# Wind Turbine Performance Measurements by Means of Dynamic Data Analysis

**Friis Pedersen, Troels; Wagner, Rozenn; Demurtas, Giorgio**

*Publication date:*
2016

*Document Version*
Publisher's PDF, also known as Version of record

DTU Vindenergi

# Wind Turbine Performance Measurements by Means of Dynamic Data Analysis

DTU Vindenergi Report 2015

Troels F Pedersen, Rozenn Wagner, Giorgio Demurtas

DTU Wind Energy E-0082

June 2015

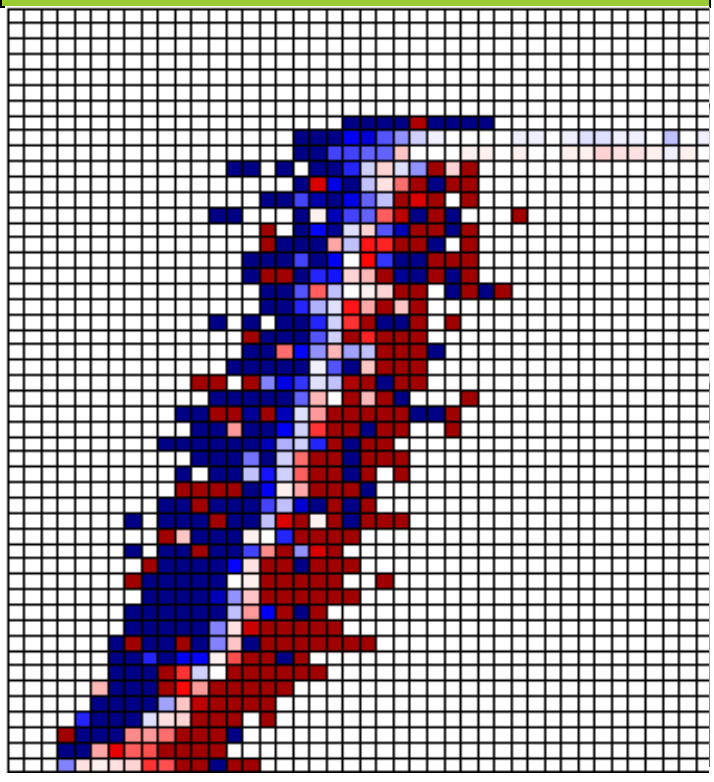

DTU Vindenergi
Institut for Vindenergi

**Authors:** Troels F Pedersen, Rozenn Wagner, Giorgio Demurtas
**Title:** Power performance measurements by means of dynamic data analysis
**Institute:** Wind Energy Division

**DTU Wind Energy E-0082**
**June 2015**

**Abstract (max 2000 char.):**
The state of the art power performance measurement method refers to the IEC61400-12-1 standard from 2005 [1]. A method for faster power curves was proposed by researchers at Oldenburg university in 2004. The method was called Langevin power curve method and advantages was claimed to be that power curves could be made faster with 1Hz dataset. In the FastWind project the Langevin power curve method was used on real power curve measurement datasets with the purpose to evaluate the method for practical use.
A practical guide to application of the method to real power curve measurement data was made. The study showed that the method has a range of parameter settings that the user must consider. Additionally to the wind speed binning power binning is needed but power binning size is not specified. Determination of drift in each bin is described with a general formula but in practice several additional tools have been developed by authors to try to make the drift field and fixed point determination more robust.
A sensitivity analysis with nacelle lidar data showed drift determination was not very dependent on the time steps applied, leading to use of time steps of 2-3 points for each dataset. Power bin size should be fixed. Data averaging with 5 sec data was more distinct for determination of the fixed points than 2 and 1 sec data. With the nacelle lidar the Langevin method seemed to produce a power curve that was comparable to the IEC power curve.
Analysis of the Langevin method with spinner anemometer data showed that fixed points were very sensitive to bin size and to requirement of minimum amount of data in each bin. The Langevin method failed to produce acceptable robust power curves comparable to the IEC power curve. Simple binned averaging of data with shorter time averages gave better results than the Langevin power curve method.

**Contract no.:**
EUDP-2009-I
J.nr. 64010-0425

**Sponsorship:**
Energiteknologisk Udviklings-
Og Demonstrations Program EUDP

**Front page:**
Drift field for Langevin power curve analysis

**ISBN: 978-87-93278-28-8**

**Pages:** 91
**Tables:** 1
**References:** 18

Technical University of Denmark
DTU Wind Energy
Frederiksborgvej 399
Building 125
4000 Roskilde
trpe@dtu.dk
www.vindenergi.dtu.dk

# Preface

The present summary report is the final report on the EUDP research project “FastWind – Faster turbine development and sharper wind farm monitoring using Dynamic Data Analysis. The project was financed by EUDP, Energiteknologisk Udviklings- og Demonstrations Program (EUDP-2009-I, J.nr. 64010-0425). The project was implemented in a cooperation consortium. From the start of the project the consortium consisted of DTU and Vestas A/S. During the project Vestas A/S withdraw from the project and the project was finalized with DTU alone.

DTU, Risø Campus, June 2015

# Content


Abstract ..... 6

1. Introduction ..... 7

2. The Langevin model for power curve measurements ..... 8
2.1 Introduction ..... 8
2.2 Binning of data ..... 8
2.3 Drift field reconstruction ..... 8
2.4 Simplified drift field reconstruction ..... 9
2.5 Fixed points determination ..... 9
2.6 Application summary of the Langevin method ..... 9
2.7 Application of dynamic data analysis on different types of data sets ..... 10

3. Dynamic data analysis on a pitch-regulated MW size wind turbine ..... 11
3.1 Ordinary IEC power curve ..... 12
3.2 Dynamic data analysis using four hours of spinner anemometer measurements and the method of bins (IEC) ..... 12
3.3 Dynamic data analysis using the Langevin method and four hours of spinner anemometer measurements ..... 17
3.4 Comparison of methods ..... 17

4. Dynamic data analysis on stall-regulated 500kW wind turbine data ..... 19
4.1 Ordinary IEC power curve ..... 21
4.2 Dynamic data analysis using the method of bins and 58 hours of spinner anemometer measurements ..... 21
4.3 Dynamic data analysis using the Langevin method and 58 hours of spinner anemometer measurements ..... 22
4.4 Comparison of methods ..... 24

5. Dynamic data analysis on a multi-megawatt turbine at Høvsøre ..... 26
5.1 Data set ..... 26
5.2 Ordinary IEC power curve ..... 26
5.3 Fast power curve with Langevin method ..... 27
5.4 Derivation of the drift curves and fixed points to the nacelle lidar data ..... 33

6. Dynamic data analysis on 2MW pitch-regulated wind turbine ..... 37
6.1 Power curve based on 10min averages and IEC binning ..... 37
6.2 Power curve based on 30sec averages and IEC binning ..... 39
6.3 Power curves based on 1 sec samples and IEC binning ..... 41
6.4 Power curves based on 1 sec samples and Langevin method ..... 44
6.5 Comparison of power curves based on different methods ..... 47

7. Discussion on dynamic data analysis ..... 52
7.1 Power curve determination ..... 52

8. Conclusions....54

References....55

Acknowledgements....57

# Abstract

The state of the art power performance measurement method refers to the IEC61400-12-1 standard from 2005 [1]. A method for faster power curves was proposed by researchers at Oldenburg University in 2004. The method was called Langevin power curve method and advantages was claimed to be that power curves could be made faster with 1Hz dataset. In the FastWind project the Langevin power curve method was used on real power curve measurement datasets with the purpose to evaluate the method for practical use.
A practical guide to application of the method to real power curve measurement data was made. The study showed that the method has a range of parameter settings that the user must consider. Additionally to the wind speed binning power binning is needed but power binning size is not specified. Determination of drift in each r bin is described with a general formula but in practice several additional tools have been developed by authors to try to make the drift field and fixed point determination more robust.
A sensitivity analysis with nacelle lidar data showed drift determination was not very dependent on the time steps applied, leading to use of time steps of 2-3 points for each dataset. Power bin size should be fixed. Data averaging with 5 sec data was more distinct for determination of the fixed points than 2 and 1 sec data With the nacelle lidar the Langevin method seemed to produce a power curve that was comparable to the IEC power curve.
Analysis of the Langevin method with spinner anemometer data showed that fixed points were very sensitive to bin size and to requirement of minimum amount of data in each bin. The Langevin method failed to produce acceptable power curves comparable to the IEC power curve. Simple binned averaging of data with shorter time averages gave significantly better results than the Langevin power curve method.

.

# 1. Introduction

The state of the art power performance measurement method refers to the IEC61400-12-1 standard from 2005 [1]. According to this standard at least 180 hours of 10 min averaged data shall be included in the power curve. However, due to wind speed variability and wind direction variability it often takes 1-3 month to perform a power performance measurement. Many efforts have been made to reduce the measurement period for a power curve measurement. A lot would be gained with shorter measurement times. For prototype wind turbines more options could be verified in shorter time, reducing expensive costs on test station pads and making development time to market shorter. For production wind turbines performance could be followed more intensely. SCADA data are often based on 1Hz data, so fast data are available on individual turbine level. Power curves based on shorter time-windows might provide closer control of power performance, and thus reveal degradation of performance if changes occur on the wind turbine.

A method for faster power curves was proposed by researchers at Oldenburg university [2-12] starting in 2004. The method has been called Markovian power curves and Langevin power curves. The advantages of the method was claimed to be that it considered the dynamic effects of the power performance by using fast scanned data in the range of 1Hz. The method would be able to extract a power curve in shorter time than the IEC standard [1] and also to generate a turbulent independent power curve. Most of the references [2-12] analysed the Langevin power curve method based on an artificial power curve made from a wind turbine model.

The present report presents the results of the aim to implement the Langevin power curve method and also shorter time averages (Dynamic Data Analysis - DDA) to real measured wind turbine data. No attempts were made to further develop the Langevin method. Only the practical aspects and robustness of the method compared with the more simple short time average binning was the focus in this analysis. An analysis of the robustness of the Langevin procedure was made early in this project and presented in [14].

The implementation of the method was made in several steps. First, the articles [2-12] have been studied. A master project study was run in parallel [13]. A practical operational description of the Langevin power curve method was made, see chapter 3.6. And then the method was implemented on four different measured power performance datasets from four different wind turbine types. The types of wind measurements also varied from hub height mast cup anemometer measurements to spinner anemometer measurements to nacelle lidar measurements.

# 2. The Langevin model for power curve measurements

## 2.1 Introduction

The Langevin power curve method uses measurements sampled at high sampling frequency. From the Nyquist-Shannon sampling theorem, for a correct reconstruction of the signal the sampling frequency should be at least twice higher than the maximum frequency present in the signals for power and wind. Due to the nature of wind and electric power of a wind turbine, where signal frequencies may reach a few Hz a practical sampling frequency of at least 10 Hz should be used. As a result of this short period between measurements, the correlation between the wind speed and the power is much lower compared to a standard IEC power curve made with 10 min averaged measurements. The scatter is therefore higher than what is normally seen for an IEC power curve made with 10 min averaged values.

The concept behind the Langevin method lays in the model of the dynamics of the power curve where the power output is considered as a set of univariate Langevin processes which lead to definition of the drift and of the fixed points. The drift is a measure of the tendency of the power to increase in time (positive drift) or to decrease (negative drift) in time. The fixed points identify the power curve, through a value of power and a value of wind speed. There is one fixed point for each wind speed bin. The scatter in the measurements cause some measurements to be located above the power curve (hence above a specific fixed point of power), while others are located below. Points above the power curve will generally tend to have a decreasing power (negative drift), since the power tend to go towards the fixed point. However, the average drift must be based on a high variety of drift values for each wind speed bin.

In [13] it was found that the influence of the wind direction on the correlation between wind speed and power was important, and for his analysis he used a wind sector of ± 25 º, centred on the direction between met-mast and wind turbine.

## 2.2 Binning of data

As described in [2-12] the measurements of wind turbine power output and wind speed are binned according to wind speed bins and power bins. The size of the wind speed bin used in general in [2-12] is the same as the IEC standard [1] and was 0.5 m/s. The power bins vary somewhat from 10 kW to 50 kW. It is argued that the number of bins should not be too high because a high number of drift data are needed for each bin.

## 2.3 Drift field reconstruction

The objective of this step of the calculation is to determine, for each wind-power bin the value of the drift. The drift is found for the time step τ going towards zero:

$$D_i^1(P) = \lim_{\tau \to 0} \frac{1}{\tau} \langle P(t+\tau) - P(t) | u_i \rangle$$

For each specific wind and power bin, the drift is calculated as follows:

- Investigate the change of power in the original time series for a time step τ.

- From each time series, find $\Delta P = P(t+\tau) - P(t)$ and let τ be going towards zero (eventually make a linear regression through origo for several τ values, i.e. 1 to 10).
- Average the power differences $\langle \Delta P \rangle$ for each time step. At this point, averaged time series should show a tendency to increase for the power bins below the power curve, and a tendency to decrease for the bins above the power curve.
- Find the drift from the average power difference divided by the time step $\langle \Delta P \rangle / \tau$ or find the drift by making a linear fit of $\Delta P$ as function of $\tau$ forced through the origin.

The procedure is repeated for each wind speed and power bin, so that a complete drift field is obtained.

## 2.4 Simplified drift field reconstruction

The drift is defined for $\tau \to 0$. However, the simplest way to calculate the drift on the basis of discretized data is to simply calculate the difference between two consecutive values of power. $\Delta P = P(t+1) - P(t)$. This can easily be made on the original time series, obtaining a drift time series. The drift is not calculated where the time series is not continuous. The drift should for the turbine sizes examined in the project be within a range of about ±100 kW/s. Higher rate of change of the power is likely to be the result of some problem in the analysis or in the measurements rather than a real (extreme) variation of power. However, it might be observed in some cases. A condition of a minimum number of measurements might be used prior to calculation of the mean drift in a wind and power bin, to avoid excessive variability.

## 2.5 Fixed points determination

The fixed points are determined from the drift field. The objective is for a specific wind speed bin to find the zero drift. The drift coefficient of a specific bin is plotted as function of power (see figures of appendices). The drift graphs should show a decreasing drift for increasing power. A linear fitting might be applied, and the value of the fixed point (in kW) be found for drift equal to zero. For some bins there might be several crossings, however, of the zero. In [13] it is suggested to do an integration of the drift over the power variation and take the absolute minimum of the integral plotted as a function of power. In [14] it is suggested to interpolate the drift values with a cubic spline.

## 2.6 Application summary of the Langevin method

The Langevin method was summarized in the following steps:

1. Load the time series measurements of $u_i$ (horizontal wind speed), $P_i$ (power output), $\rho_i$ (air density).
2. Normalize power (stall regulated rotor) or wind speed (actively controlled rotor) of time series data to standard air density with the method described in the standard IEC61400-12-1 [1] to find $u_{in}$.and $P_{in}$.
3. Calculate $\Delta P_{in} = P_{in}(t+\tau) - P_{in}(t)$ of the normalized power data from the time series data using the smallest appropriate $\tau$, where the time series is continuous in time. Remove measurements where it was not possible to calculate $\Delta P_{in}$.
4. Make a binning of wind speeds of 0.5 m/s bin size centered on full and half wind speeds
5. Make a binning of power into an appropriate amount of bins, for example about 50 bins

6. Average all wind speeds in each wind speed bin to obtain the wind speed fixed point $u_{fixed} = \langle u_{in} \rangle$
7. Average all $\Delta P_{in}$'s for each power bin to find $\langle \Delta P_{i,j} \rangle$.
8. Find the drift coefficient $D_{i,j} = \langle \Delta P_{i,j} \rangle / \tau$ to obtain the drift for each power bin
9. For each wind speed bin make a plot of the drift as a function of power bin and determine the fixed point as $P_{fixed} = P | D_{i,j} = 0$
10. Table and plot the power curve $P_{fixed}$ as function of $u_{fixed}$

## 2.7 Application of dynamic data analysis on different types of data sets

The power curve of four wind turbine models was calculated first with a traditional IEC method [1] (several hundred hours of 10 min averaged measurements and binning) to serve as reference power curve. Then we obtained power curves by use of the Langevin method as described in the previous chapters, and finally we used the method of bins based on short time averages.

# 3. Dynamic data analysis on a pitch-regulated MW size wind turbine

The wind turbine was part of a wind farm made of  wind turbines aligned in a single row, almost east to west, in an open flat area. The turbine under consideration was the 4$^{th}$ counting from west. The rotor diameter was 90 m and the hub height 80 m. The wind turbine was mounted with a spinner anemometer [15]. At a direction of 215 degrees from the wind turbine there was an IEC61400-12-1 compliant met-mast instrumented with cup anemometer at hub height and wind vane on a boom at 78 m height.

The sampling frequency was 10 Hz for both the spinner anemometer and the electric power output. Time series were filtered with moving average to 1Hz. Figure 1 shows 30 seconds of measurements relative to a wind speed and power in the slope of the power curve. Because of the high variability of the power, the measurements were averaged to 1 second. This averaging period was sufficient to smooth out most of the variations in the power, as shown graphically by the bold black line (1 second moving average). If the power signal was sampled with a frequency of 1 Hz instead of 10 Hz, the signal would have been quite different, as represented by the green dotted line (each dot represent a sample). The same treatment was applied to the wind speed measured time series.

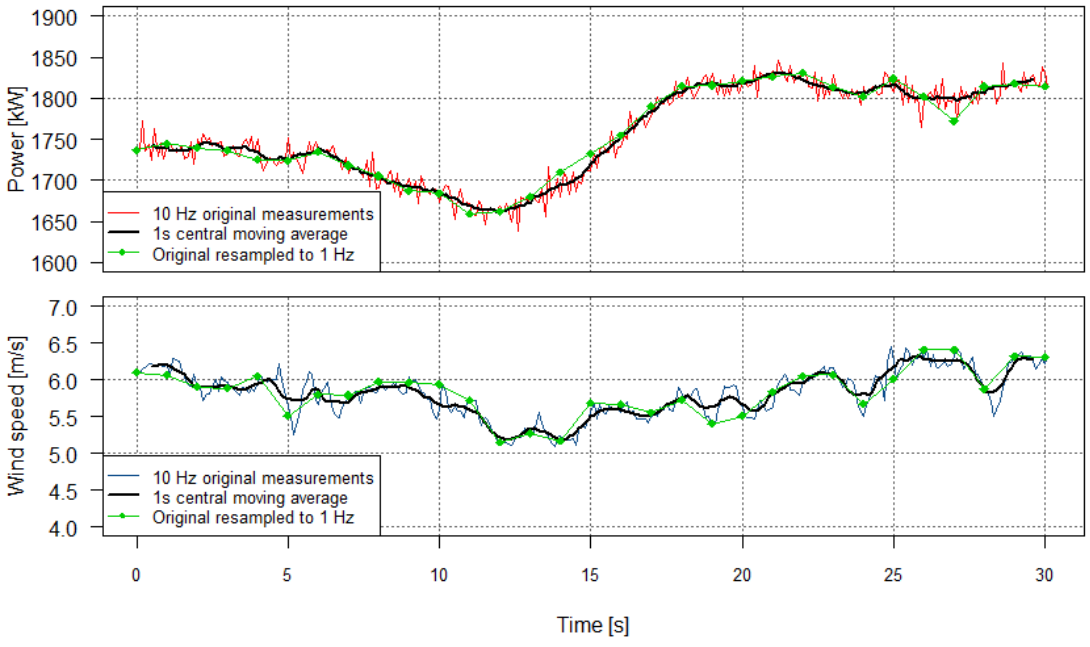


**Figure 1 Time series showing 30 seconds of measured power and horizontal wind speed (by spinner anemometer). One seconds central moving average in black, and in green the original signal resampled at one second intervals.**

## 3.1 Ordinary IEC power curve

The wind speed was simultaneously measured by the met-mast and by the spinner anemometer installed on the turbine. The selected valid wind direction sector as calculated from the IEC standard was 101-229 degrees. However we only used 120 to 210 degrees, which is 90 degrees wide and is centered onto the direction 165 degrees to have some safety margins to avoid wind turbine wakes. A narrower sector should increase further the correlation between mast wind speed and turbine power.

The spinner anemometer was calibrated for yaw misalignment measurements [16], but wind speed calibration and the nacelle transfer functions was not determined. As a consequence, the power curve by the spinner anemometer differs significantly from the one by the met-mast (Figure 2). This discrepancy is not an issue for the present analysis, which aims at comparison of the power curve made with the IEC method of the analysis of the Langevin method and with short time averaging. Therefore, the power curve (shown in red in Figure 2) is used as the reference power curve and other power curves are related to this one. The correlation between power and wind speed is much better for the spinner anemometer than for the met-mast, as seen by the scatter of the power. This is a result of the reduced distance between the wind speed sensor and the turbine rotor.

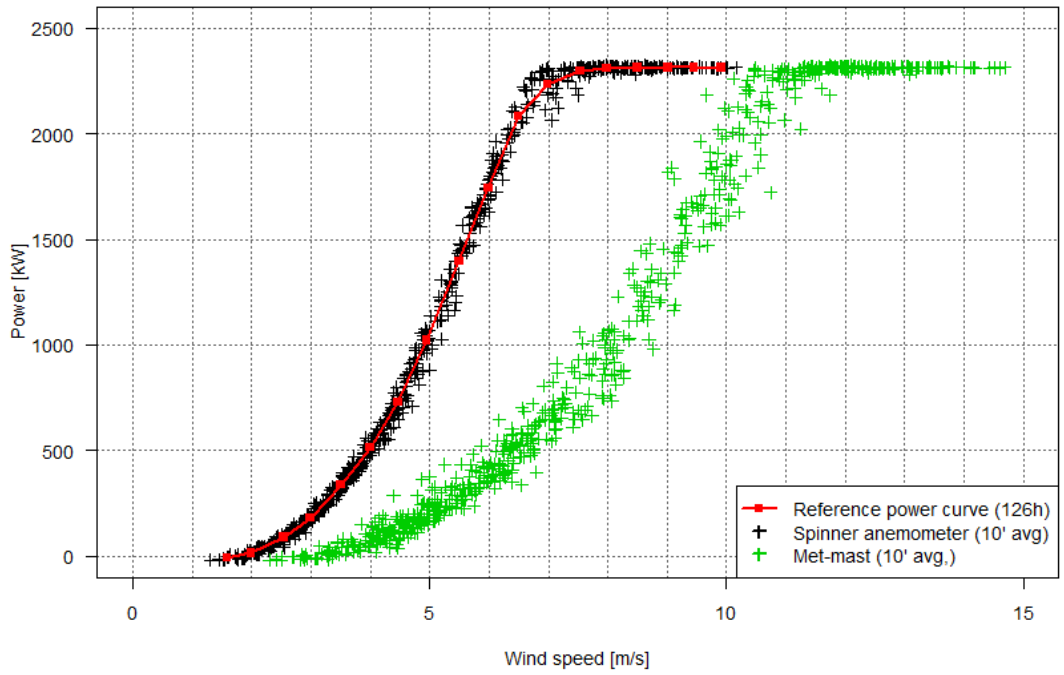


**Figure 2 Power curve by met-mast (green) and spinner anemometer (red) without a calibration factor.**

## 3.2 Dynamic data analysis using four hours of spinner anemometer measurements and the method of bins (IEC)

The period of measurements was selected in order to cover the whole wind speed range. Four periods of one hour were identified, as shown in the (not continuous) time series of Figure 3. The periods are (UTC+1 time, or Danish normal time) :
2014-09-15 h 06-07; 2014-12-08 h 09-10; 2014-12-08 h 15-16; 2014-12-02 h 08-09

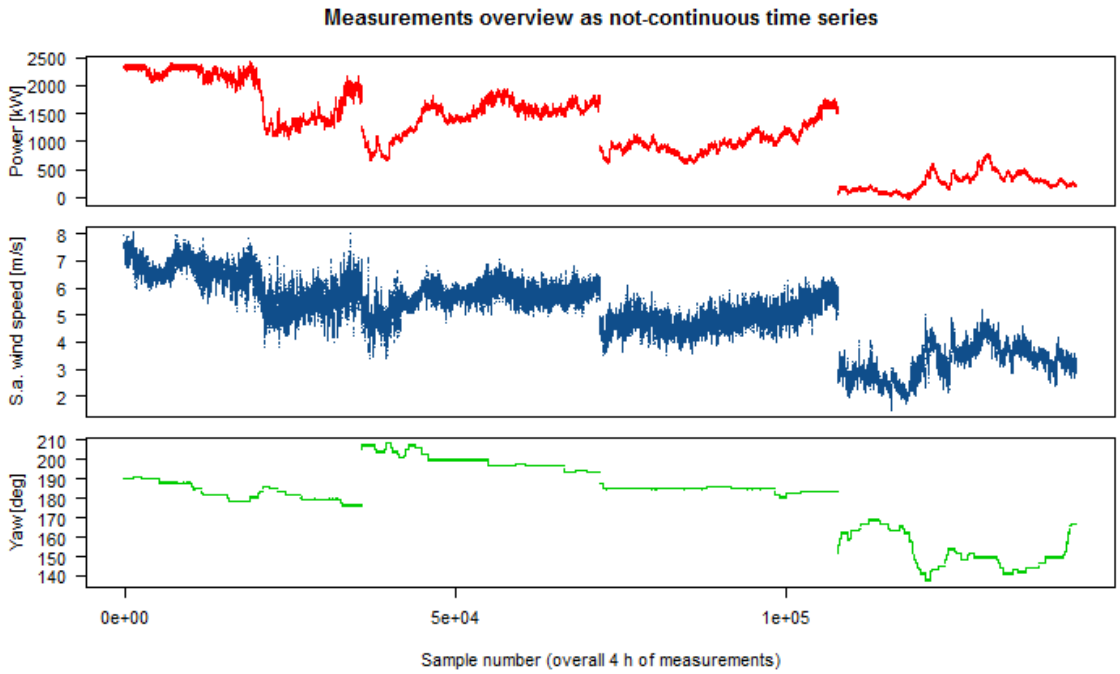


**Figure 3 Not continuous time series of the four hours of measurements of 10Hz data used for the DDA. Red is the power output, blue is the horizontal wind speed by the spinner anemometer (not calibrated values). Green is yaw position of the wind turbine (approximating the wind direction).**

A scatter plot of 10Hz data between wind speed and power is shown in Figure 4. The same data averaged to 1Hz are shown in Figure 5. The scatter is seen to be reduced significantly, as well as the amount of data is reduced ten times.

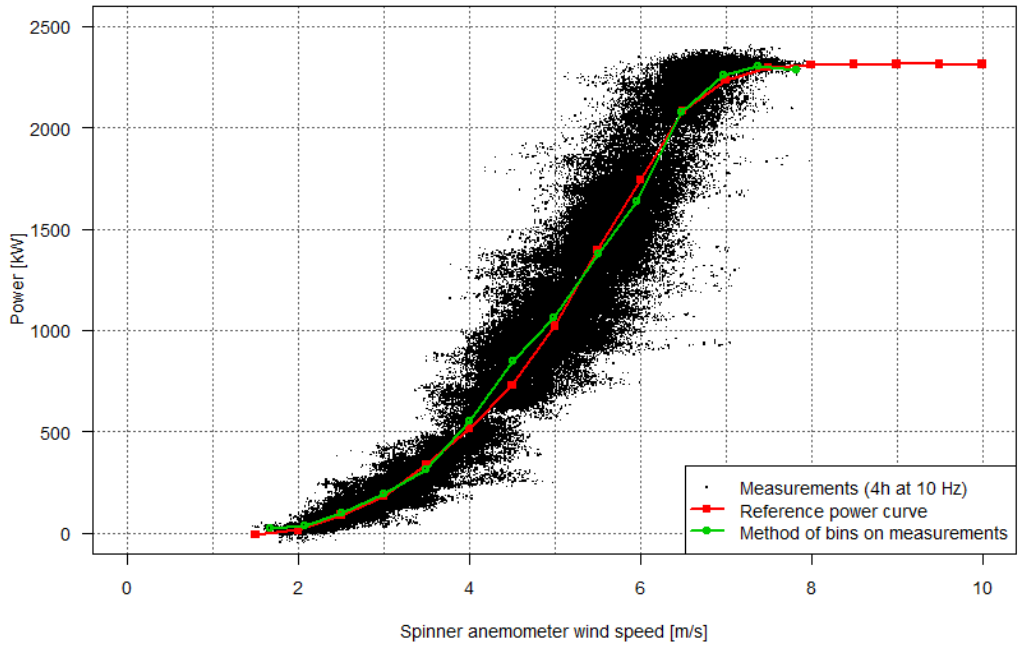


**Figure 4 Fast power curve data. In black 10Hz sampled data. In red binned reference power curve with IEC standard 10min averaging. In green binned power curve with 10Hz data.**

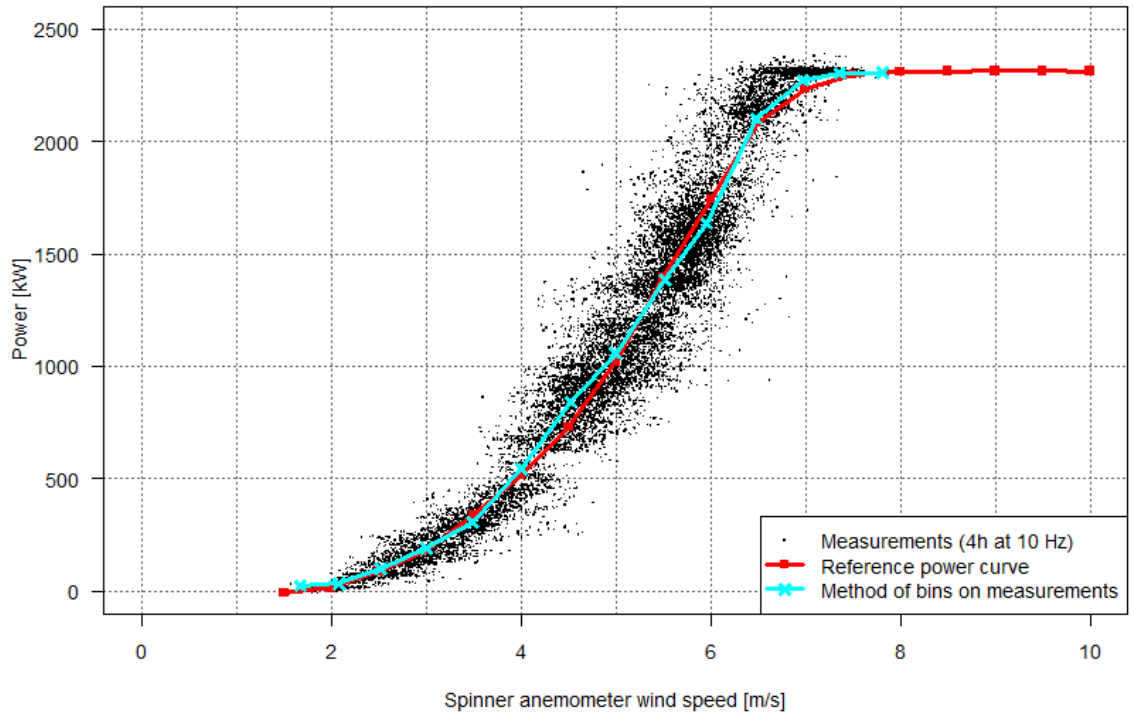


**Figure 5 Fast power curve data. In black 10 Hz measurements averaged to 1s, In blue binned power curve with 10 Hz measurements averaged to 1s.**

The deviations between the reference power curve and the fast power curve seems to be due to the uneven distribution of measurements along the power values. This is more visible in Figure 6.

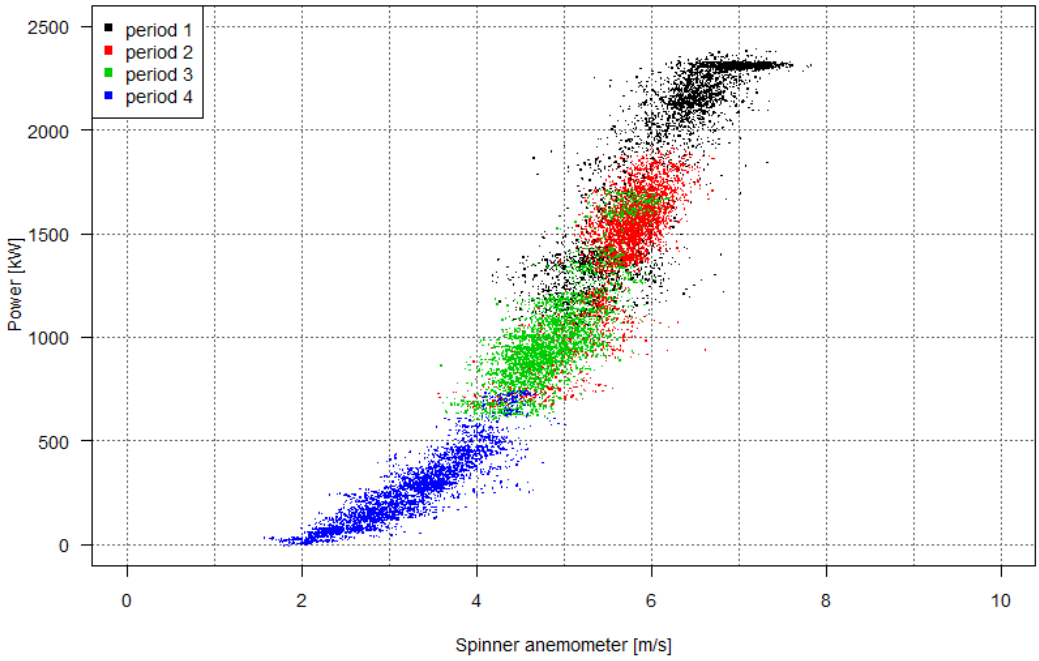


**Figure 6 10 Hz measurements averaged to 1s, shown with a colour for each hour of the dataset.**

Few measurements in a certain power bin will increase the uncertainty of the average bin power (and speed). On the other hand, missing values of power (due to insufficient amount of data, or an uneven distribution along the power curve) will result in a deformed average value.
As seen in Figure 6, there is a gap in power between the four data sets. This is clearly visible also in the count of the measurements binned according to the power (Figure 7).

At present the Langevin method as described in [2-12] sets no requirement regarding the amount of measurements in each power bin, as absolute value as well as difference to neighboring bins.

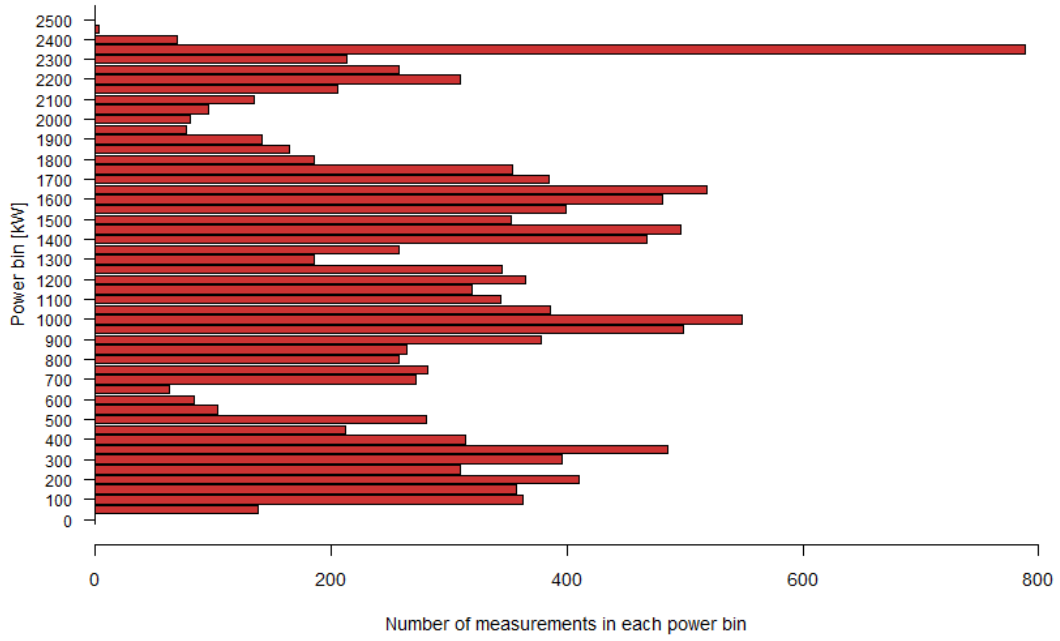


**Figure 7 Number of measurements in each power bin.**

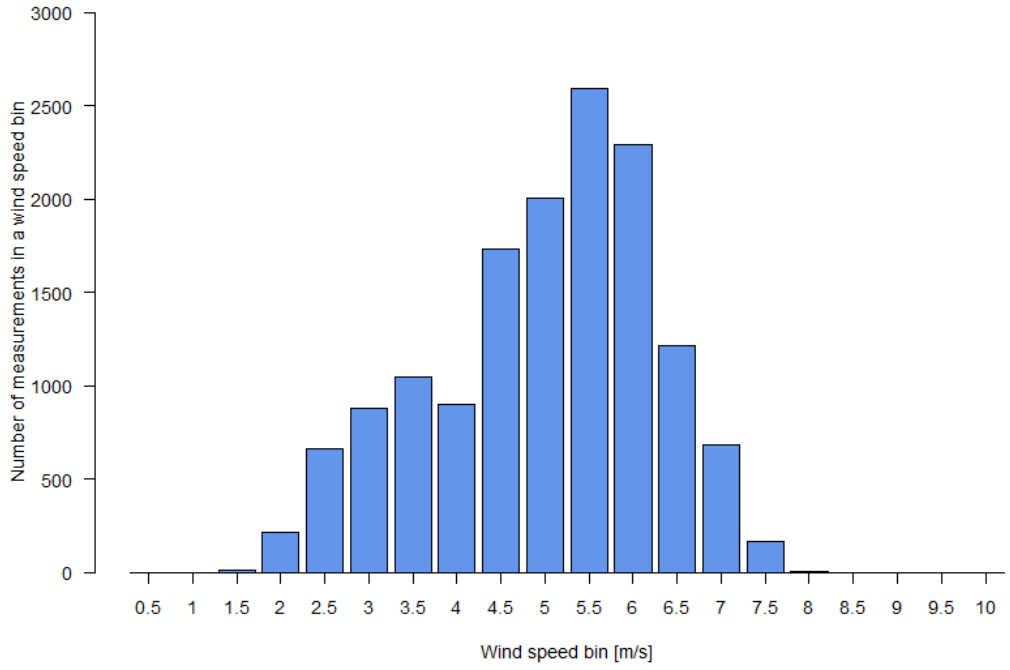


**Figure 8 Number of measurements in each wind speed bin**

## 3.3 Dynamic data analysis using the Langevin method and four hours of spinner anemometer measurements

The data-set described in section 3.1 was analyzed by use of the Langevin method. The major difficulties encountered were the determination of a robust value of the power fixed point. In fact, while the drift was expected to be decreasing in a wind speed bin for increasing power, we observed a not clear tendency. See for example the positive drift near a negative drift in bin corresponding to 5 m/s.

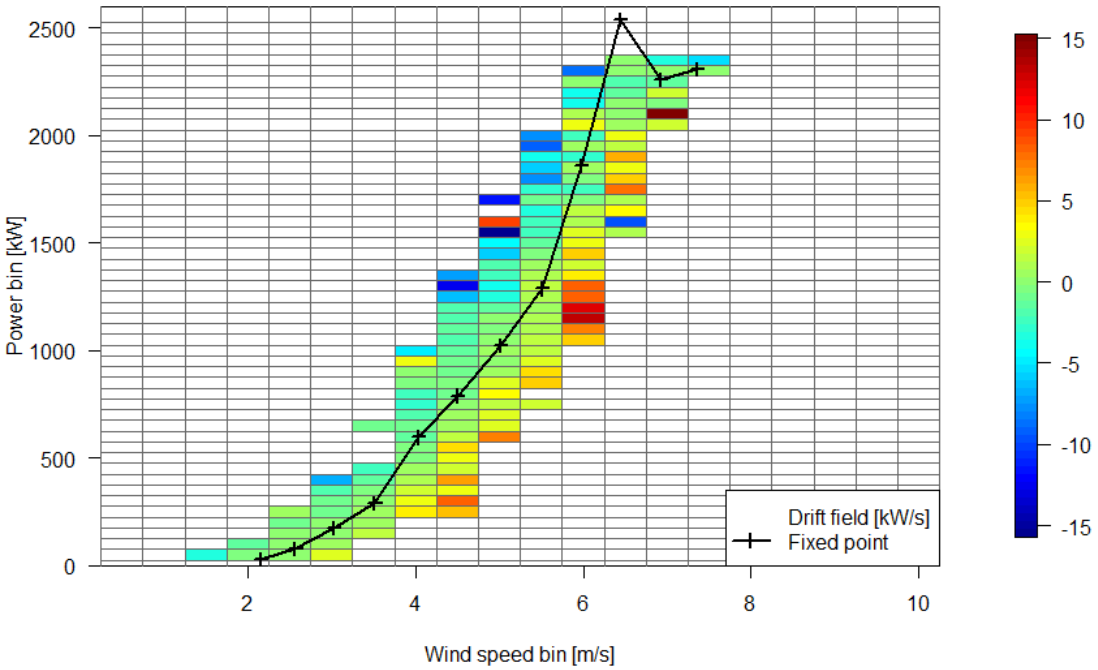


**Figure 9 Drift field and Langevin power curve (power bin is 50 kW)**

The same data showed with colors in Figure 9 are shown as drift as a function of power in appendix. Each plot corresponds to a column of Figure 9. In each figure, the vertical segment shows the value of power of the reference power curve. The drift curves (red) are crossing the zero drift (horizontal black line) in correspondence of the vertical blue mark. This value of power was obtained simply fitting a linear regression (blue line) to the drift curve. Due to the unclear shape of the drift curve, it was impossible to identify a better fitting method.

## 3.4 Comparison of methods

The power curve used as reference for comparing the methods was made on the basis of 126 hours of spinner anemometer measurements and the method of bins.

The deviations from the reference power curve are better represented in Figure 11, where the vertical scale shows the difference between each of the three methods and the reference power curve. The deviation between use of the method of bins or use of the Langevin method seems comparable.

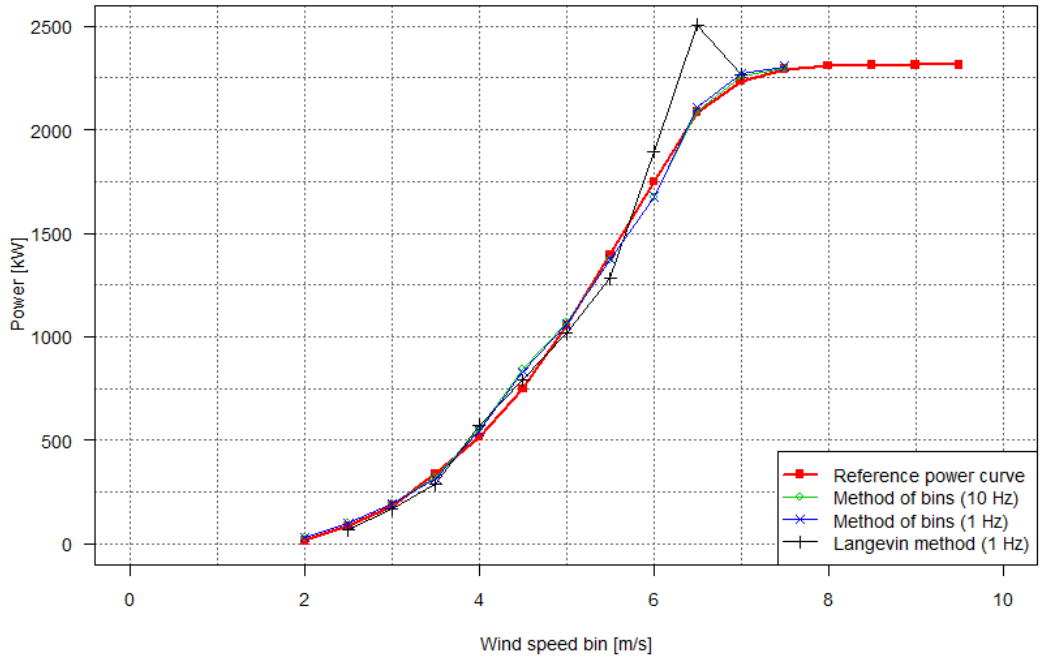


**Figure 10 Comparison of power curves made with different methods**

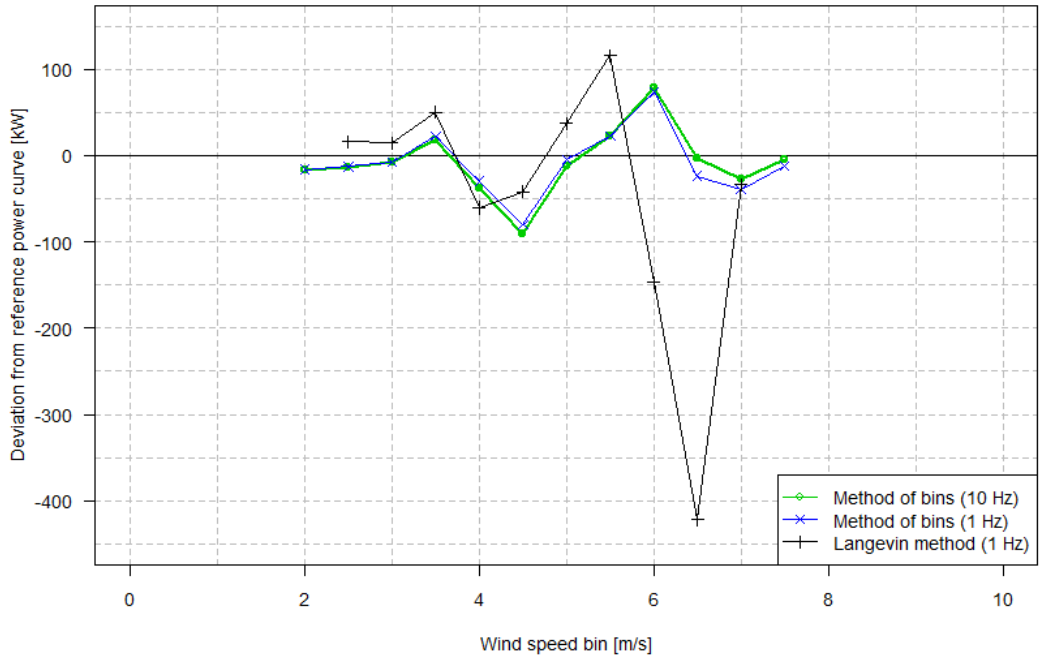


**Figure 11 Deviations from the reference power curve of three power curves made using 4 hours of measurements at 10 Hz.**

# 4. Dynamic data analysis on stall-regulated 500kW wind turbine data

The wind turbine is installed at DTU Wind Energy Risø campus. The wind turbine is part of a row of wind turbines. A met-mast is erected at the direction 283º in front of the wind turbine and equipped with wind speed and wind direction measurements at hub height. The wind direction sector that guarantees an undisturbed wind flow is 90º wide, cantered at 283º.

The wind turbine is also measuring the wind by use of a spinner anemometer. For the period of measurements used in this report, the spinner anemometer was calibrated (which means that it is measuring correctly the wind speed at the centre of the rotor plane in stopped condition). The nacelle transfer function is not applied, since the objective is here to compare the methods rather than obtaining an absolute power curve made with the met-mast and IEC61400-12-1 method.

In chapter 3.1 the methods were jeopardized by the uneven distribution of measurements in the power bins, which was causing the values of the power curve made with only 4 hours of measurements to deviate from the reference power curve. In the present case the analysis was repeated on a much higher amount of measurements, 58 hours.

This chapter compares a reference power curve (chapter 4.1) to a power curve derived from a short interval of measurements and a high periodicity. The measurement system delivers the power sampled at 35 Hz, while the spinner anemometer is sampled at 10 Hz. 30 seconds of such measurements are shown in red and blue colour in Figure 12. Note that the resampled signal and the averaged signal have discrepancies. Therefore, in order to catch the real dynamic content of the physical parameter, a sampling frequency of 0.5 Hz or 1 Hz is insufficient.

The power signal presents a variation that repeats with a constant periodicity. This variation is due to the blade passing the tower, and has a constant period since the rotational speed of the turbine is constant.

In order to remove this variation, that is not due to the wind, from the signal, the power signal and the wind signal are averaged at 2 seconds intervals. The time series of power, wind speed, and yaw position of the wind turbine are shown in Figure 14 as 0.5 Hz averaged signals.

The calculation of the power curve with the method of bins on original data (10Hz) and on 1s averaged data (chapter 3.1.2) showed that the resulting power curves are very similar. Therefore, this scale of averaging (from 10-35 Hz down to 1-0.5 Hz) can be used to reduce the amount of data to analyze by a factor of 10-30, without compromising the results.

The power was corrected to standard air density at the moment of importing the time-series from the database into the analysis software.

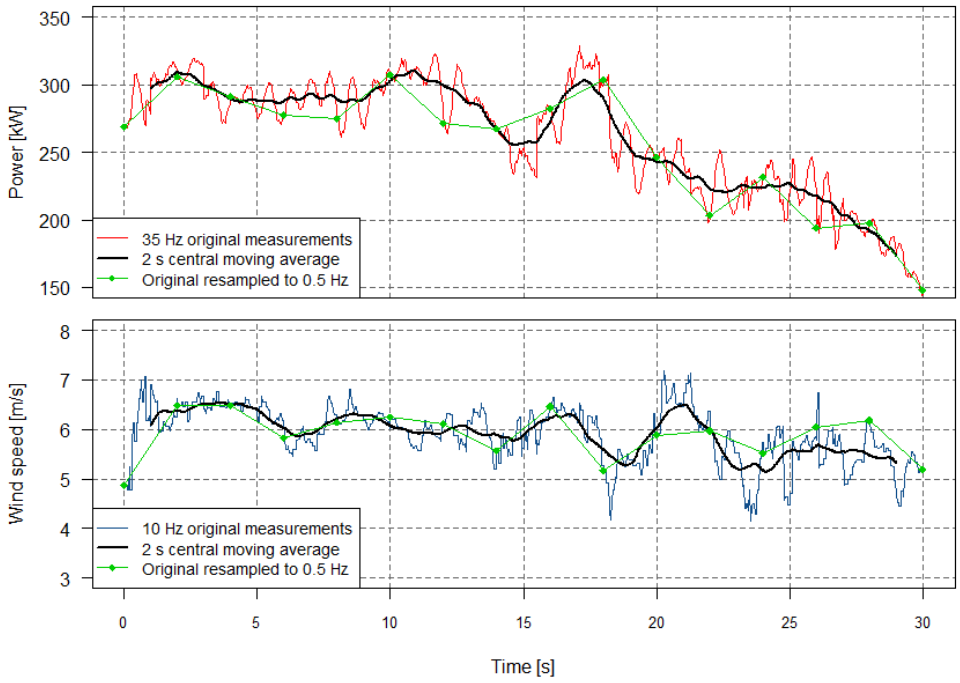


**Figure 12 30 seconds time series of measured power and horizontal wind speed (by spinner anemometer). Two seconds central moving average in black and in green the original signal resampled at two second intervals.**

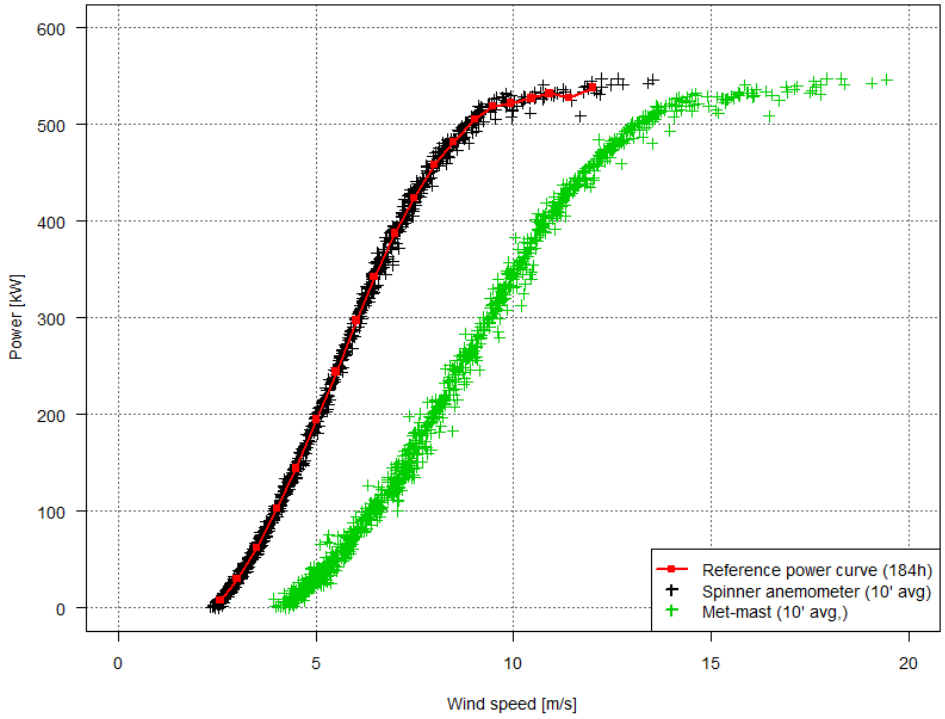


**Figure 13 Reference Power Curve, measured with the spinner anemometer on a 500 kW stall regulated wind turbine. IEC method of bins.**

## 4.1 Ordinary IEC power curve

The reference power curve (Figure 13) is measured using the spinner anemometer and the method of bins. Green points shows for reference the power curve measured with the met-mast.

## 4.2 Dynamic data analysis using the method of bins and 58 hours of spinner anemometer measurements

The reference power curve determined previously compares well with the one obtained with the method of bins applied to 58hours of 2s averaged measurements.

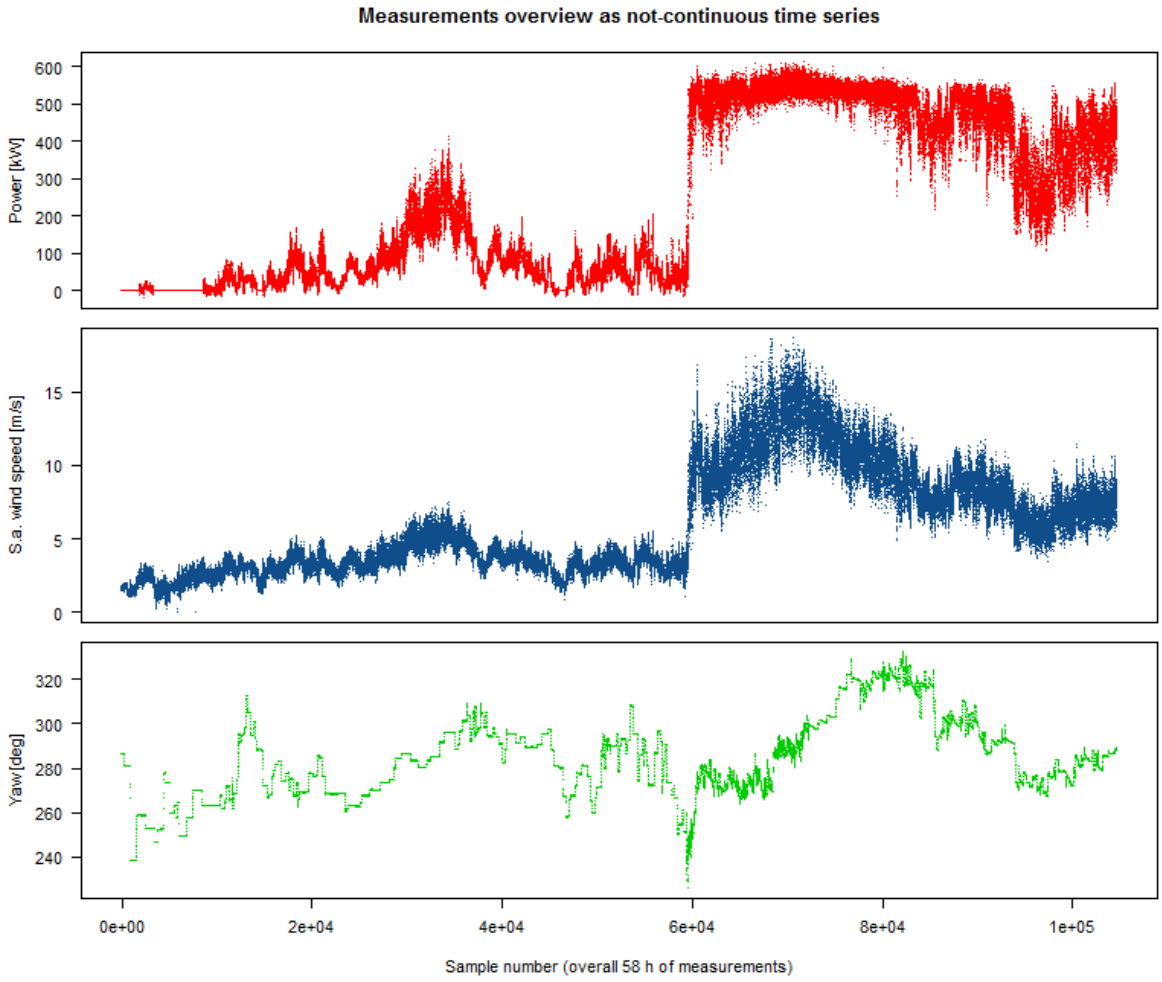


**Figure 14 Time series of 58 hours of 2s averaged measurements**

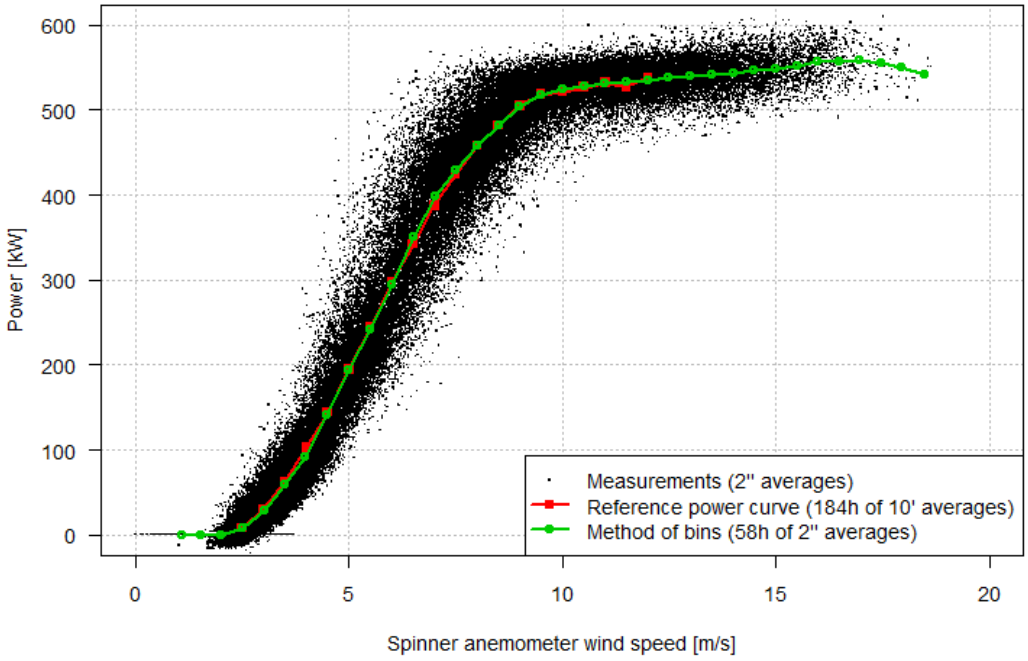


**Figure 15 Power curves of the Nordtank 500kW wind turbine using spinner anemometer**

## 4.3 Dynamic data analysis using the Langevin method and 58 hours of spinner anemometer measurements

The Langevin method applied to 58 hours of 2s measurements gave the drift field as represented in Figure 16. The determination of the fixed points gave unexpected results in the band between 200 kW and 450 kW. In fact, the drift curves did not present a decreasing tendency, or were very close to the value of zero drift for a broad range of power values.

The linear fitting applied to the drift curves gave, for several bins, a value of power very distant from the expected one and definitely inconsistent. See drift curves in appendix.

The reason for this inconsistency might be due to the insufficient amount of measurements available in the power bins that had a bad estimation of the power curve. See Figure 17 and Figure 18.

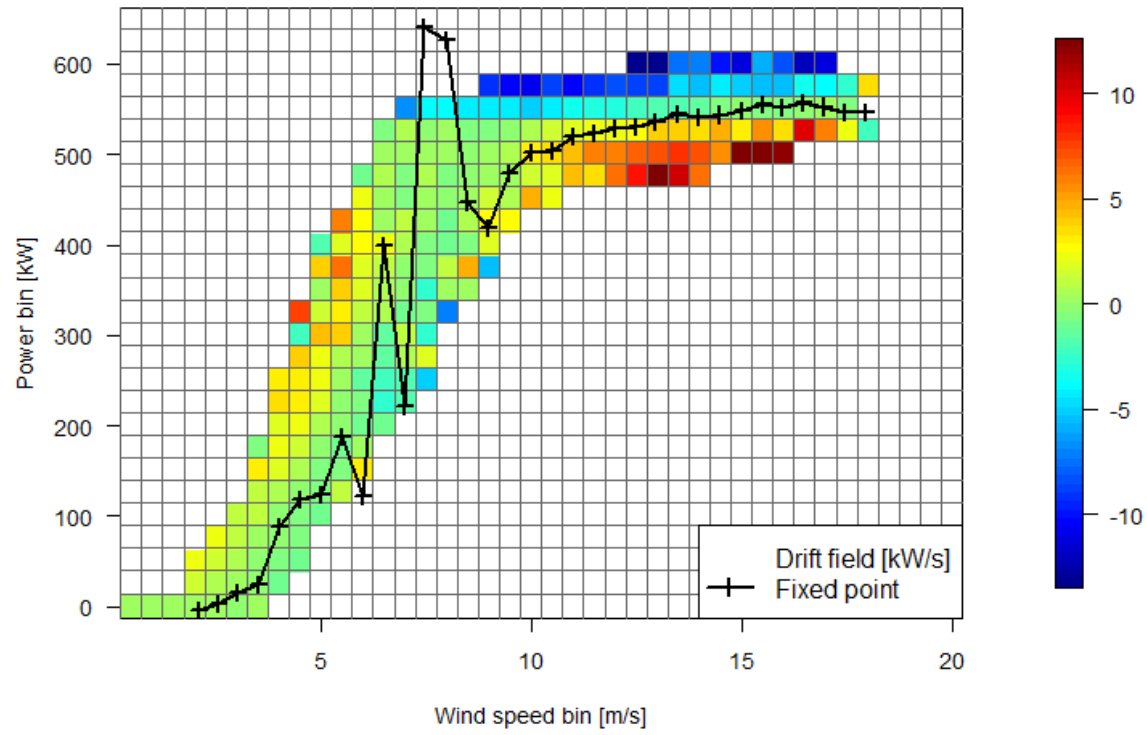


**Figure 16 Drift field for 56 h of 2s averaged measurements (power bin is 50 kW)**

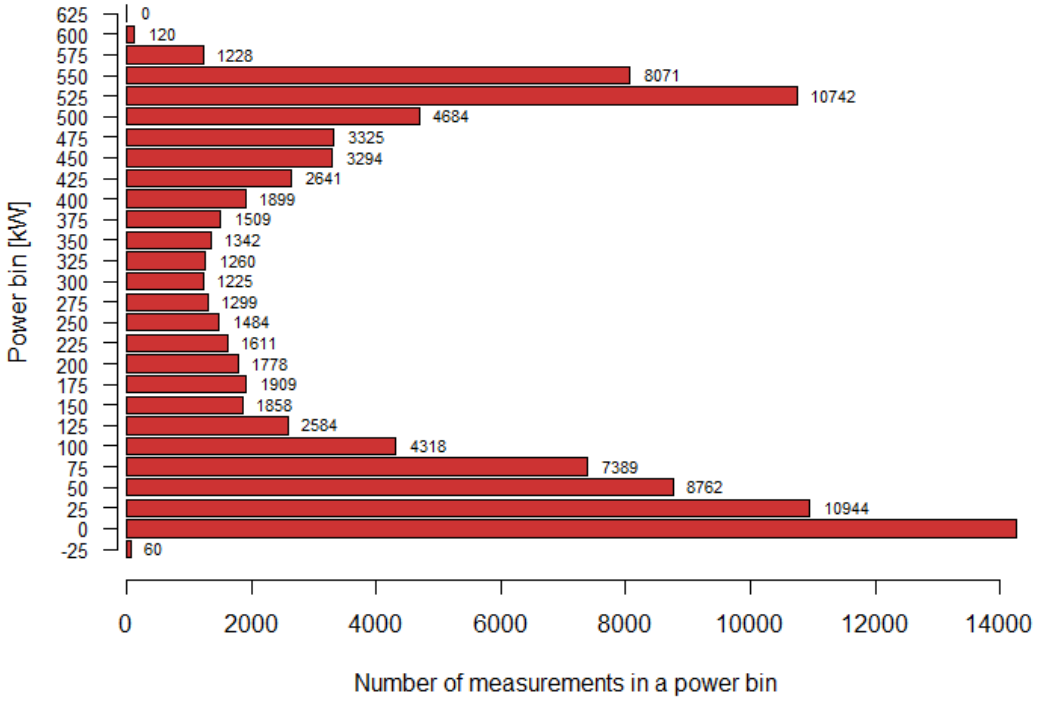


**Figure 17 Number of measurements in each power bin**

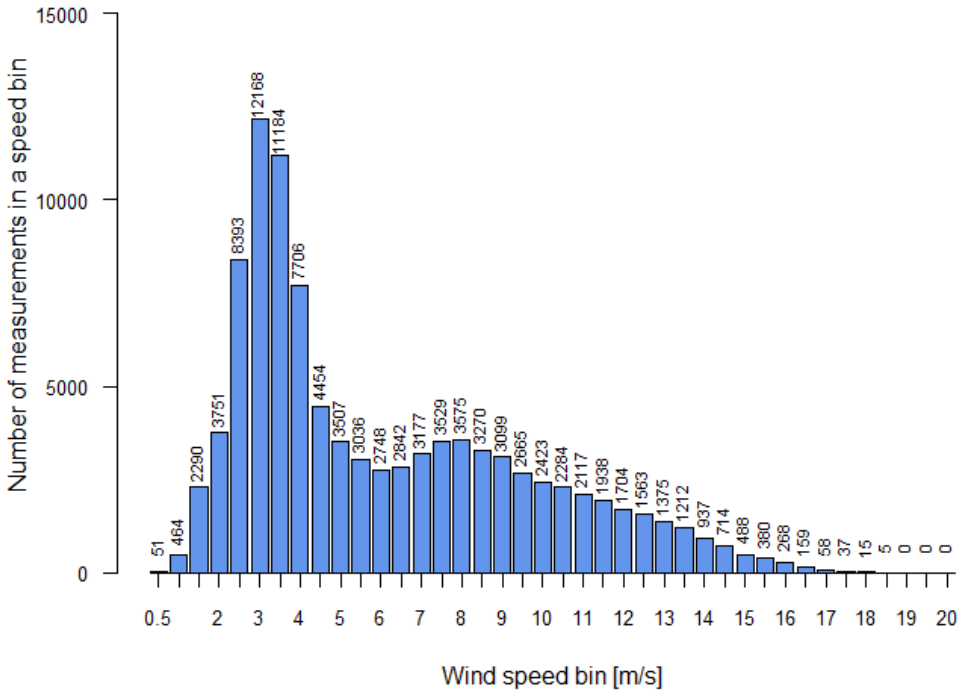


**Figure 18 Number of measurements in each wind speed bin**

## 4.4 Comparison of methods

The power curve calculated with the method of bins and Langevin method are shown in Figure 19 along with the reference power curve. The reference power curve was calculated with the method of bins applied to 184 hours of 10' averaged values. The other two curves were calculated from the same dataset of 58 hours of 2 seconds averages. For the comparison, all the values of power were calculated at the wind speed bin center with linear interpolation.

As minimum, in a power bin there are about 1200 measurements (2 second averages), that correspond to 40 minutes of measurements. Compared to the method of bins, the Langevin method, see Figure 20, seems to have problems for those power bins with fewer measurements. On the other hand, the method of bins reproduced the reference power curve much more accurately.

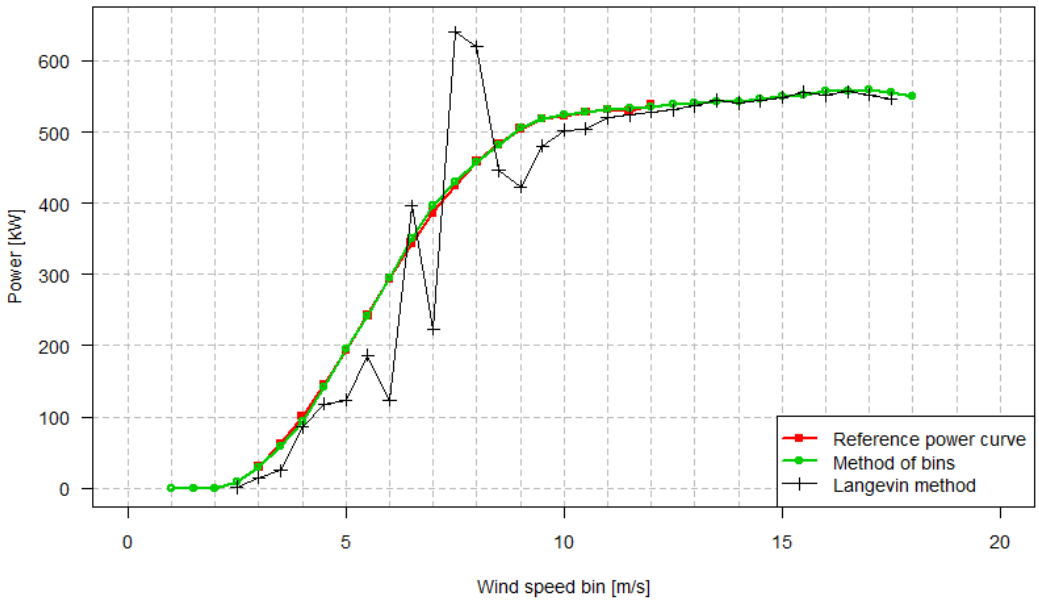


**Figure 19 Comparison of power curves calculated with different methods**

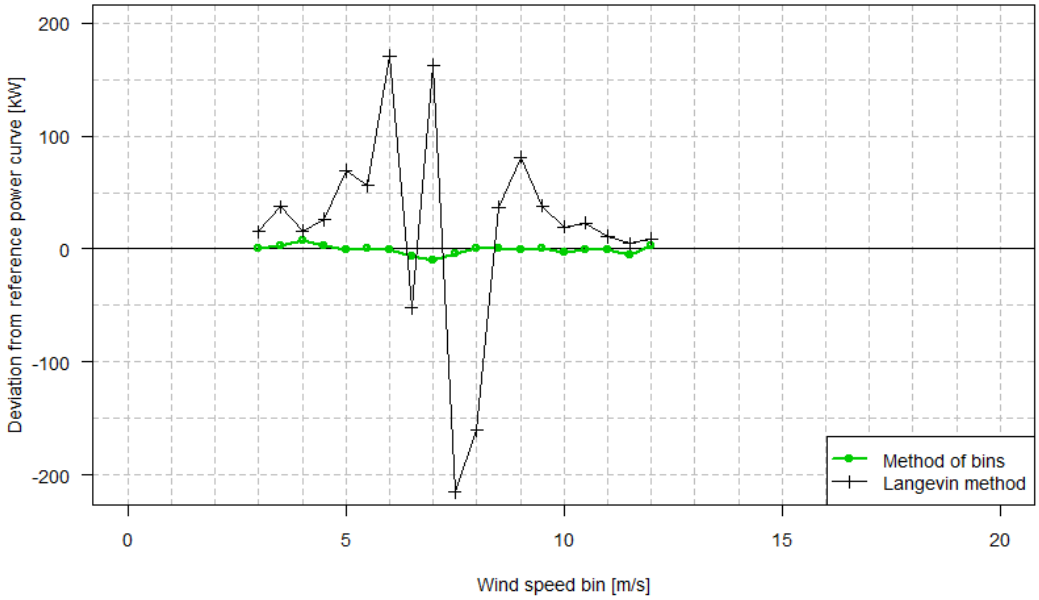


**Figure 20 Deviation from the reference power curve. Maximum deviation for the method of bins is 9.85 kW at 7m/s.**

# 5. Dynamic data analysis on a multi-megawatt turbine at Høvsøre

## 5.1 Data set

The measurements resulted from a measurement campaign carried out at DTU's test station for large wind turbines, in Høvsøre on the west coast of Denmark. The site counts 5 multi megawatt wind turbines aligned along the North-South direction. A hub height met mast compliant with the IEC 61400-12-1 requirements stands on the west side of each turbine for power performance measurement.

One of these 5 turbines has been used for the following analysis. The turbine data (power, status and yaw) were sampled at 35Hz. The met mast data were acquired at 1 Hz. A 2 beam pulsed nacelle lidar was installed on the turbine nacelle roof, behind the rotor and sensing the wind speed upstream of the turbine [18].

Only two months of 1Hz mast data were available.

## 5.2 Ordinary IEC power curve

The 10 minute average wind speed and power data were filtered and averaged according to the requirement of the IEC 61400-12-1 standard [1] and in order to have reliable lidar data [13] in a common dataset.

The final data set only counts about 160 hours of data, which is 20 hours too short to fulfil the IEC requirements. Nevertheless, after binning the data in wind speed bins of 0.5m/s, all the bins counted more than 3 points for the wind speeds between 4 and 20m/s (included). Figure 21 shows the bin averaged power curve derived from the 10 minute mean data for the met mast cup anemometer an the nacelle lidar.

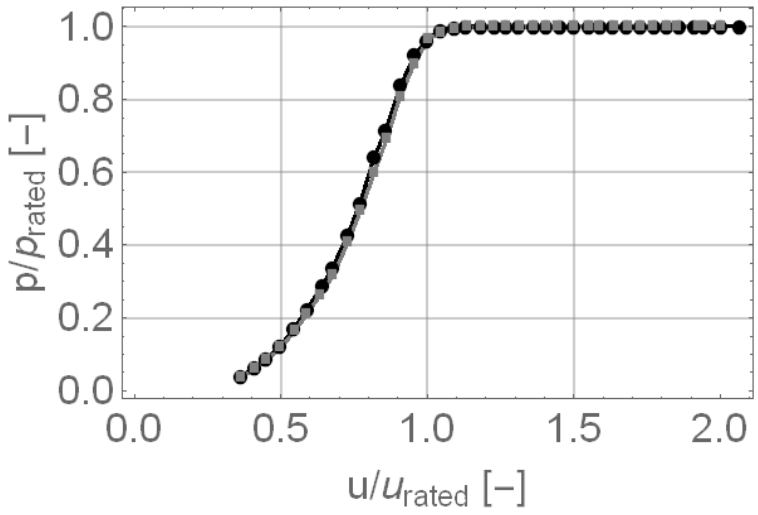


**Figure 21 Bin averaged power curve obtained with mast cup anemometer wind speed measurements (black), with nacelle lidar wind speed measurements (gray).**

## 5.3 Fast power curve with Langevin method

In order to apply the Langevin method, the turbine data were first averaged down to 1Hz. Figure 22 shows the power scatter plot obtained with the 1 Hz date from the turbine power and the mast mounted cup anemometer wind speed.

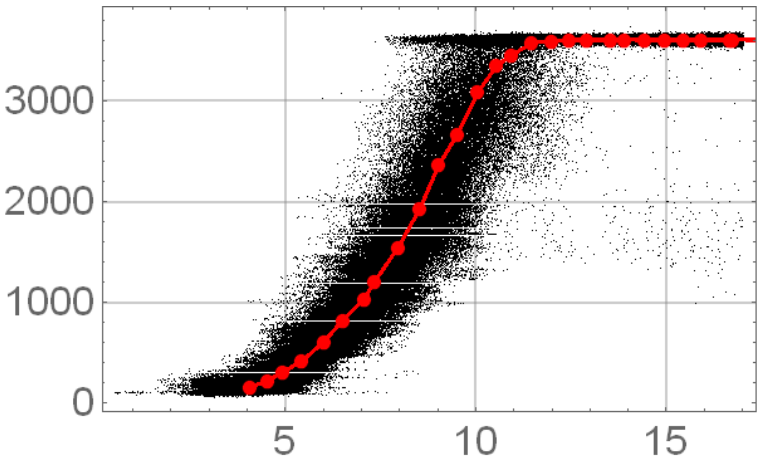


**Figure 22 Power curve scatter plot with 1Hz data from mast and turbine (Black); power curve from bin-averaging of 10 minute mean data (red).**

Before applying the DDA method to the lidar data, the first steps of the Langevin method were applied to the data from the mast and the turbine in order to make a sensitivity analysis of the drift curves to the number of steps to account for to determine the drift coefficient (τ), to the method used to bin the data within the wind speeds bins (power binning) and to the data frequency (e.g. block averaging time).

### 5.3.1 Sensitivity to τ

In this analysis, the drift coefficients were derived with a linear regression on τ time steps after t. τ was varied from 1 to 10. Since 1 Hz data are used in this analysis, one step equals to 1 second. This practically required to store, for each of the time step of the time series, the power values for the 10 following seconds. The data were binned according to the wind speed and power values at time t. The wind speed bins had a fixed size of 0.5 m/s and the power sub-bins a fixed size in the order of 100kW. In each wind speed and power sub bin, the shift in power, $\Delta P(\tau) = P(t + \tau) - P(t)$ , was averaged out for each value of τ from 1 to 10 (see example in Figure 23).

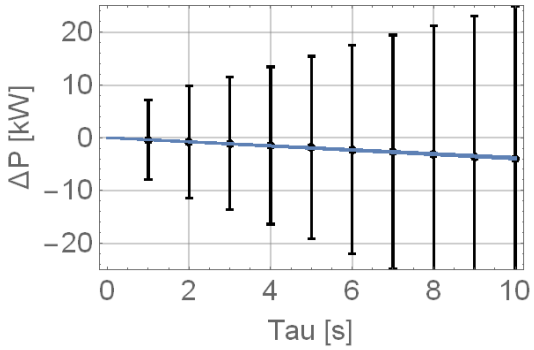


**Figure 23 Power shift as a function of τ (Tau) for the sub-bin 6m/s and 700kW. Dots represent the average value and the error bars represent the standard deviation. Blue lines show the linear regression through the average values for Tau varying from 1 to 10. In this case, the 10 lines are very similar and cannot be distinguished.**

Finally a linear regression, forced through 0, was performed through the N+1 first points (including {0,0}) with N going from 1 to 10. The drift coefficient corresponds to the slope resulting from the linear regression. Figure 24 and Figure 25 show the drift curves obtained for τ varying from 2 to 10, for two different wind speed bins. The drift curves are rather noisy and do not seem to be sensitive to the number of points (τ ) used in the regression.

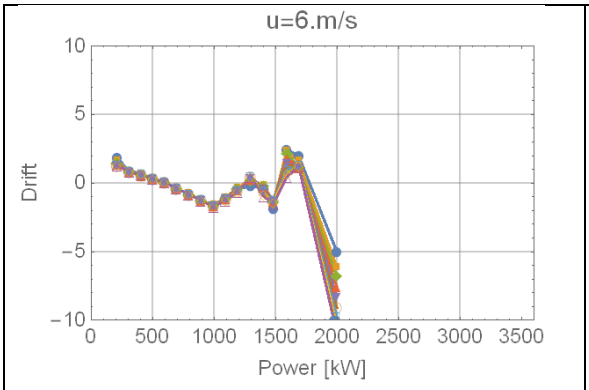


**Figure 24 Drift curves for the wind speed bin 6m/s. The various colours represent various values of Tau.**

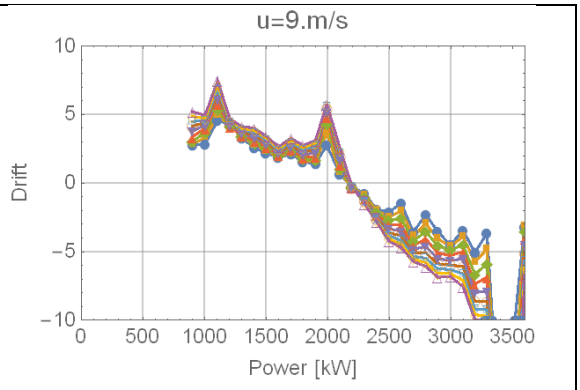


**Figure 25 Drift curves for the wind speed bin 9m/s. The various colours represent various values of Tau.**

τ starts making a difference around 9m/s where the power range is much larger, and therefore so is the drift variation, within the wind speed bin, see Figure 26. Delta P is not as linear for large values of τ, as shown in [13]. In the rest of the analysis we have therefore chosen to use τ =2.

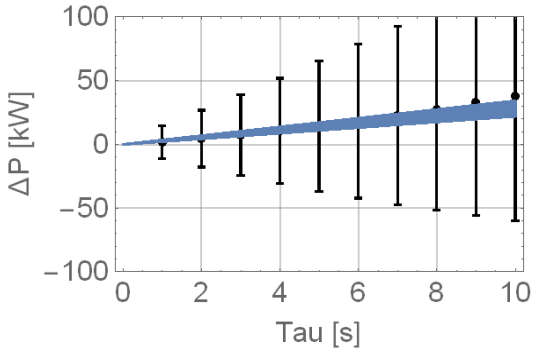


**Figure 26 Power shift as a function of τ for the sub-bin 9m/s and 1500kW. Dots represent the average value and the error bars represent the standard deviation. Blue lines show the linear regression through the average values for Tau varying from 1 to 10.**

### 5.3.2 Sensitivity to power binning

Three different ways of binning the power values were tested and compared:

1. The power sub-bins were given a fixed range of 100kW. In this case the number of data can vary quite a lot from one sub-bin to another.
2. All power sub bins in one wind speed bin counted the same number of data, and that number depends on the number of data in the wind speed bin, and therefore the number of data in the power sub-bins can vary from one wind speed bin to another. In this case, the power sub bin range is variable within the same wind speed bin, it is smaller in the ranges where there are a lot of data, and it is larger in the power ranges counting little data
3. The power sub bins were given fixed number of data points of 200. In this case as well, the range of the sub bin is variable.

The number of data in every sub bin is shown in Figure 27 for the three binning method.

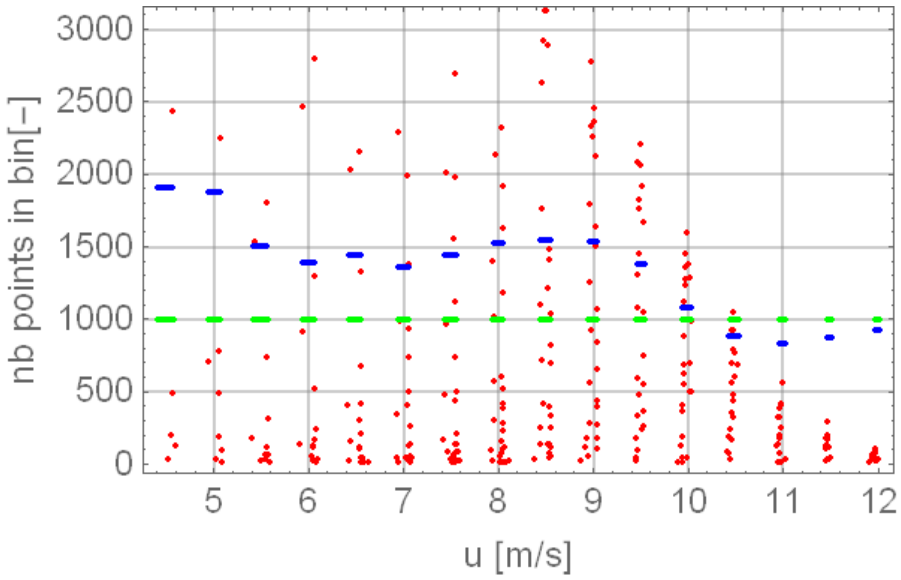


**Figure 27 Number of data in every sub-bin as a function of the mean wind speed in the sub bin. Sub bin size defined by maximum range of 100kW (Red); Sub bin size defined by a constant number of data in all sub bins in the same wind speed bin (blue), sub bin size defined by 200 data points/sub bin (green).**

Figure 28 and Figure 29 show the drift curves obtained with the 3 different binning methods for two different wind speed bins. Methods 2 and 3 provide more points around 0, but the drift curves are also noisier than that obtained with Method 1. A fixed point should therefore be easier to determine with method 1. Moreover, it makes more sense to derive drifts coefficient for bins that are limited in range. Indeed the drift coefficient is expected to vary as we move away from the fixed point. If bins with very large range are allowed, the variations in drift coefficient may be blended and the extracted drift for a large power sub bin might not be representative. Finally, the risk of binning with a fixed range is to have large variation in number of data per bin, and having some bins with very few data points. However more data points are expected around the fixed points, which should make the drift curve reliable around the fixed points even with a fixed sub-bin range.

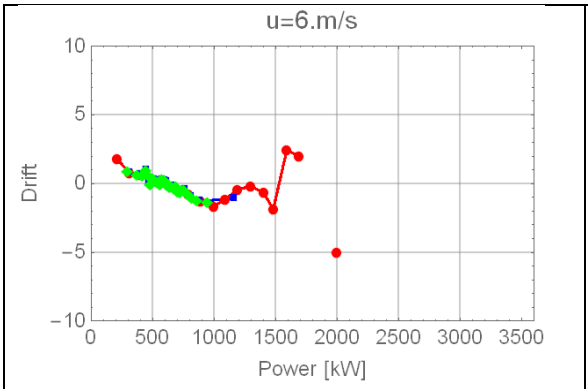


**Figure 28 Drift curves obtained with 1Hz data in wind speed bin 6m/s and for the methods to make the power sub-bins (same colour code as Figure 26)**

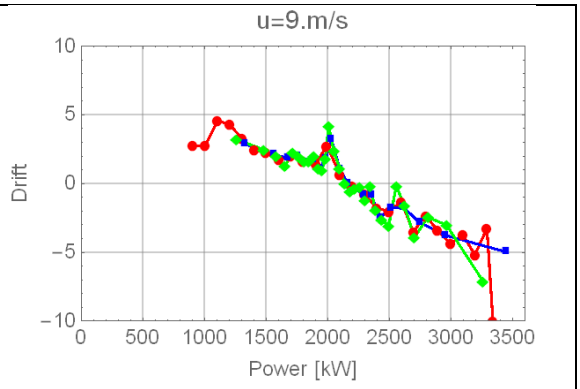


**Figure 29 Drift curves obtained with 1Hz data in wind speed bin 9m/s and for the methods to make the power sub-bins (same colour code as Figure 26)**

### 5.3.3 Sensitivity to averaging

Finally the 1Hz data were block-averaged over 2s (0.5Hz) and 5s (0.2 Hz) periods. For each of the 3 datasets, the data were binned in wind speed bins with a fixed range of 0.5m/s and in power with a fixed range of 100kW. For each sub-bin the drift coefficient was derived by linear fitting using $\tau = 2$ (i.e. considering only one time step after the considered time t). Note though that the unit time step is by definition of different lengths for the three datasets: 1s, 2s and 5s respectively).

Figure 30 shows the resulting drift curves for the 3 datasets, for 6 different wind speed bins. The slope of the drift curve increases as the averaging time increases and this appears more and more clearly as the wind speed increases. It is interesting to observe that the drift curves obtained with the three datasets cross 0 around very similar power values. It therefore seems that the fixed points are not very sensitive to the averaging time but they are easier to identify for larger averaging time.

It can also be noted that in Figure 30, power sub-bins counting less than 50 points were removed. This smoothed out the drift curves quite significantly (usually discarding bins away from the fixed point) however the drift curves are still rather noisy and sometimes cross 0 several times. Multiple fixed points are possible but in the case of the 8m/s wind speed bin, it rather looks like the results of outliers. More than 50 points per sub-bins are probably required to have reliable drift coefficients.

The drift curves obtained from the 0.2Hz dataset were linearly interpolated and the fixed points were derived as the smallest power value for which the drift curve crossed 0 (i.e. only one fixed point per bin was allowed). The fixed points are shown in Figure 31 together with the IEC power curve (see section 5.2). The two curves are rather similar.

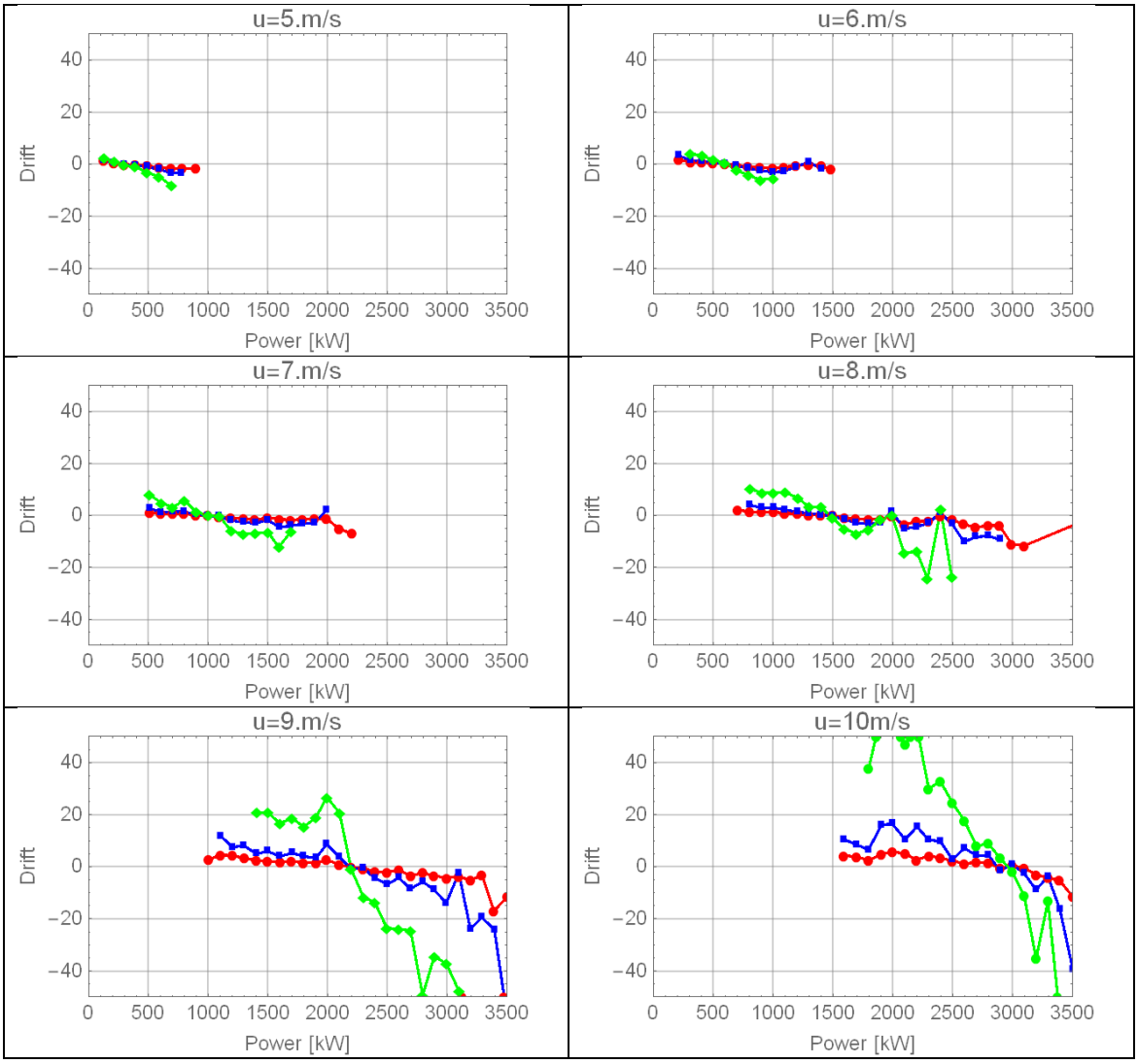


**Figure 30 Drift curves for 6 wind speed bins obtained with three different averaging time; Red: 1s; Blue:2s; Green: 5s (only shown for every second bin between 5 and 10 m/s). Bins counting less than 50 points were discarded.**

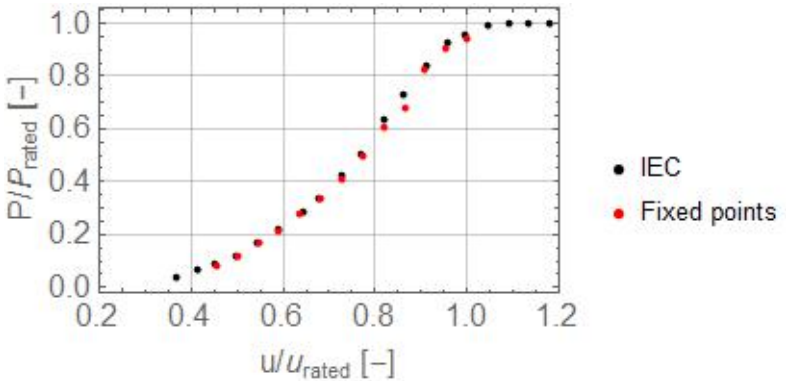


**Figure 31 Fixed points obtained with 0.2Hz dataset and IEC power curve.**

## 5.4 Derivation of the drift curves and fixed points to the nacelle lidar data

### 5.4.1 Lidar data

The lidar used in this measurement campaign was a 2-beam nacelle lidar prototype from Avent Lidar technology (see more details in [17]). A stream of pulses is emitted on each line-of-sight alternatively. The horizontal wind speed is reconstructed from two consecutive radial wind speed measurement along the two line-of-sights.

The lidar system own signal processing was supposed to remove the radial wind speed measurements when the CNR was below a certain threshold indicating that the laser beam had been blocked by one of the blade and could not return a reliable signal. Horizontal wind speed values were therefore not available for every second (this lidar prototype did not provide horizontal wind speed regularly contrary to a cup anemometer that is sampled with a given frequency, e.g. 10 Hz. When the blades do not block the beam significantely, the lidar normally provides values every 0.5 second. But due to the beam blacakge by the blades, horizontal wind speed values are available irregularly.) it was therefore chosen as a compromise to the lidar measurement characteristics and the results from the previous sensitivity analysis to average down the lidar horizontal wind speed over 5 seconds. Figure 32 shows the comparison of those lidar wind speeds to the 5 second block averaged wind speed from h the cup anemometer. On average, the lidar wind speed is close to the cup anemometer wind speed (also found in [17]) but the scatter is rather large. This may be due to several reasons:

- The cup anemometer is sampled at 10Hz whereas the lidar 5 second averaged wind speed can result from 1 to 10 horizontal values;
- The lidar always measures upstream whaile the mast measures at a fixed position;
- The lidar measures over a volume of about 67m (distance between the 2 beams) X 60m (range gate length)X a few centimeters (beam width);
- The lidar beam heights varies with the turbine nacelle tilting (see [17]);
- The lidar reconstruction algorithm assumes horizontal homogeneity (i.e. that the wind speed sensed by both beams is identical) which is of course not true instantaneously. (The instantaneous deviations however average out when we consider 10 minute mean wind speed, therefore resulting in a good comparison with the cup anemometer wind speed.)

Figure 33 and Figure 34 show the power curve scatter plot obtained with the 5 second blocked averaged data from the cup anemometer and from the lidar respectively. The two figures result from simultaneous datasets. The scatter is smaller in Figure 34 than in Figure 33. It might mean that the fact that the lidar measures upstream, and therefore the lidar wind speed has a higher correlation with the wind at the turbine, than the cup anemometer measuring at a fixed position (independently of the wind direction and therefore not always measuring the wind speed upstream of the turbine) has a greater impact than the lidar measurements features, like the measurement over a volume, etc.

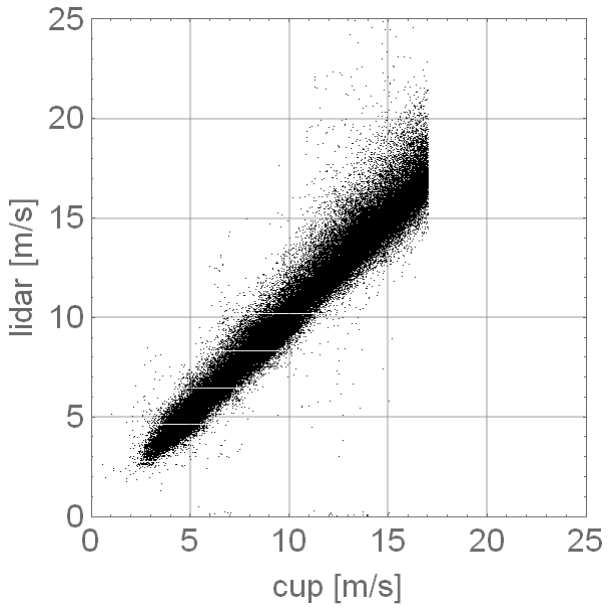


**Figure 32 Five second block averaged wind speed from the 2 beam lidar vs cup anemometer (In order to fasten the calculation, data with a cup anemometer wind speed above 17 m/s were not considered here. This has no significant consequence on the analysis since it way beyond rated wind speed).**

On the other hand, the lidar is sometime providing erroneous wind speed values as for example we can observe points at rated power with wind speed below 0.8 rated wind speed in Figure 34. There was not obvious explanation for those points. However since they are clearly wrong wind speed values the dataset (including both lidar and cup anemometer wind speeds) was filtered so that:

1. So that lidar wind speeds were larger than 3m/s;
2. And points with a power above 97.2% of rated power and a lidar wind speed below 82% of rated wind speeds were discarded.

The rest of the analysis is still done on concurrent measurements of the cup anemometer and the lidar.

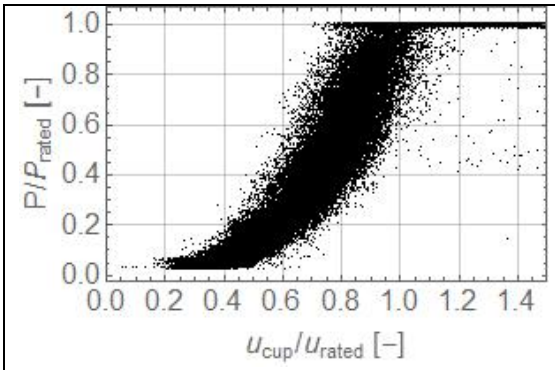


**Figure 33 Power curve scatter plot with 5s averaged cup anemometer wind speed**

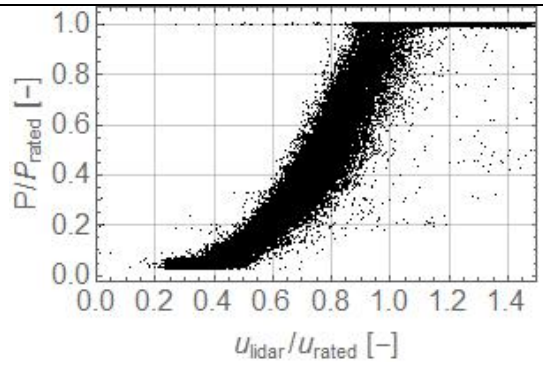


**Figure 34 Power curve scatter plot with 5s averaged lidar horizontal wind speed**

### 5.4.2 Application of Langevin method to the lidar data

For each dataset, the data were binned in wind speed bins with a fixed range of 0.5m/s and in power with a fixed range of 100kW. For each sub-bin the drift coefficient was derived by linear fitting using $\tau = 2$ (i.e. considering only one time step after the considered time t). Figure 35 shows the resulting drift curves for the 3 datasets, for 6 different wind speed bins. The average slope of the drift curves is larger for the lidar than for the cup anemometer. This might be due to the better correlation between the lidar wind speed measurement and the turbine power time series because the lidar always measures upstream.

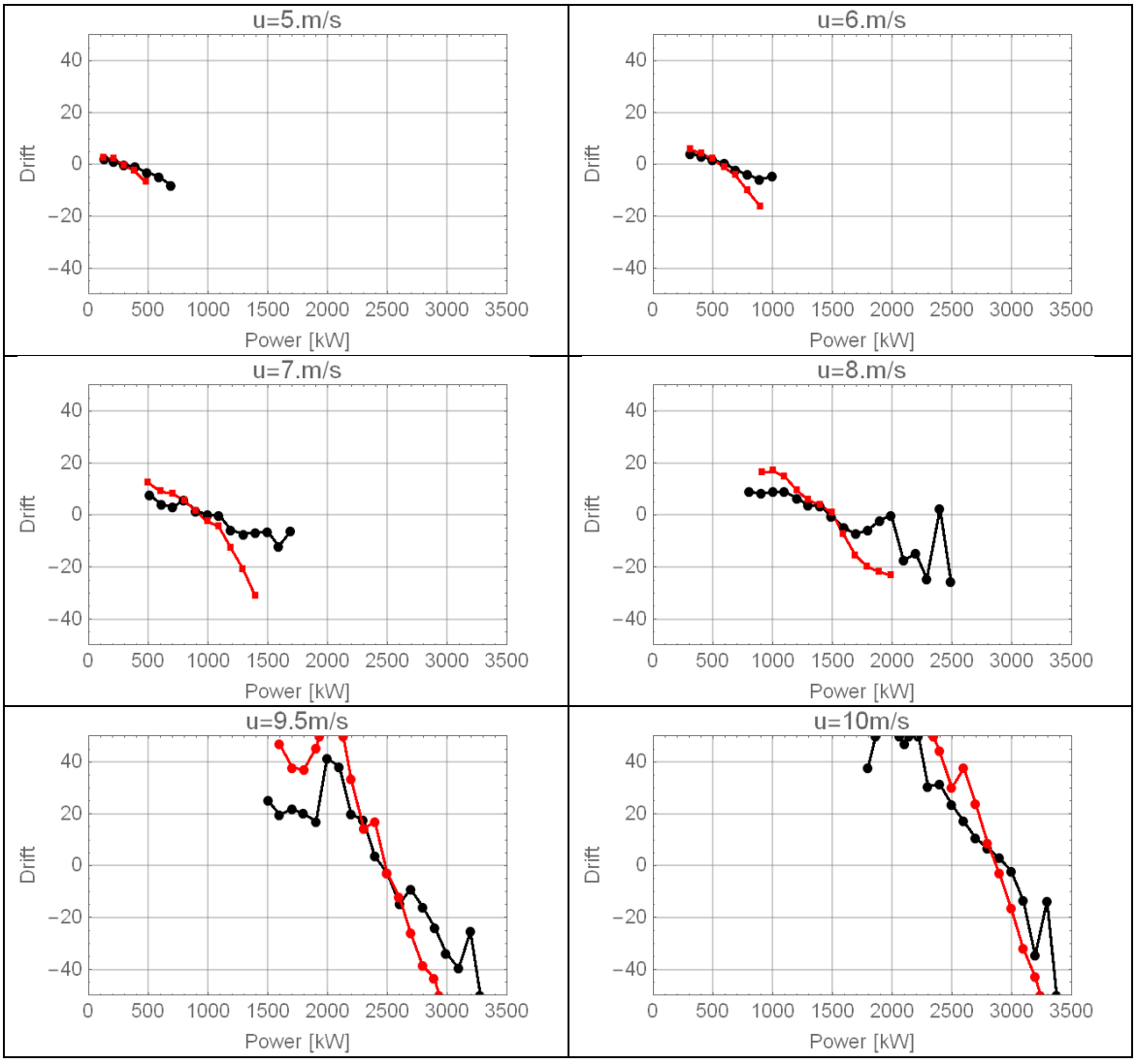


**Figure 35 Drift curves for 6 wind speed bins; Black: cup anemometer; Red: Lidar. Bins counting less than 50 points were discarded.**

The drift curves were linearly interpolated and the fixed points were derived as the smallest power value for which the drift curve crossed 0 (i.e. only one fixed point per bin was allowed). The fixed points are shown in Figure 36 together with the IEC power curve.

The fixed points obtained with the two instruments are rather similar, except around 77% of rated speed.

For most wind speed bins, the drift curves obtained with the two instruments cross 0 for very similar power values (see Figure 35). However for 77% of rated speed, as shown in Figure 37, the drift curve derived from the cup anemometer data shows a strange behaviour as it almost reaches 0 around 49% of rated power (where the lidar drift curve actually crosses 0) but then it increses again and decreses again and finally crosses 0 around 56% of rated power.

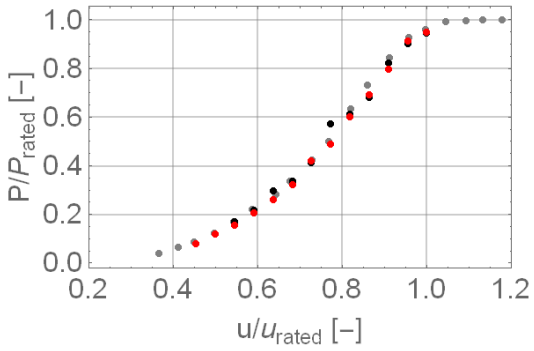


**Figure 36 Fixed points for the cup anemometer (black) and for the lidar (red) and IEC power curve (gray).**

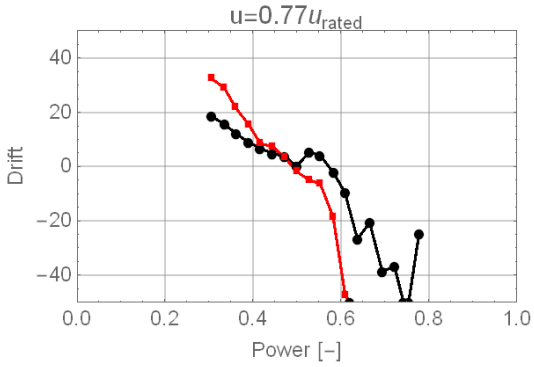


**Figure 37 Drift curves for wind speed bin 77% of rated speed; Black: cup anemometer; Red: Lidar. Bins counting less than 50 points were discarded.**

# 6. Dynamic data analysis on 2MW pitch-regulated wind turbine

Dynamic data analysis was analysed on a 2MW size pitch-regulated wind turbine. Wind speed, wind direction, air temperature and air pressure were measured on a nearby mast. On the turbine the electric power and the nacelle wind speed and spinner anemometer wind speed were monitored. Data were measured for a time period of five month. Data were organized with three different averaging times:10min, 30sec and 1Hz. The different power curve analysis results were related to an ordinary IEC power curve based on mast wind speeds with 10min averaging time, using data from the whole period but filtered for a free measurement sector of 40°. In the following only power curves measured with the spinner anemometer are considered. Objectives are to evaluate the Langevin method and not absolute or relative power curves. In this relation the spinner anemometer has an advantage compared to mast wind speed measurements or nacelle wind speed measurements. The spinner anemometer has a high cross-correlation with power so there is no time lap between measurement of wind speed and power. The spinner anemometer is also not disturbed by blade wakes as it is placed in front of the blades.

## 6.1 Power curve based on 10min averages and IEC binning

The five month of 10min data were sorted for the free sector of 40° leaving 1970 datasets for the power curve. The wind speeds were normalized to standard air density 1.225kg/$m^3$. The data were binned with 0.5m/s wind speed bins and the power curve is shown in Figure 38.

The power curve with the spinner anemometer and 10min data shows a rather narrow band of power which indicates a good correlation of measured wind speed with power. This is expected because the spinner anemometer measures the power in the centre of the rotor. However, the 10min averaging is smoothing the power curve at cut-in and at wind speeds just before nominal power is reached.

In addition to the power curve based on the five month of data a shorter database of 14 days of data was analysed but only 282 10 min datasets remained. This period is not enough for an IEC power curve but it covered the whole range of wind speeds of the power curve from cut-in to 20m/s. The data should be sufficient to cover the expected required amount of data for fast power curves with dynamic data analysis. The 10min average power curve for the 14 days period is shown in Figure 39.

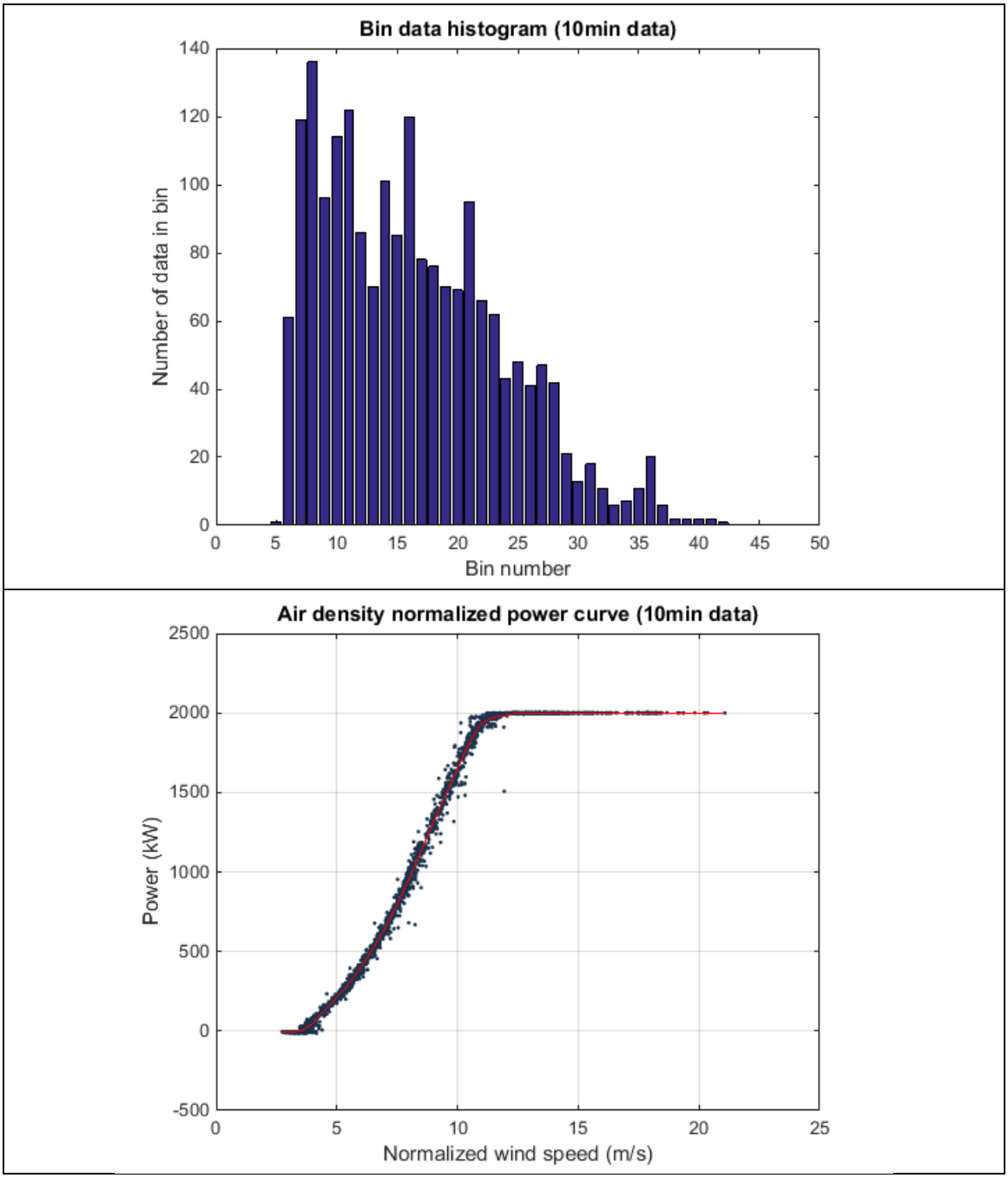


**Figure 38 IEC power curve of 2MW wind turbine based on spinner anemometer and 10min data for a five month period (1970 datasets)**

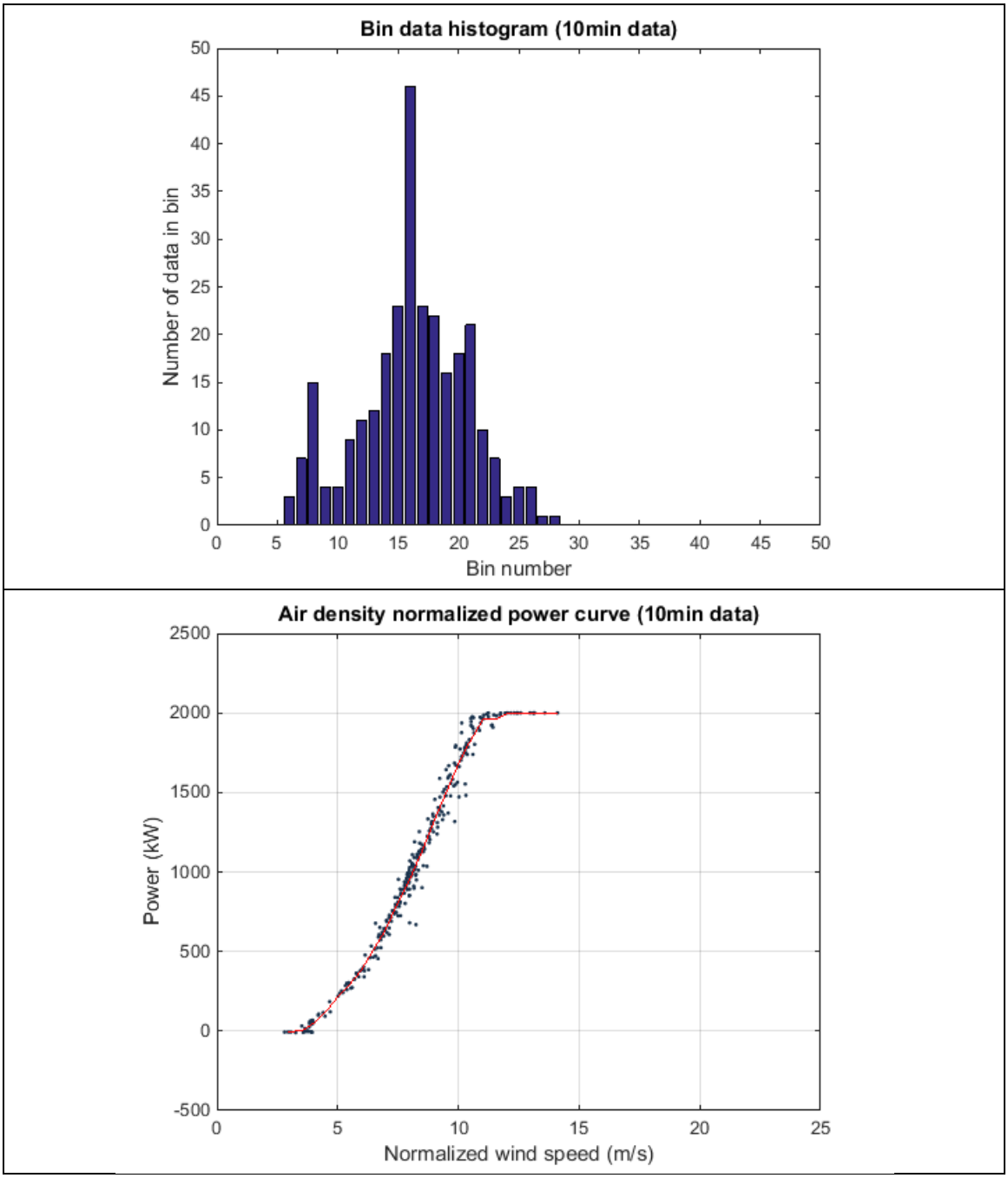


**Figure 39 IEC power curve of 2MW wind turbine based on spinner anemometer and 10min data for a 14 days period (282 datasets)**

## 6.2 Power curve based on 30sec averages and IEC binning

The five month of 30sec data were sorted for the same free sector of 40° leaving 41688 datasets for the power curve. The wind speeds were normalized to standard air density 1.225kg/m$^3$. The data were binned with 0.5m/s wind speed bins and the power curve is shown in Figure 40.

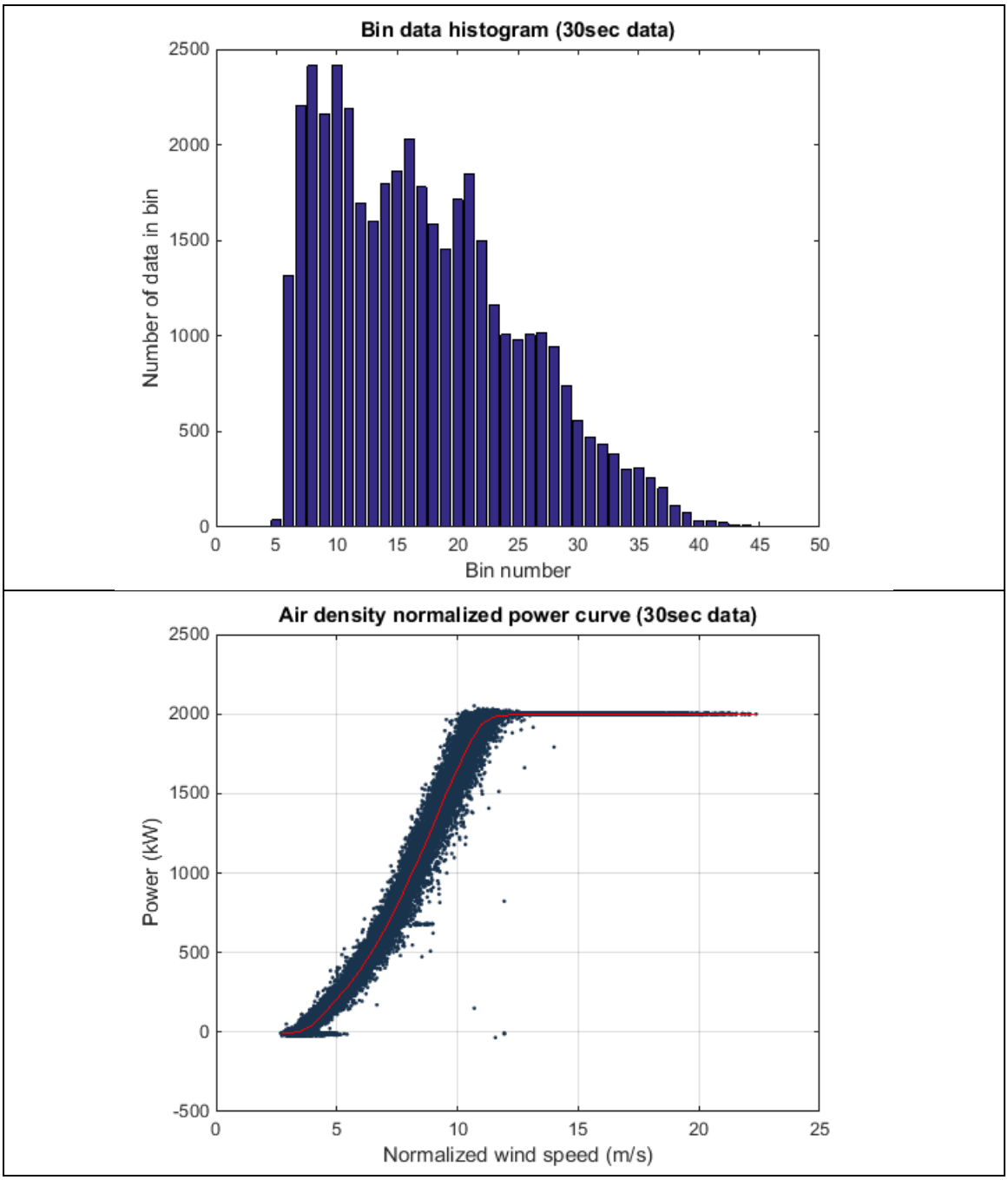


**Figure 40 Power curve of 2MW wind turbine based on spinner anemometer and 30sec data for a five month period (41688 datasets)**

The power curve for the shorter 12 days measurement period is shown in Figure 41 with 6275 datasets.

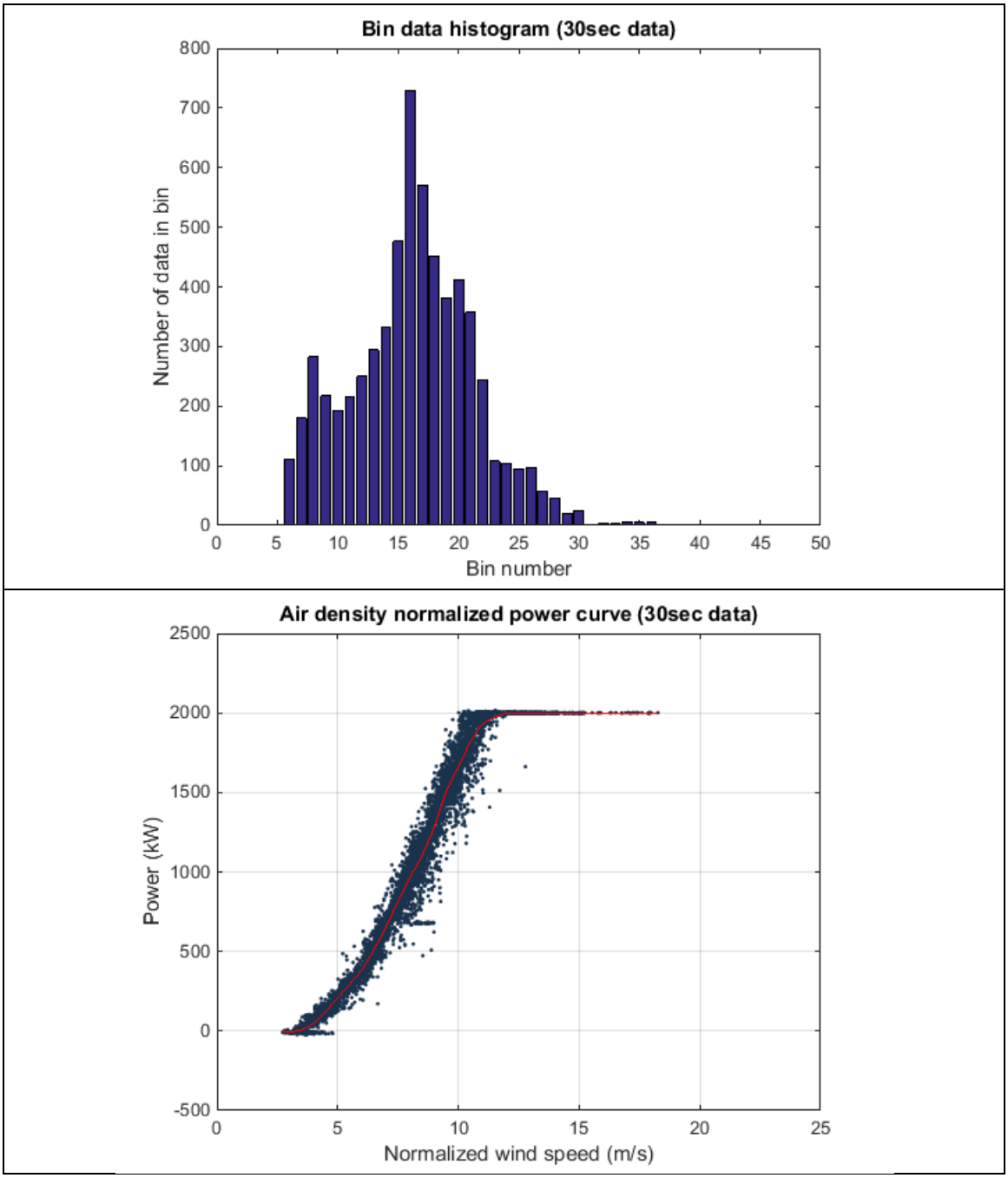


**Figure 41 Power curve of 2MW wind turbine based on spinner anemometer and 30sec data for a 14 days period (6275 datasets)**

## 6.3 Power curves based on 1 sec samples and IEC binning

For the 1 sec sampled data only the 12 day period was selected. The raw data are shown in Figure 42. The air density during the measurement period is shown in Figure 43. A histogram of the data for each wind speed bin and an air density normalized power curve using method of bins is shown in Figure 44.

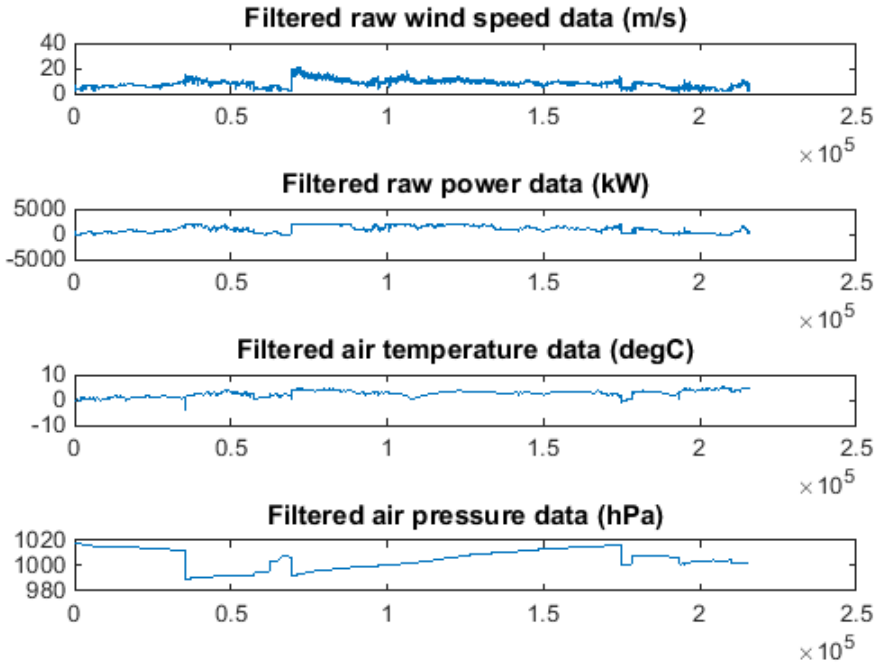


**Figure 42 1Hz raw data for 14 days period (sector filtered down to 2.5 days)**

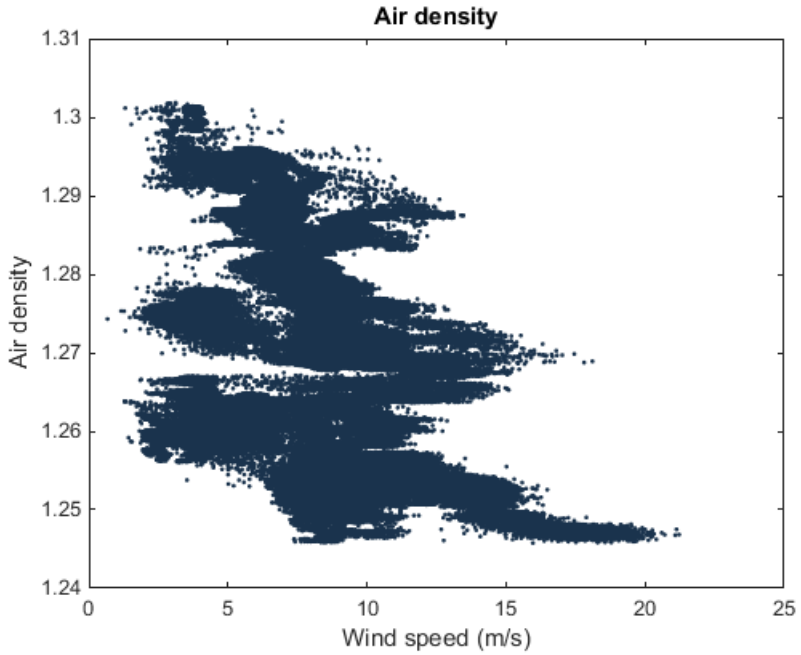


**Figure 43 Air density as function of wind speed for 1Hz data**

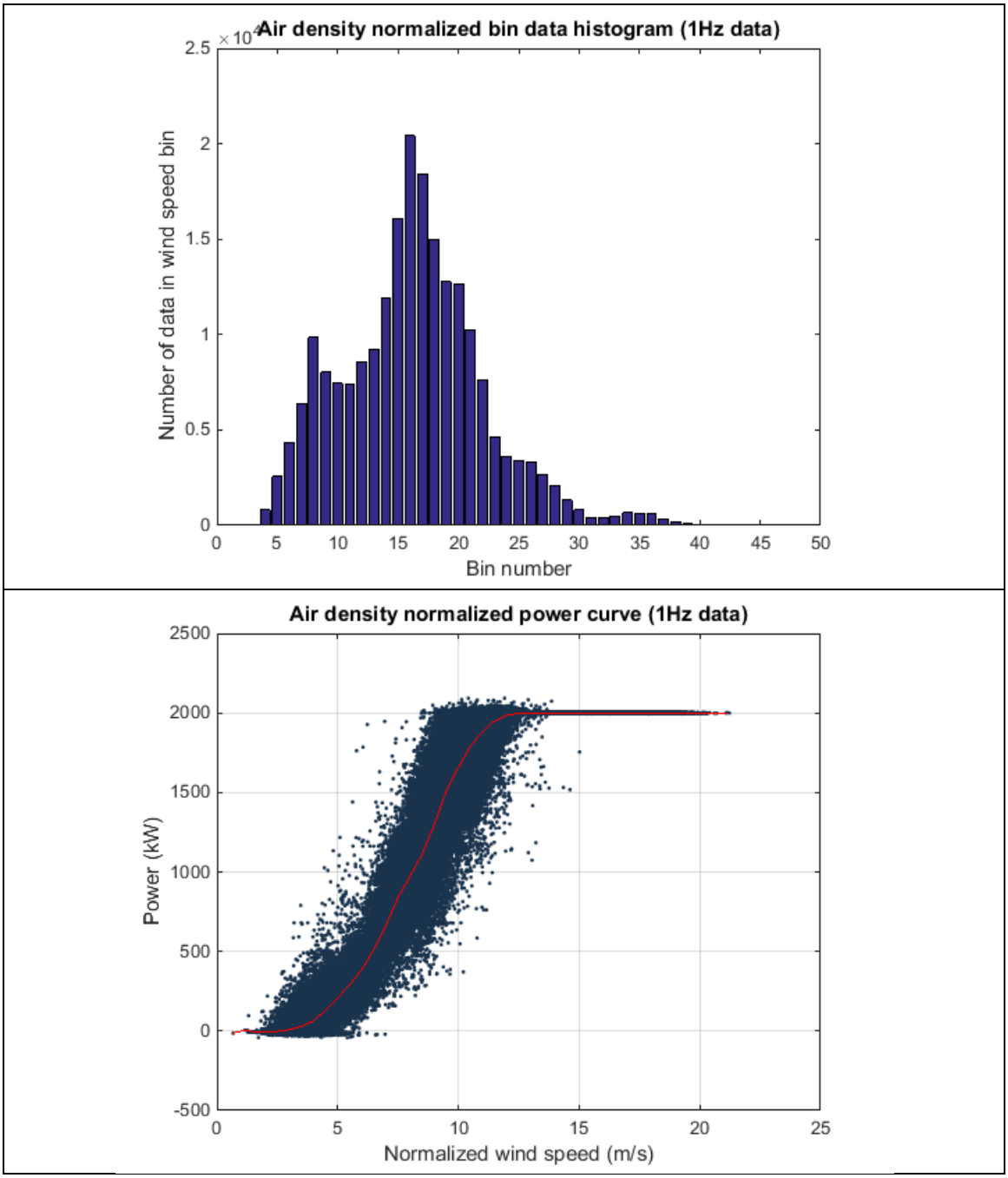


**Figure 44 Power curve of 2MW wind turbine based on spinner anemometer and 1 Hz data for a 14 days period (215708 datasets)**

The power curve based on 10 min averaged data do comply well with the power curve based on 30 sec averaged data. However, the power curve based on 1 sec data deviates from the other two in that the power curve is smoothened in both ends. This effect is opposite to the effects seen on mast measurements where the cross correlations of wind speeds and power is significantly lower. The reason for the 1 sec data to achieve this effect is due to a combination of the high spreading of wind data and the method of bins when coming close to the rooftop nominal power.

## 6.4 Power curves based on 1 sec samples and Langevin method

The same 1Hz sampled data for the 14 days period were analyzed with the Langevin method. The raw data are shown in the previous chapter with the same wind speed bin data histogram. For the Langevin power curve analysis the maximum power was set to 2500kW. The number of bins was set to 50 with each bin being 50kW in size. The amount of data per wind speed and power bin is shown in Figure 45. The drift field was calculated with a time steps of 2, corresponding to 2 seconds and only bins with more than 10 data were included. The drift field is shown in Figure 46.

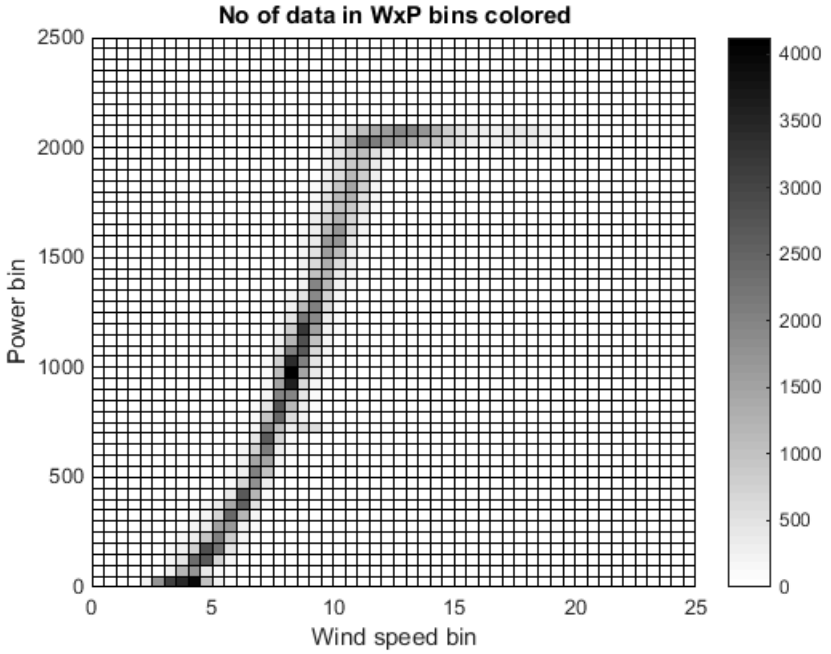


**Figure 45 Amount of data per wind speed and power bin for the Langevin analysis**

For each wind speed bin the drift per power was plotted (see annex B). A linear regression was made, and the power for the drift equal to zero was found. The resultant Langevin power curve is shown in Figure 47. In order to analyse the sensitivity to parameter settings the amount of power bins was reduced from 50 to 48. The result is shown in Figure 48. In Figure 49 the required amount of data for each power bin was set to 500 instead of 10. The power curves are seen to be significantly sensitive to these parameter changes.

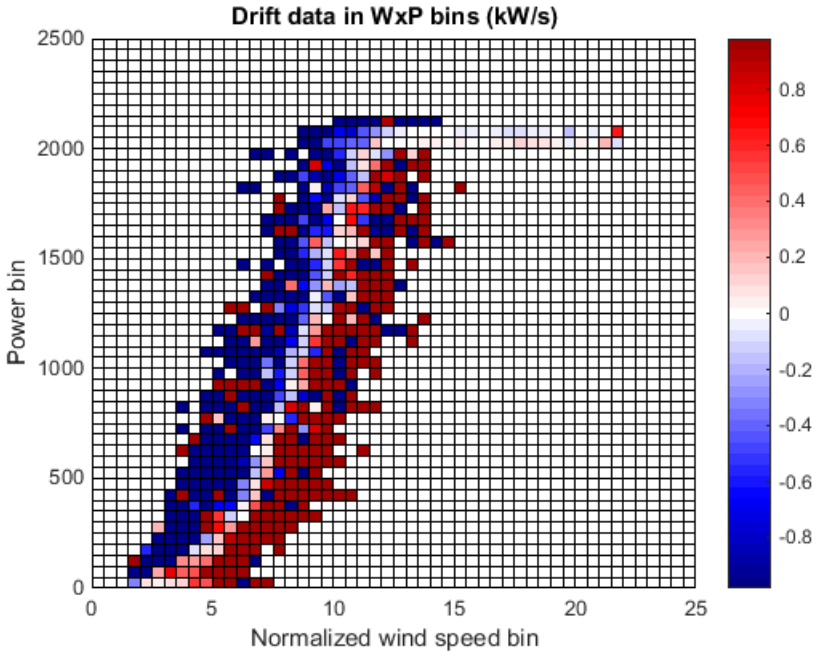


**Figure 46 Average drift for each wind speed and power bin for the Langevin analysis**

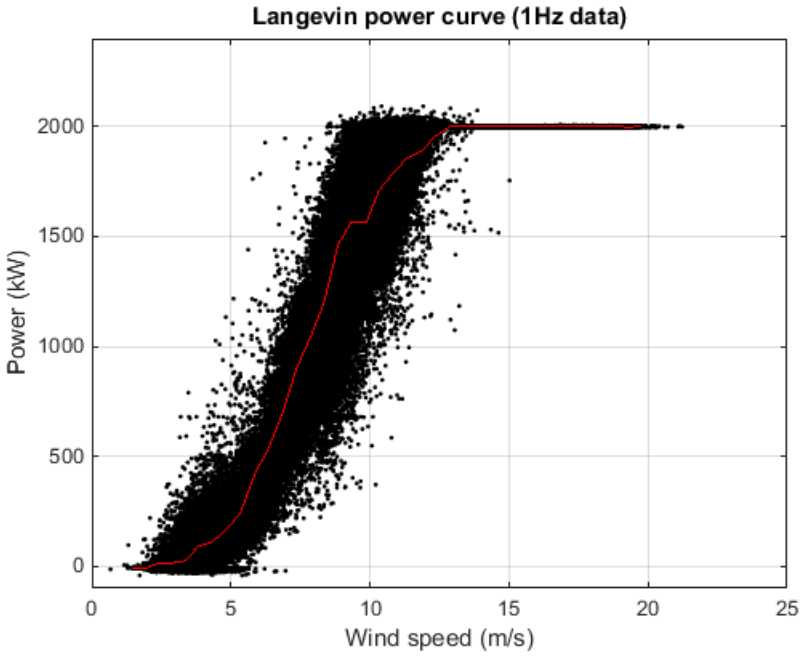


**Figure 47 Langevin power curve of 2MW wind turbine based on spinner anemometer and 1 Hz data for a 14 days period (215708 datasets) and with 50kW power bins with at least 10 points per bin and linear fit of drift to power**

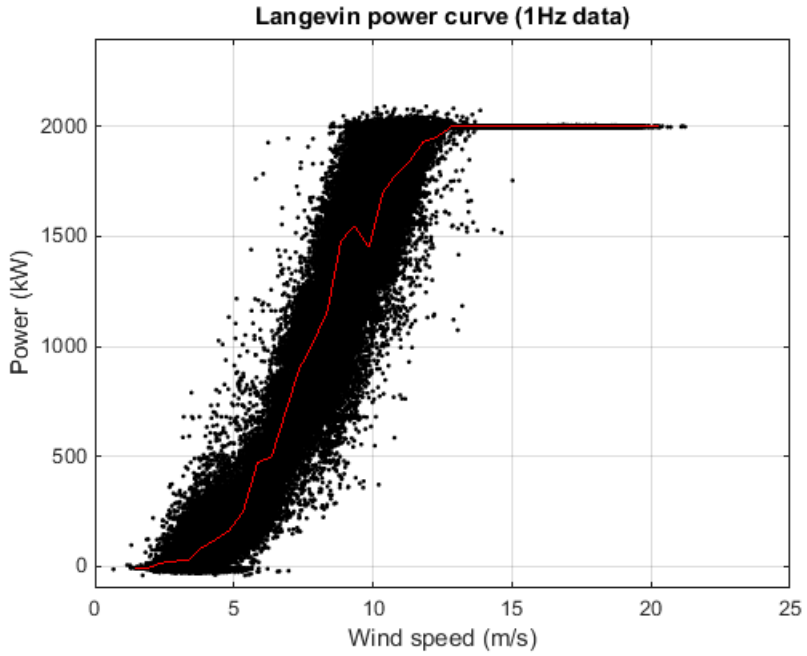


**Figure 48 Langevin power curve of 2MW wind turbine based on spinner anemometer and 1 Hz data for a 14 days period (215708 datasets) and with 48kW power bins with at least 10 points per bin and linear fit of drift to power**

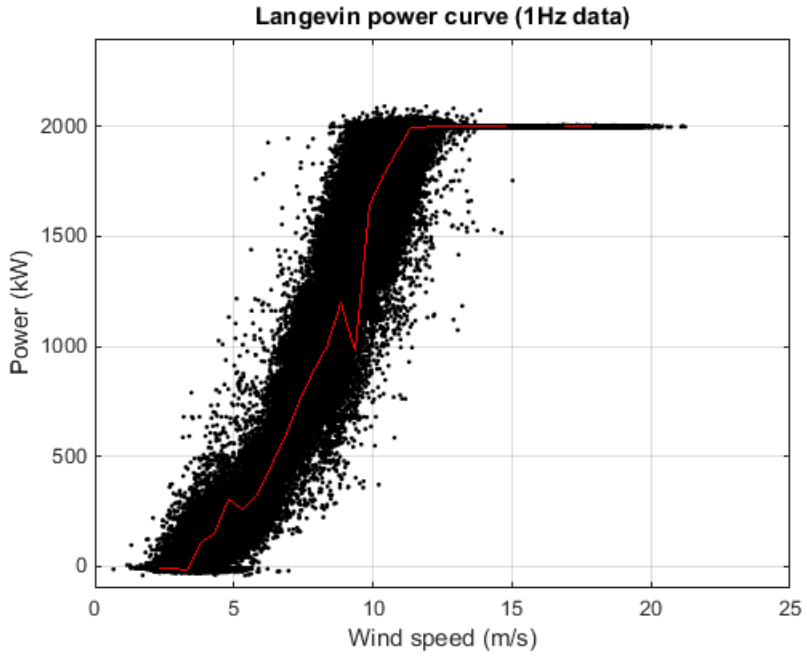


**Figure 49 Langevin power curve of 2MW wind turbine based on spinner anemometer and 1 Hz data for a 14 days period (215708 datasets) and with 50kW power bins with at least 500 points per bin and linear fit of drift to power**

## 6.5 Comparison of power curves based on different methods

In the following the power curves are compared. The averaging times of the data, the measurement period and the simple binning and averaging is compared to the Langevin method using 1Hz data.

The 5 month period of measurements resulted in 1970 10min datasets corresponding to 328 hours or effectively 13.7 days of data in the free measurement sector. The measurement time and the effective database for the different averaging times are shown in Table 1. It should be mentioned that the measurement sector is only 40° in the prevailing wind sector. From the table it is seen that the time for the effective measurement database is significantly smaller (a factor of 6-10) than the whole measurement time.

**Table 1 Effective measurement database from measurements in the Tjæreborg wind farm. Number of datasets are related to the amount of hours and days**

| Total measurement time | 5 month | 14 days |
|---|---|---|
| 10min averaging | 1970 ~ 328.3h ~ 13.7days | 282 ~ 47.0h ~ 1.96days |
| 30sec averaging | 41688 ~ 347.4h ~ 14.5days | 6275 ~ 52.3h ~ 2.18days |
| 1sec averaging | | 215708 ~ 59.9h ~ 2.50days |

Measurements with 10min averages for periods of 5 month and 14 days are compared in Figure 50. The data seem to compare quite well. The same quite good comparison is seen for 30sec averages in Figure 51. The same can be said about the comparison of 10min and 30sec data for the 5 month period, Figure 52, and the 14 days period, Figure 53. However, for the 14 days period differences starts to be seen at about nominal power and this is due to the limited amount of data for the 10min average power curve which was 282 datasets corresponding to 47 hours of data in the filtered sector. For the 14days period, Figure 54, the 30sec and 1sec data shows smooth curves but for the 1sec data the power curve is smoothed out at the upper and lower ends. This is surprising because we would normally expect this behavior for longer time averages because the unlinear power is averaged over a larger wind speed interval. The same is seen when comparing 10min averages over 5 month with 1sec averages over 14 days, Figure 55.

The Langevin power curves based on 1sec averages and 14days compared with 10min averages over 5 month or 1sec averages over 14 days are shown in Figure 56 and Figure 57. The Langevin power curves do not compare well with neither the 10min power curve or the 1sec power curve.

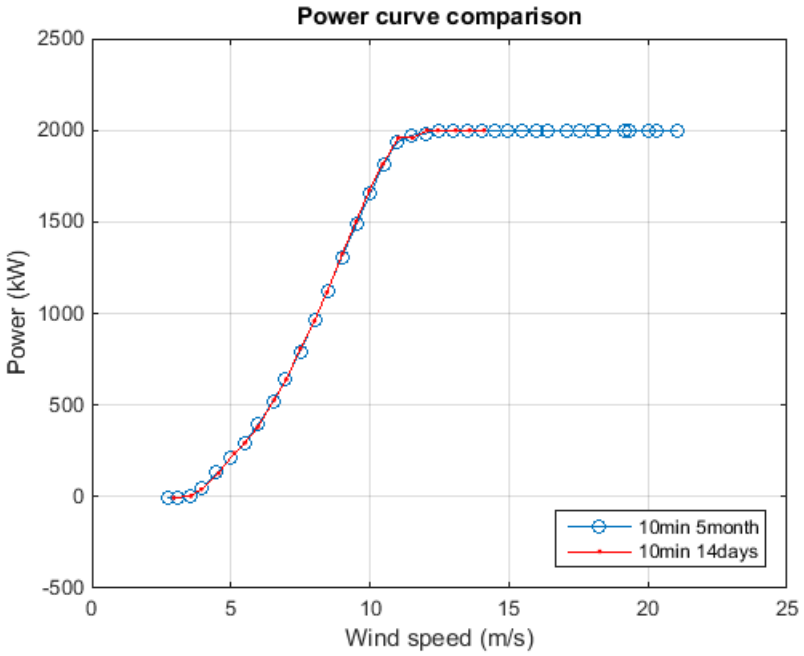


**Figure 50 Comparison of 10min average power curves over 5 month and 14 days**

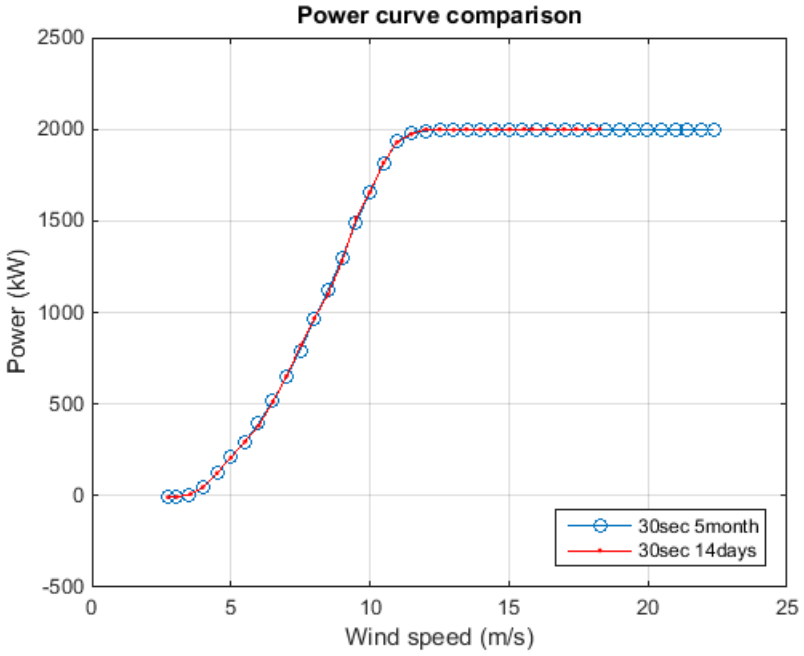


**Figure 51 Comparison of 30sec average power curves over 5 month and 14 days**

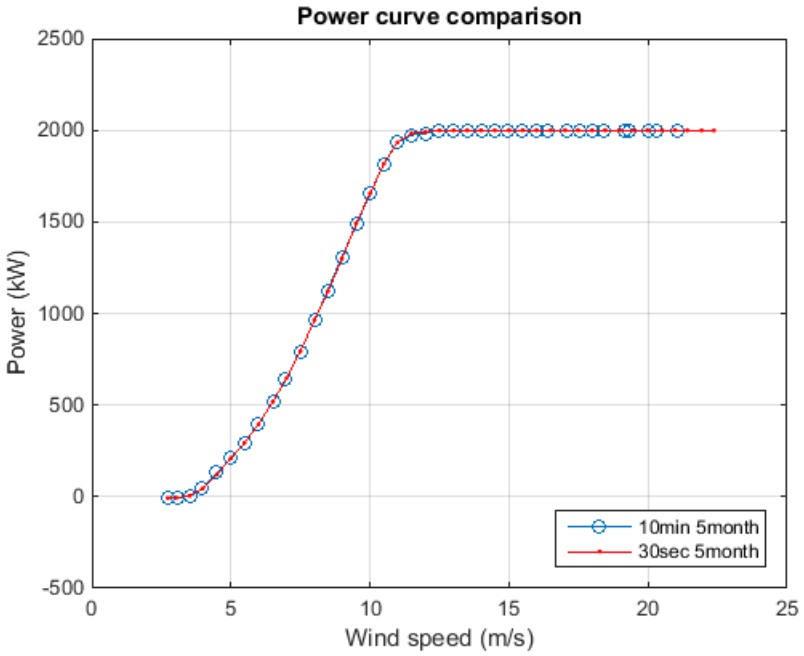


**Figure 52 Comparison of 10min average power curve over 5 month with 30sec power curve over 14 days**

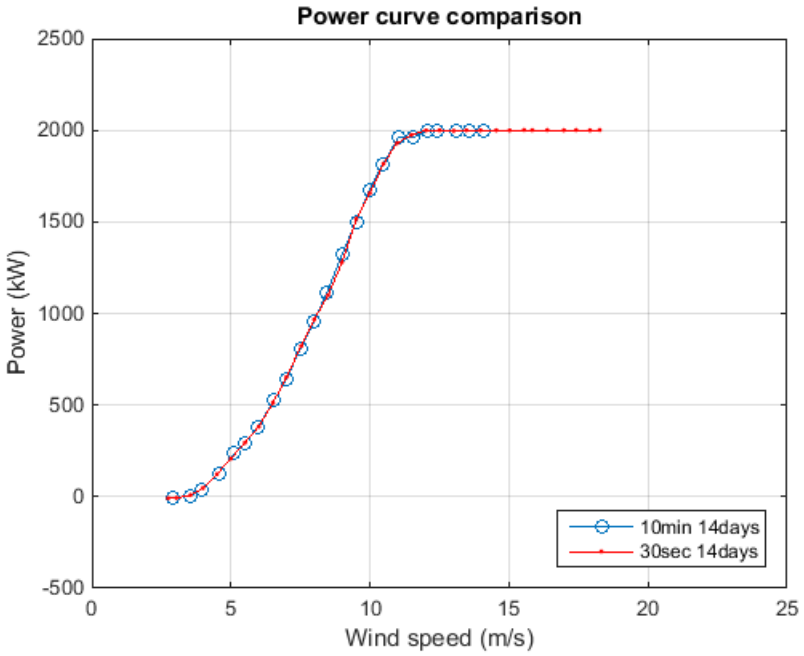


**Figure 53 Comparison of 10min average power curve with 30sec power curve over 14 days**

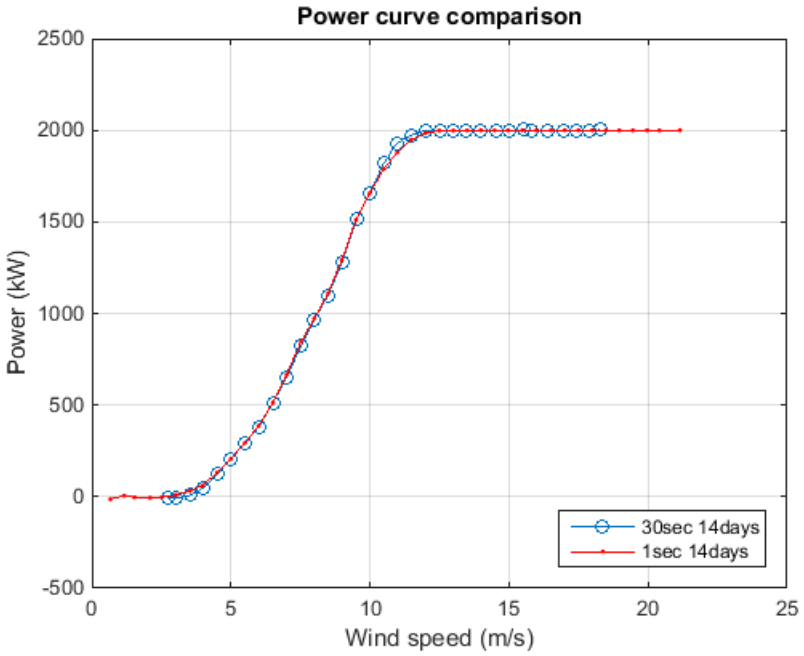


**Figure 54 Comparison of 30sec average power curve and 1sec power curve over 14 days**

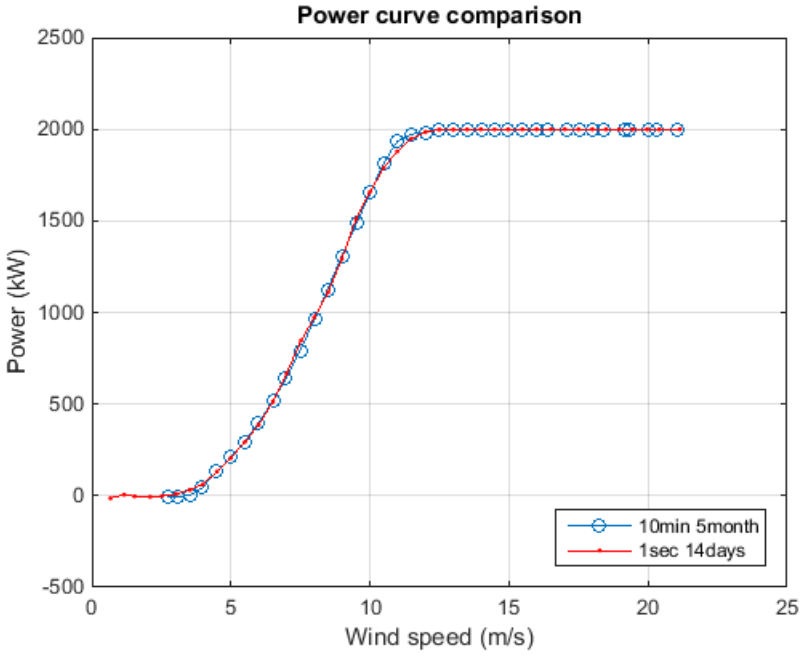


**Figure 55 Comparison of 10min average power curve over 5 month with 1sec power curve over 14 days**

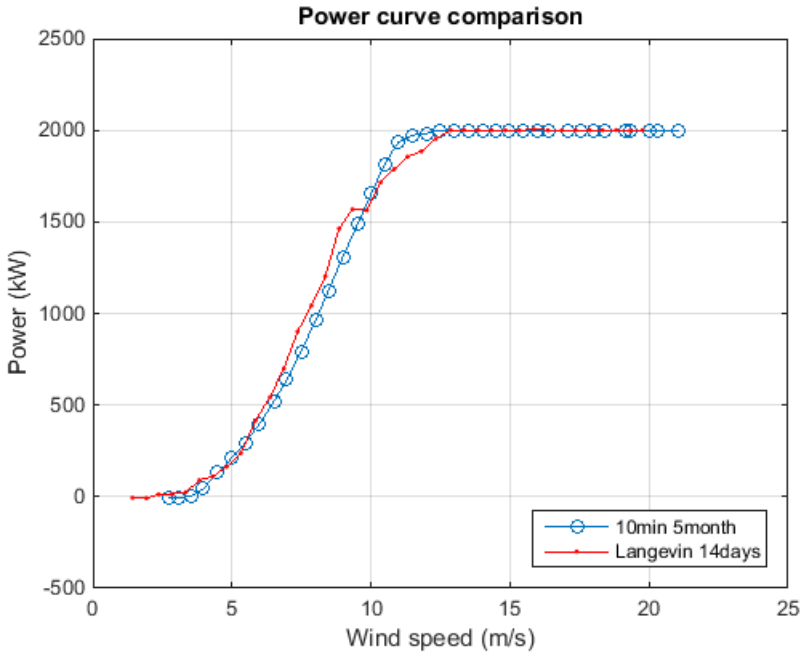


**Figure 56 Comparison of Langevin power curve over 14 days with 10min average power curve over 5 month**

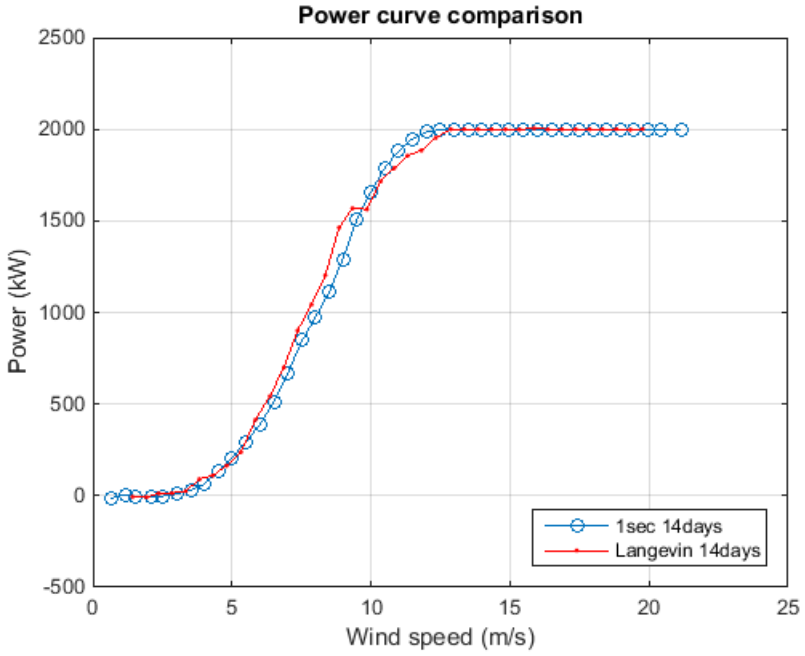


**Figure 57 Comparison of Langevin power curve over 14 days with 1sec average power curve over 14 days**

# 7. Discussion on dynamic data analysis

## 7.1 Power curve determination

The main objective of using dynamic data analysis was to make power curves faster than the IEC standard method. The idea was to use shorter time averaged data that generated a larger database. In this analysis different averaging times used on the same basic measurement database has been considered. In using the simple wind speed binning of 0.5m/s bins from the IEC standard and averaging the power and wind speeds for each bin the power curves made from different averaging times and varying measurement periods has been compared. Also different measurement principles have been analysed. Traditional mast measurements, lidar measurements and spinner anemometer measurements have been used on different types of wind turbines. The variability of methods and datasets should therefore comprise a sufficient database to evaluate applicability and robustness of the methods used.

The Langevin method has been developed and investigated by several authors from a theoretical point of view prior to this analysis. The results of the developments and investigations promised a method that could be used to make faster power curves. In this project the Langevin method, as proposed in several articles, was investigated in detail. The method was described in a few steps necessary to apply the method on a dataset, and the method was used on several datasets.

The steps for application of the Langevin method itself reveal a number of subjective issues that already reduces simplicity and robustness compared to the simple IEC procedure. In the Langevin method the power is also sorted into bins which is a further complication compared to the IEC method. In the analysis using the spinner anemometer the power bin size has a substantial influence on the results, even for a small difference. A change of bin size from 50kW to 48kW made a significant change on the result as shown in Figure 47 and Figure 48. The drift in each bin is also varying a lot. The method implies that the differential of the power with the wind speed is used to generate the drift field. Several authors have used different methods to derive the drift field but no consensus can be extracted from the literature. The amount of data in each wind speed and power bin is not described either. Some authors recommend numbers. A recent author recommends 600 data for each bin but more than 2400 for bins close to nominal power. These recommendations are close to the database requirements in the IEC standard. The fact that if the time necessary to gather the measurements for the Langevin method is the same as for the IEC method, then there is no advantage in using the Langevin method.

In this analysis basic methods for extracting the drift field were used. The results of drift field analysis are shown in plots for each wind speed bin for the different analyses in the appendix. The graphs show that the drift in most cases is far from being continuously decreasing but in many cases crosses the zero line several times. This makes procedures for determination of the fixed points very difficult to establish. The lack of a specific method here is significantly reducing robustness of the Langevin method on real power curve measurement data. In fact it makes the method inferior to simple binning and averaging as described in the IEC standard.

The Langevin method was derived from a theoretical statistical approach. The method was tested against artificial generated power curve data where noise was added to a power curve. Obviously, the theoretical statistical approach was put into a physical framework. A physical framework must first of all consider what purpose the power curve is going to be used for. The IEC standard for power curve measurements is made for calculation of energy production. For such purposes it must be required that the power curve measurement method gives consistent results with power produced and wind speeds monitored. The simple averaging of data in wind speed bins do comply with such criteria while it is difficult to see how drift field analysis can comply. Satisfactory argumentation for the Langevin method in this respect has not been found.

# 8. Conclusions

In this project the Langevin power curve measurement method was used on real power curve measurement datasets. The purpose was to evaluate methods for making faster power curves. The Langevin method has been developed by several authors in the past by applying the method to a theoretical power curve where noise was added. Several authors concluded that the method worked well and that it had potential for making faster power curves, which means a power curve of comparable uncertainty by use of a reduced observation time.

The Langevin method was studied and a practical guide to application of the method to real power curve measurement data was made. The study showed that the method has a range of parameter settings that need to be considered. Additionally to the wind speed binning in the IEC61400-12-1 standard a power binning is needed. The method does not specify how the binning should be made. The determination of the drift in each wind speed and power bin is described with a general formula but in practice several additional tools have been developed by authors to try to make the drift field and fixed point determination more robust.

We made a sensitivity analysis with nacelle lidar data and found that drift determination was not very dependent on the time steps applied, leading to use of time steps of 2-3 points for each dataset. The power bin size was investigated for fixed bin size, fixed bin size with minimum 500 data, and fixed numbers of datasets in each bin and it was found that a fixed bin size was appropriate. Data averaging with 5 sec data is more distinct for determination of the fixed points than 2 and 1 sec data but the fixed points were not very sensitive to the bin size. With the nacelle lidar the Langevin method seemed to produce a power curve that was comparable to the IEC measured power curve with 10min data.

Analysis of the Langevin method with spinner anemometer data showed that the fixed points were very sensitive to bin size and also to the requirement of minimum amount of data in each bin. For the spinner anemometer measurements the Langevin method failed to produce acceptable power curves that were comparable to the IEC measured power curve with 10min data.

Simple binned averaging of data with shorter time averages gave significantly better results than the Langevin power curve method. With 30sec averages the power curve was very similar to the IEC measured power curve with 10min data and with 1sec averages the power curve was smoothened a little due to the high spreading of data close to the rooftop at nominal power. For determination of fast power curves or dynamic data analysis the preferred method seems to be the simple binned averaging with shorter times averaging. Especially for measurements with spinner anemometry this method seems to have good potential. This is due to the high cross correlation between wind speed and power measurements.

# References


1. IEC 61400-12-1. Wind turbines – part 12-1: Power performance measurements of electricity producing wind turbines, 2005. International Electrotechnical Commission.

2. Rauh A., Peinke J., A phenomenological model for the dynamic response of wind turbines to turbulent wind, Journal of Wind Eng. Ind. and Aerody. 92, 159-183, 2004

3. Anahua E, Barth S, Peinke J, Characterization of the Wind Turbine Power Performance Curve by Stochastic Modeling, EWEC 2006

4. Gottschall J, Peinke J. Stochastic modelling of a wind turbine's power output with special respect to turbulent dynamics. Journal of Physics: Conference Series 2007; **75**: 012045 (8pp). DOI: 10.1088/1742-6596/75/1/012045.

5. Anahua, Barth St, Peinke J, Markovian Power Curves for Wind Turbines, Wind Energy 11(3), 219–232 (2008).

6. Gottschall J, Peinke J. Power curves for wind turbines – a dynamical approach. Proceedings of EWEC 2008, Brussels, 2008.

7. Gottschall J, Peinke J. How to improve the estimation of power curves for wind turbines. Environmental Research Letters 2008; **3**(1): 015005 (7pp). DOI: 10.1088/1748-9326/3/1/015005.

8. Gottschall J, Peinke J. On the definition and handling of different drift and diffusion estimates. New Journal of Physics 2008; **10**: 083034 (20pp). [Online]. Available: http://www.njp.org/. DOI: 10.1088/1367-2630/10/8/083034 (Accessed August 2008).

9. Milan P, Mücke T, Morales A, Wächter M, Peinke J. Applications of the Langevin power curve. Proceedings of the EWEC 2010, EWEA: Warsaw, Poland, 2010.

10. Wächter M, Milan P, Mücke T, Peinke J, Power performance of wind energy converters characterized as stochastic process: applications of the Langevin power curve, Wind Energy 2011, **14**, 711-717

11. Milan P, Wächter M, Peinke J. Stochastic modeling of wind power production. Proceedings of the EWEC 2011, EWEA: Brussels, Belgium, 2011.

12. Wächter M, Heißelmann H, Hölling M, Morales A, Milan P, Mücke T, Peinke J, Reinke N, Rinn P. The turbulent nature of the atmospheric boundary layer and its impact on the wind energy conversion process. Journal of Turbulence 2012; **13**: 1–21.

13. Brown C. Fast Verification of Wind Turbine Power Curves: Summary of Project Results. Master Thesis, Technical University of Denmark, DTU Informatics (IMM-M.Sc.-2012-72), 2012

14. Gottshall J, Courtney M, On the robustness of the fixed points for a dynamical performance characteristic – or: a closer look at the Langevin power curve, Wind Energy 2014 we1718

15. Pedersen TF, Madsen HA, Møller R, Courtney, M, Sørensen NN, Enevoldsen P, Egedal P, "Spinner Anemometry – An Innovative Wind Measurement Concept", EWEC2007 Milan, paper and poster (poster award)

16. Pedersen TF, Demurtas G, Zahle F, "Calibration of a spinner anemometer for yaw misalignment measurements", Wind Energy 2014, we1798

17. Albers A, et al, Influence of Meteorological Variables on Measured Wind Turbine Power Curve, EWEC 2007

18. Wagner et al., Power curve measurement with a nacelle mounted lidar, Wind Energy 17:9, 2014

# Acknowledgements

We would like to acknowledge EUDP for the support for this project. We would also like to acknowledge Jakob Matthiesen, Vestas for discussion on the Langevin method , and Vattenfall and DONG Energy for allowing data from earlier project to be used for the analysis.

# Appendix A
# Wind speed bin drift data for Nordtank 500kW wind turbine with spinner anemometer

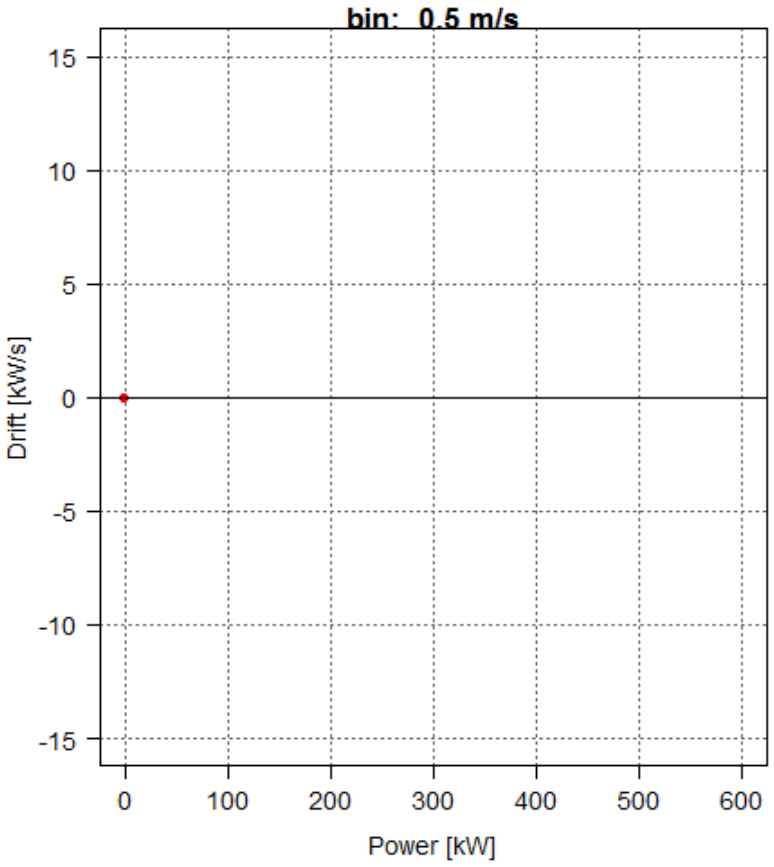

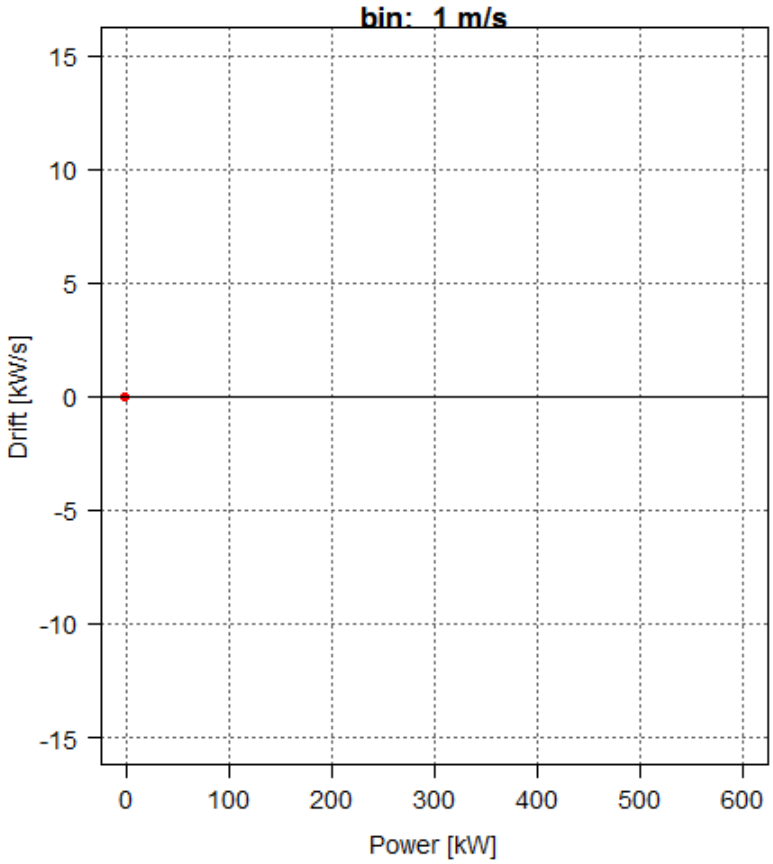
bin: 1 m/s
15
10
5
0
-5
-10
-15
Drift [kW/s]
0
100
200
300
400
500
600
Power [kW]

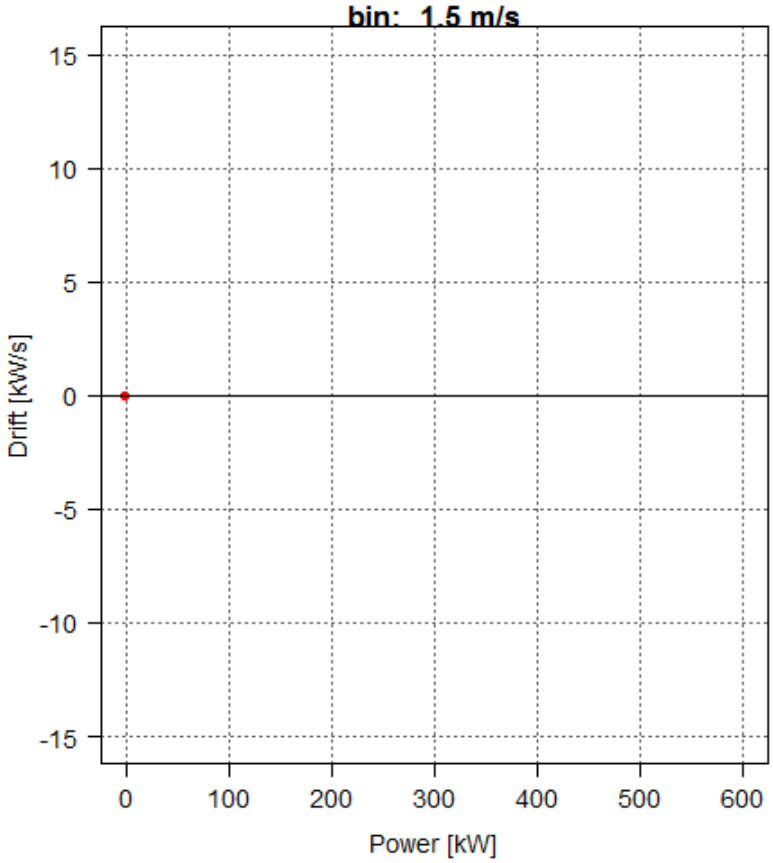
bin: 1.5 m/s
15
10
5
0
-5
-10
-15
Drift [kW/s]
0
100
200
300
400
500
600
Power [kW]

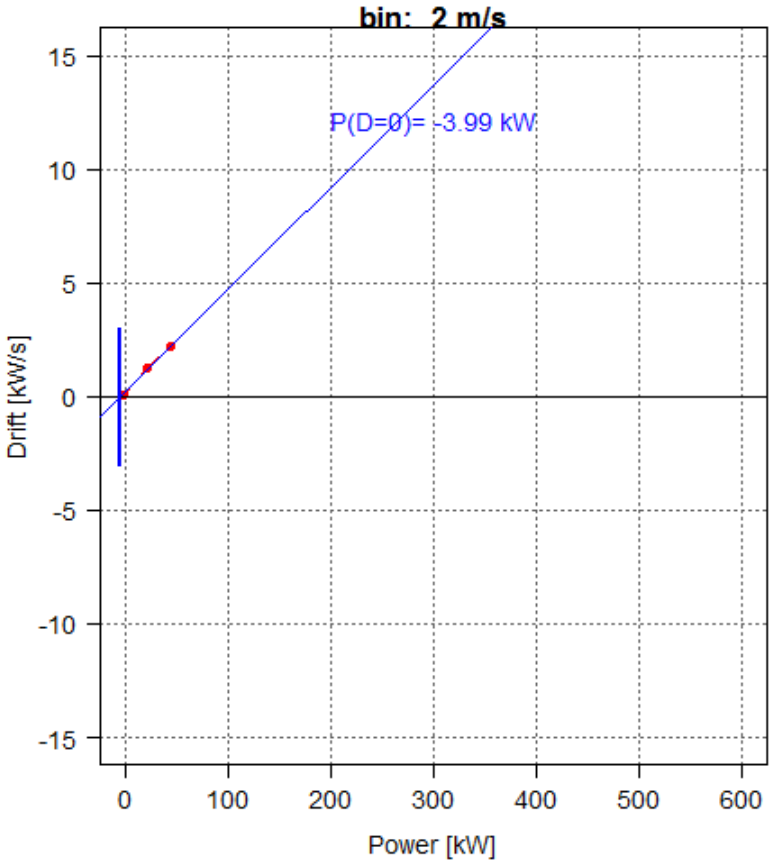
bin: 2 m/s
P(D=0)= -3.99 kW
Drift [kW/s]
Power [kW]
15
10
5
0
-5
-10
-15
0
100
200
300
400
500
600

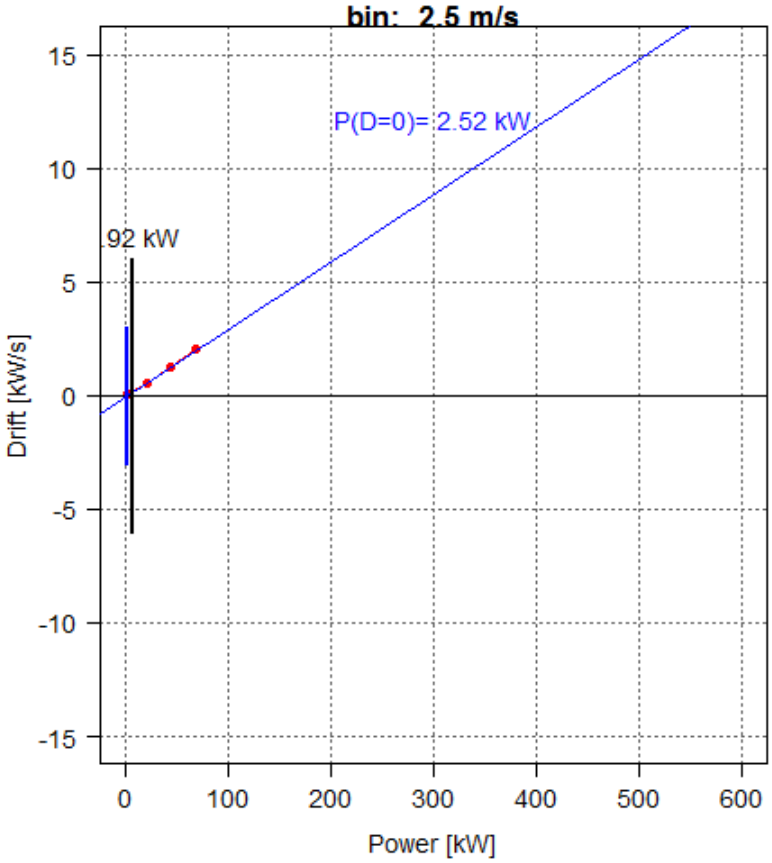
bin: 2.5 m/s
P(D=0)= 2.52 kW
92 kW
Drift [kW/s]
Power [kW]
15
10
5
0
-5
-10
-15
0
100
200
300
400
500
600

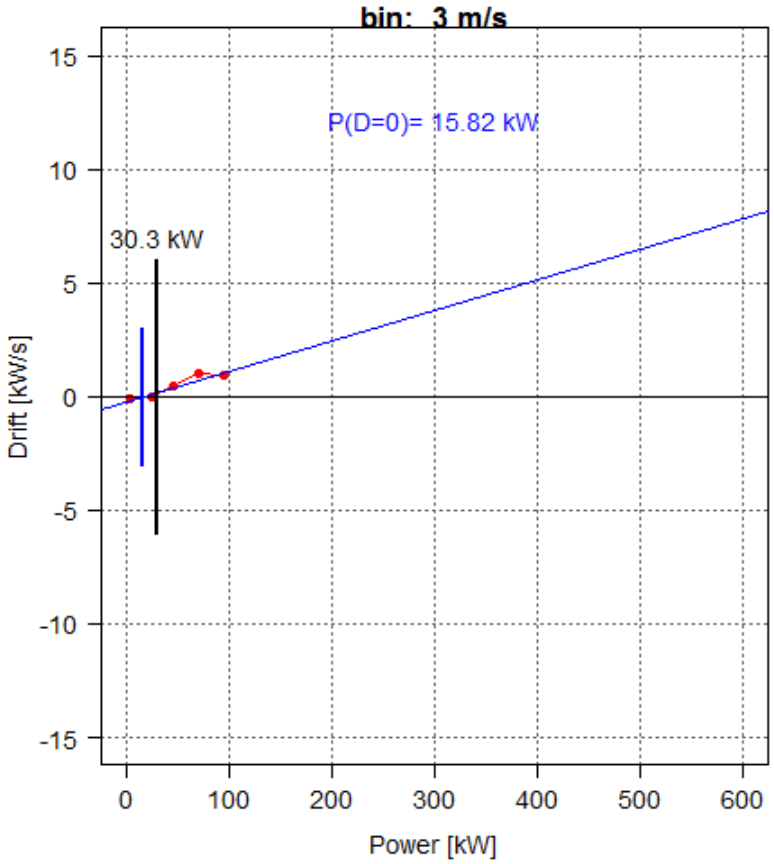
bin: 3 m/s
P(D=0)= 15.82 kW
30.3 kW
Drift [kW/s]
Power [kW]
15
10
5
0
-5
-10
-15
0
100
200
300
400
500
600

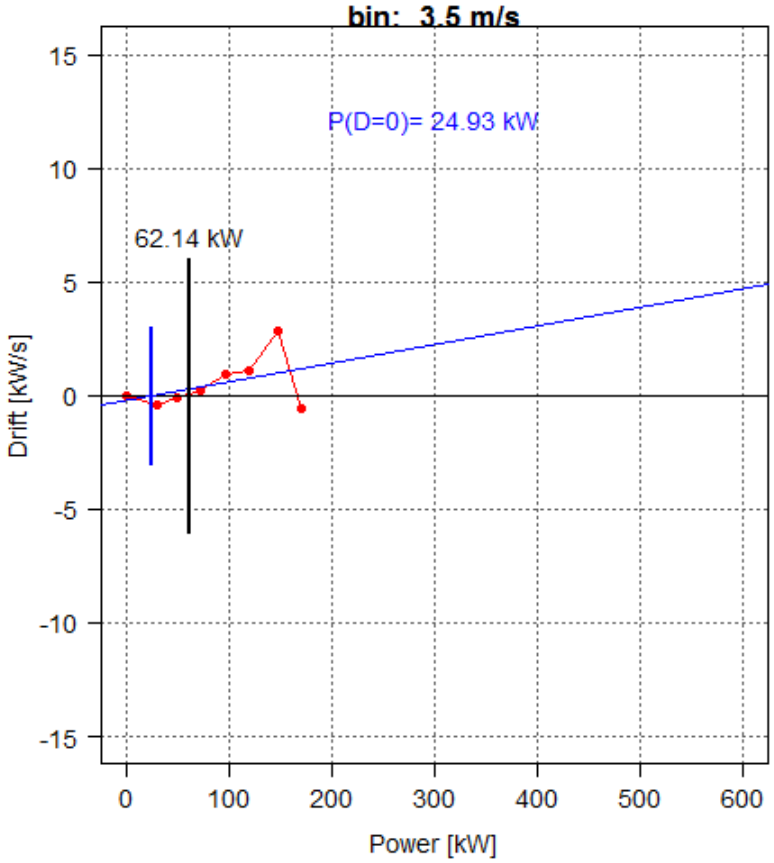
bin: 3.5 m/s
P(D=0)= 24.93 kW
62.14 kW
Drift [kW/s]
Power [kW]
15
10
5
0
-5
-10
-15
0
100
200
300
400
500
600

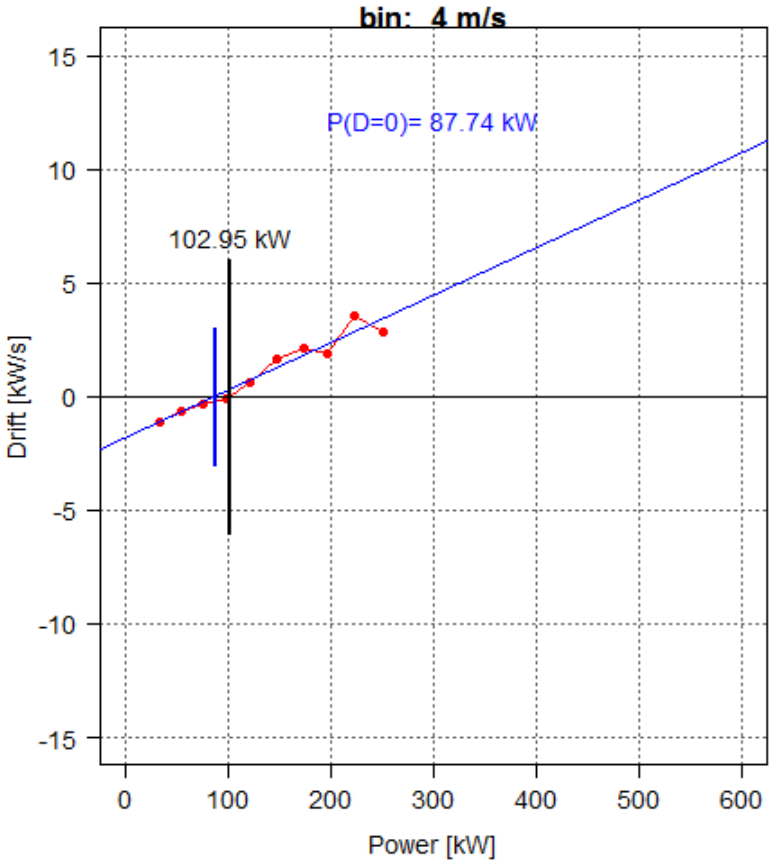
bin: 4 m/s
P(D=0)= 87.74 kW
102.95 kW
Drift [kW/s]
Power [kW]
15
10
5
0
-5
-10
-15
0
100
200
300
400
500
600

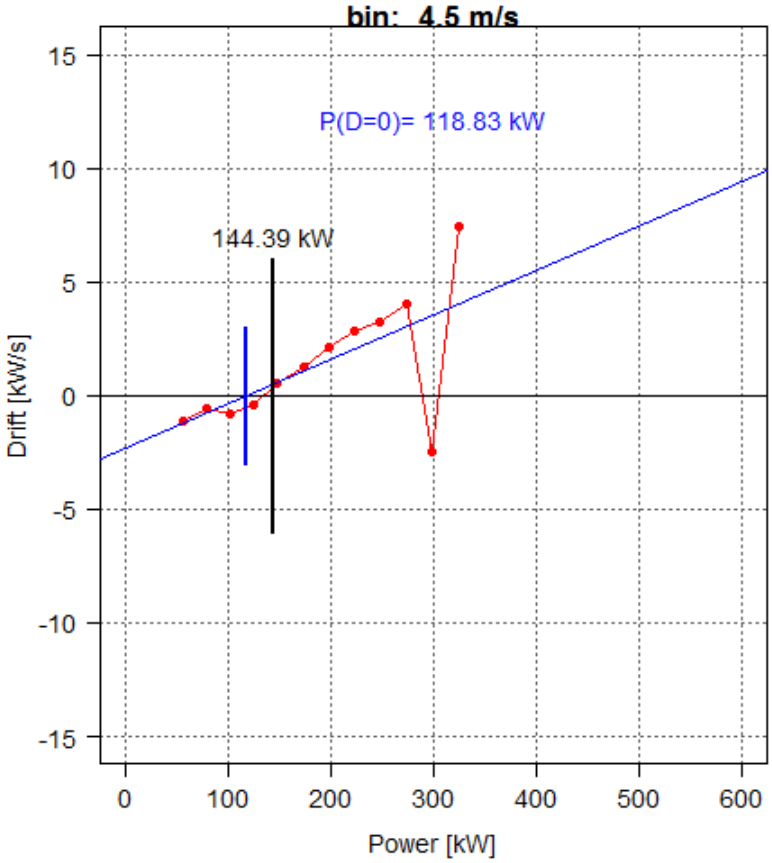
bin: 4.5 m/s
P(D=0)= 118.83 kW
144.39 kW
Drift [kW/s]
Power [kW]
15
10
5
0
-5
-10
-15
0
100
200
300
400
500
600

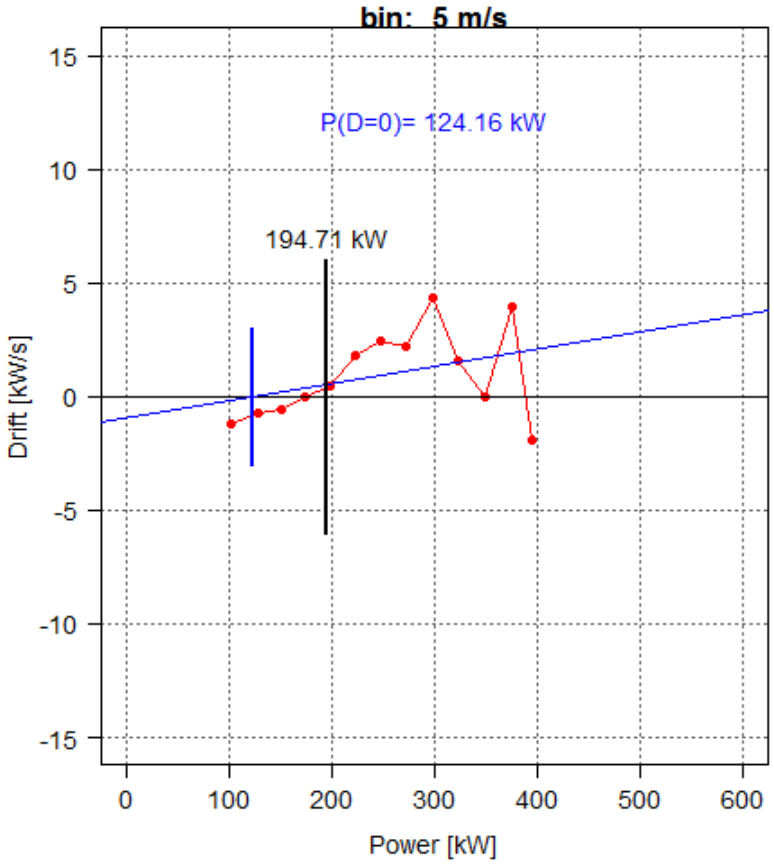
bin: 5 m/s
P(D=0)= 124.16 kW
194.71 kW
Drift [kW/s]
Power [kW]
15
10
5
0
-5
-10
-15
0
100
200
300
400
500
600

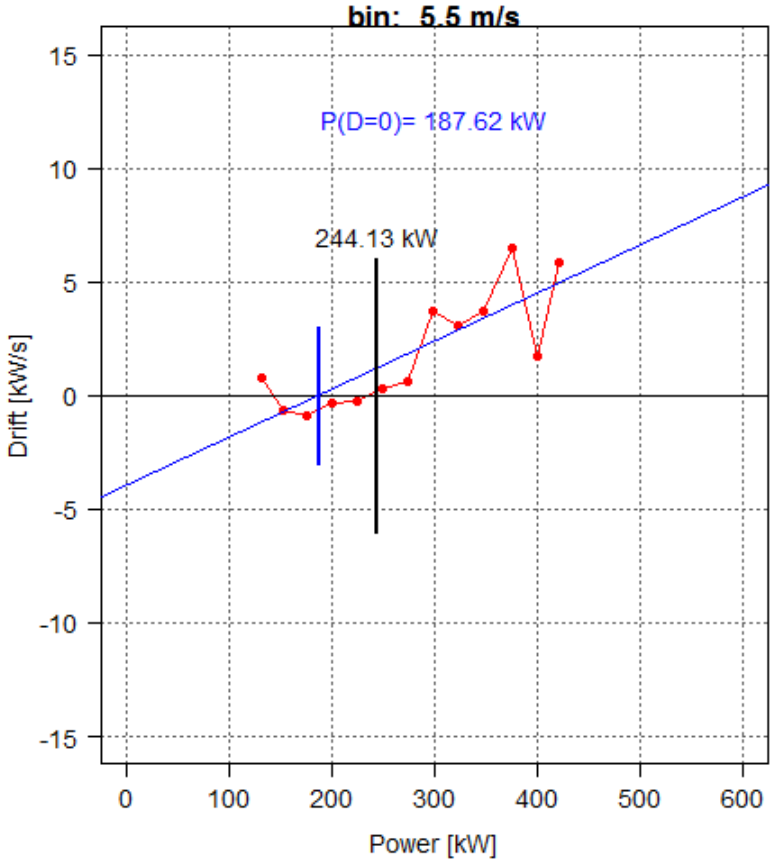
bin: 5.5 m/s
P(D=0)= 187.62 kW
244.13 kW
Drift [kW/s]
Power [kW]
15
10
5
0
-5
-10
-15
0
100
200
300
400
500
600

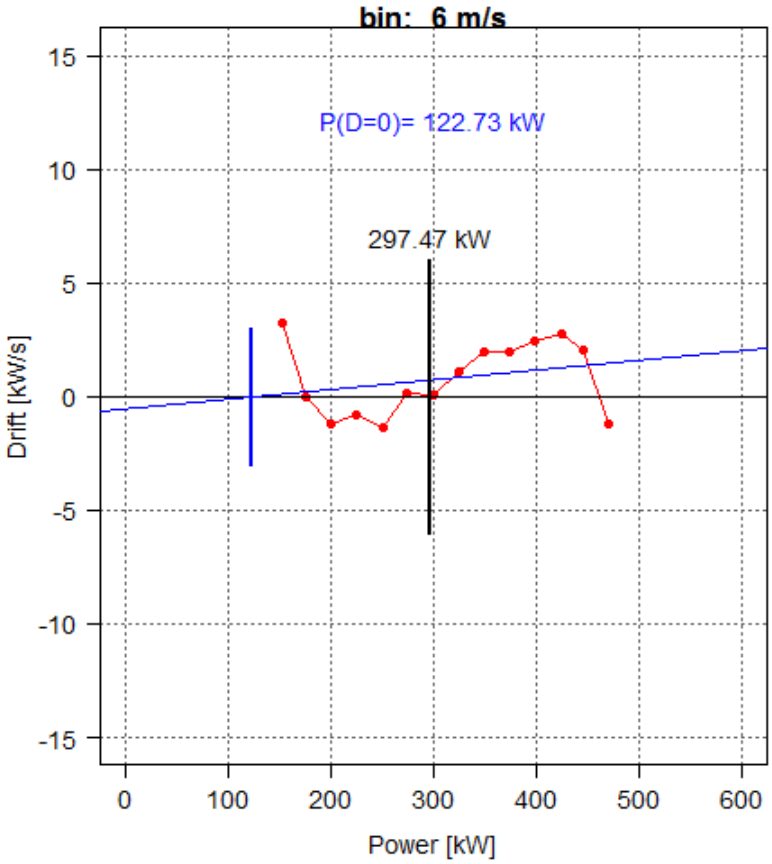
bin: 6 m/s
P(D=0)= 122.73 kW
297.47 kW
Drift [kW/s]
Power [kW]
15
10
5
0
-5
-10
-15
0
100
200
300
400
500
600

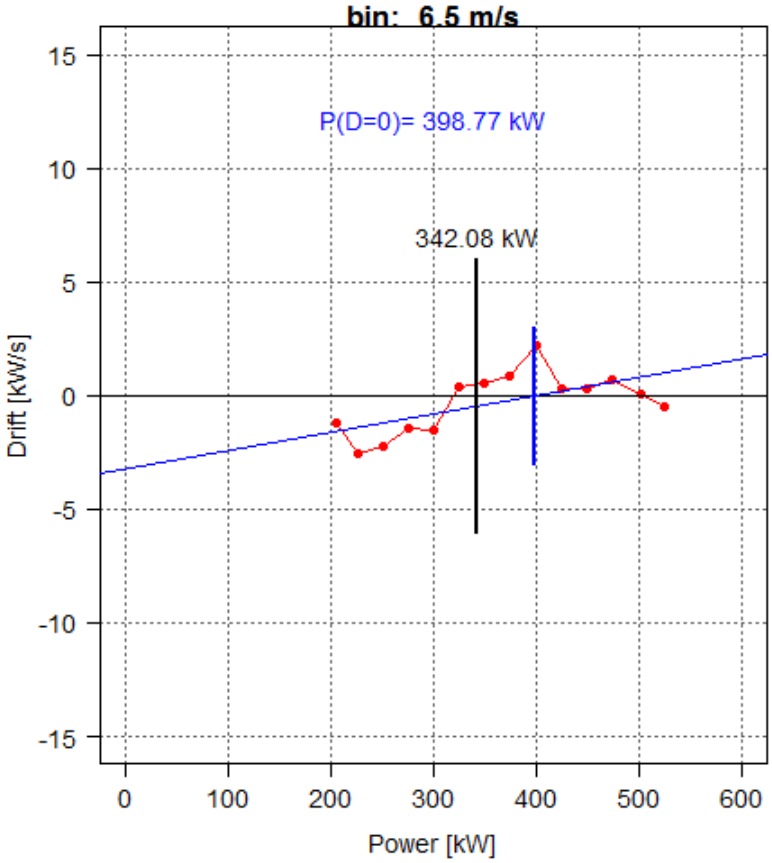
bin: 6.5 m/s
P(D=0)= 398.77 kW
342.08 kW
Drift [kW/s]
Power [kW]
15
10
5
0
-5
-10
-15
0
100
200
300
400
500
600

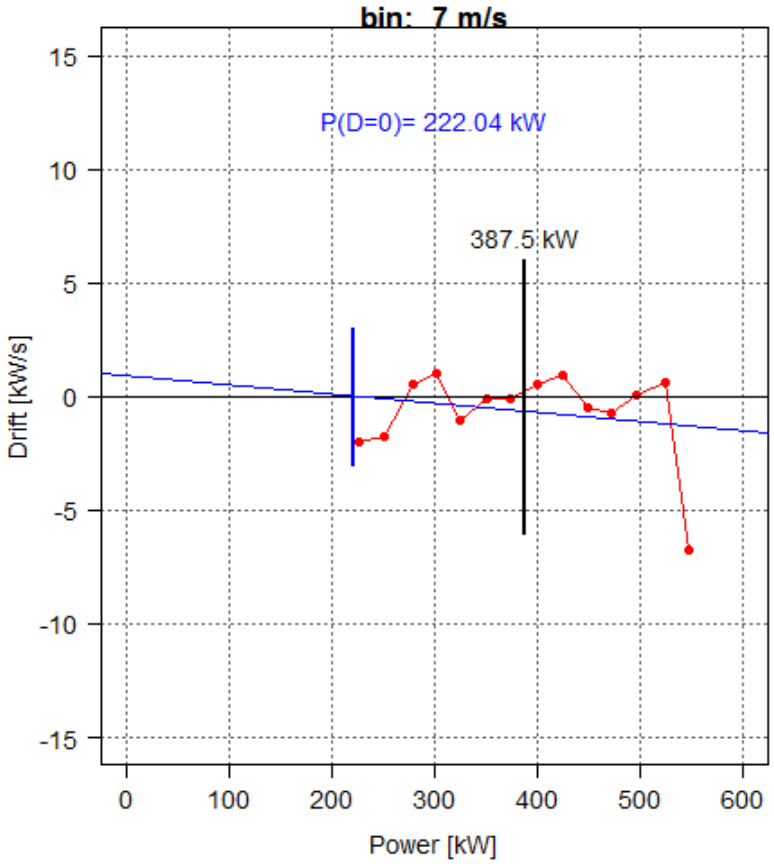
bin: 7 m/s
P(D=0)= 222.04 kW
387.5 kW
Drift [kW/s]
Power [kW]
15
10
5
0
-5
-10
-15
0
100
200
300
400
500
600

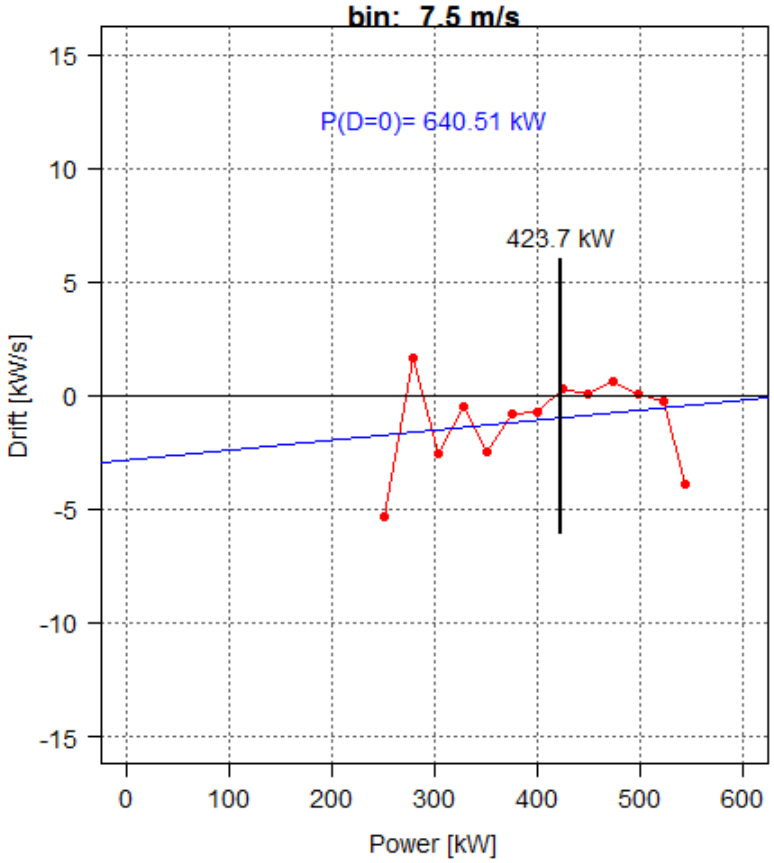
bin: 7.5 m/s
P(D=0)= 640.51 kW
423.7 kW
Drift [kW/s]
Power [kW]
15
10
5
0
-5
-10
-15
0
100
200
300
400
500
600

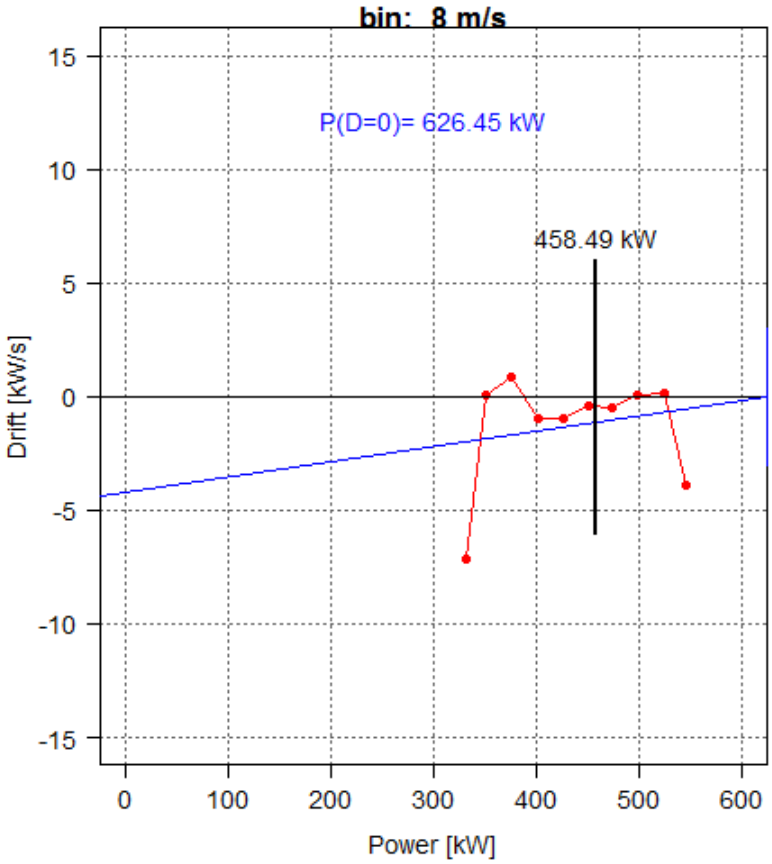
bin: 8 m/s
P(D=0)= 626.45 kW
458.49 kW
Drift [kW/s]
Power [kW]
15
10
5
0
-5
-10
-15
0
100
200
300
400
500
600

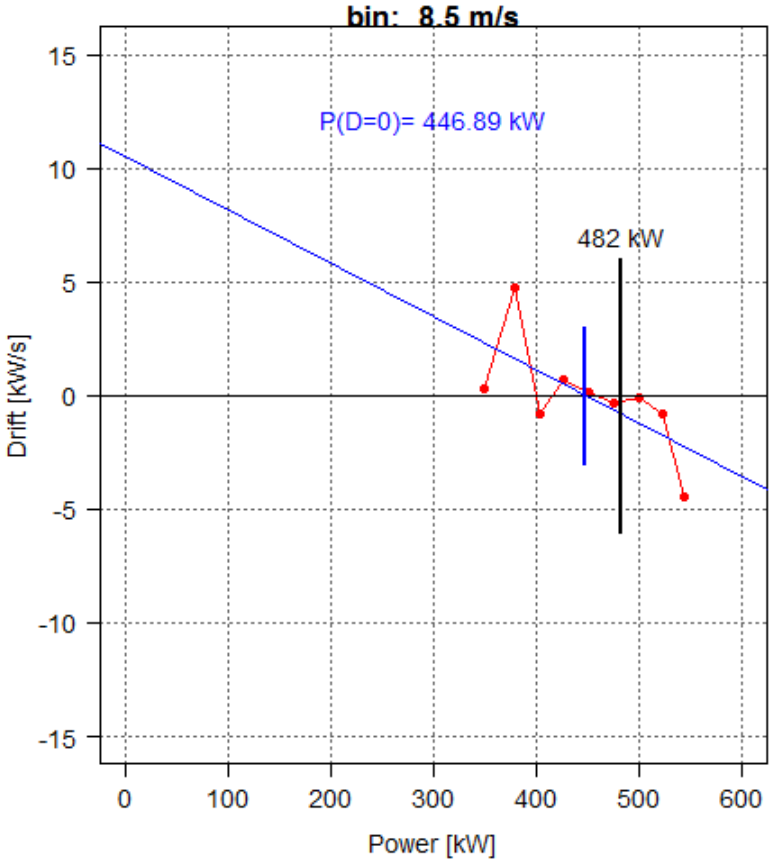
bin: 8.5 m/s
P(D=0)= 446.89 kW
482 kW
Drift [kW/s]
Power [kW]
15
10
5
0
-5
-10
-15
0
100
200
300
400
500
600

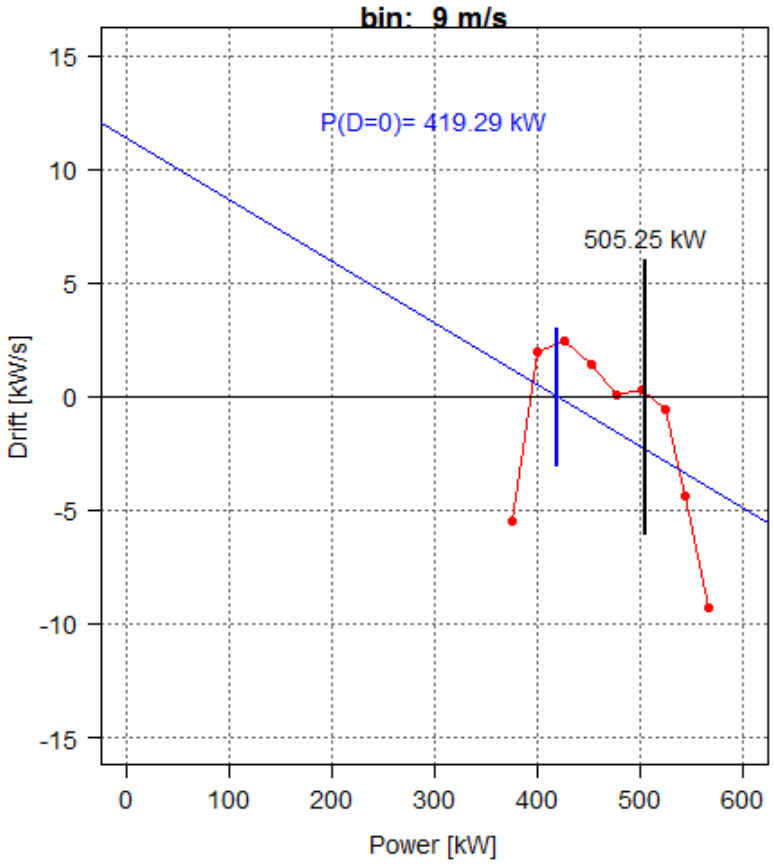
bin: 9 m/s
P(D=0)= 419.29 kW
505.25 kW
Drift [kW/s]
Power [kW]
15
10
5
0
-5
-10
-15
0
100
200
300
400
500
600

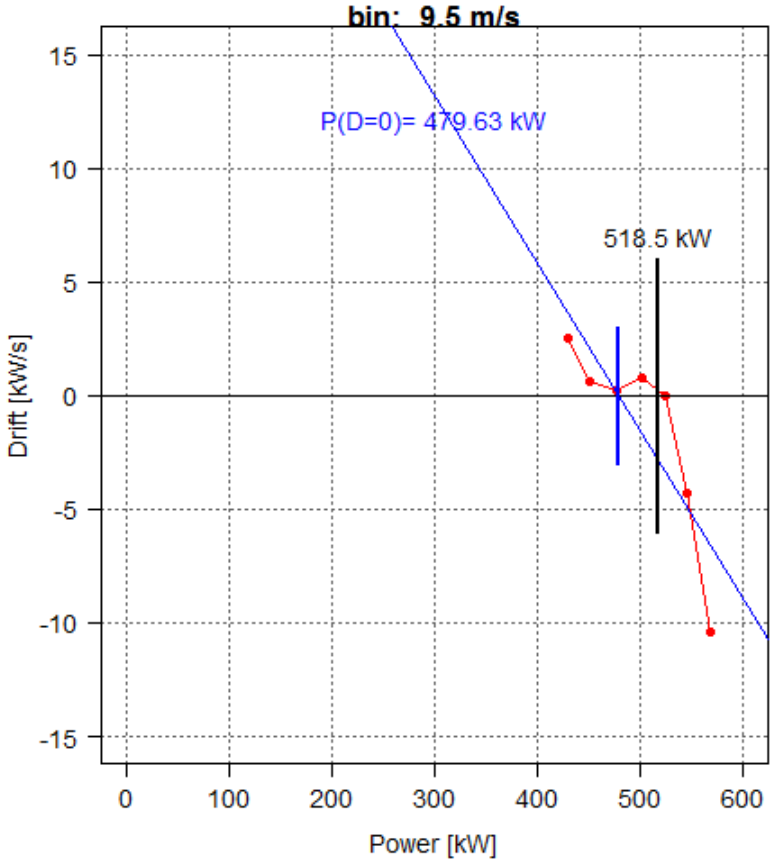
bin: 9.5 m/s
P(D=0)= 479.63 kW
518.5 kW
Drift [kW/s]
Power [kW]
15
10
5
0
-5
-10
-15
0
100
200
300
400
500
600

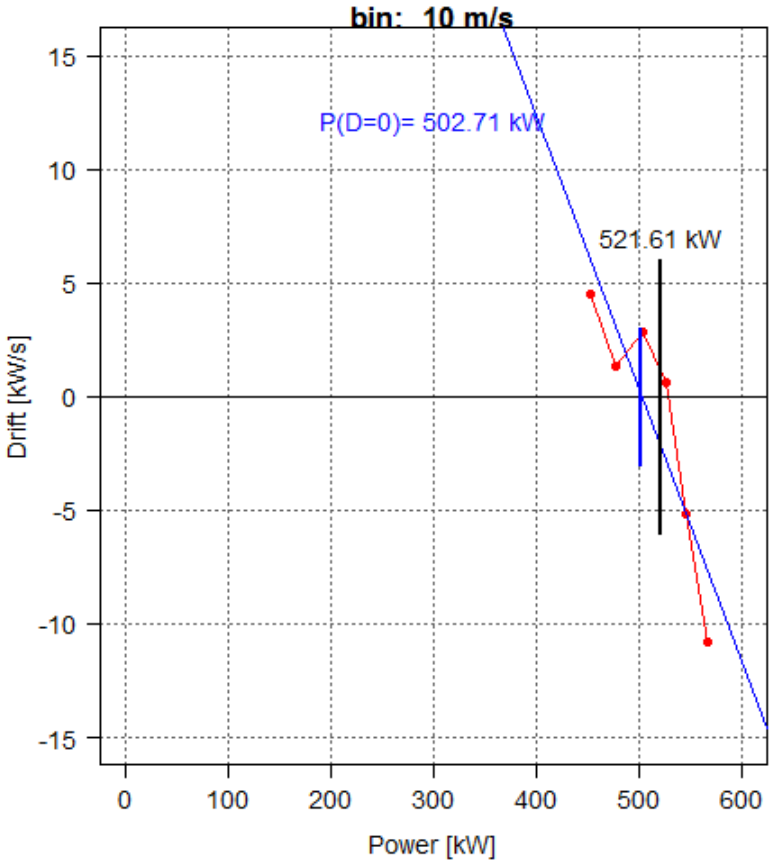
bin: 10 m/s
P(D=0)= 502.71 kW
521.61 kW
Drift [kW/s]
Power [kW]
15
10
5
0
-5
-10
-15
0
100
200
300
400
500
600

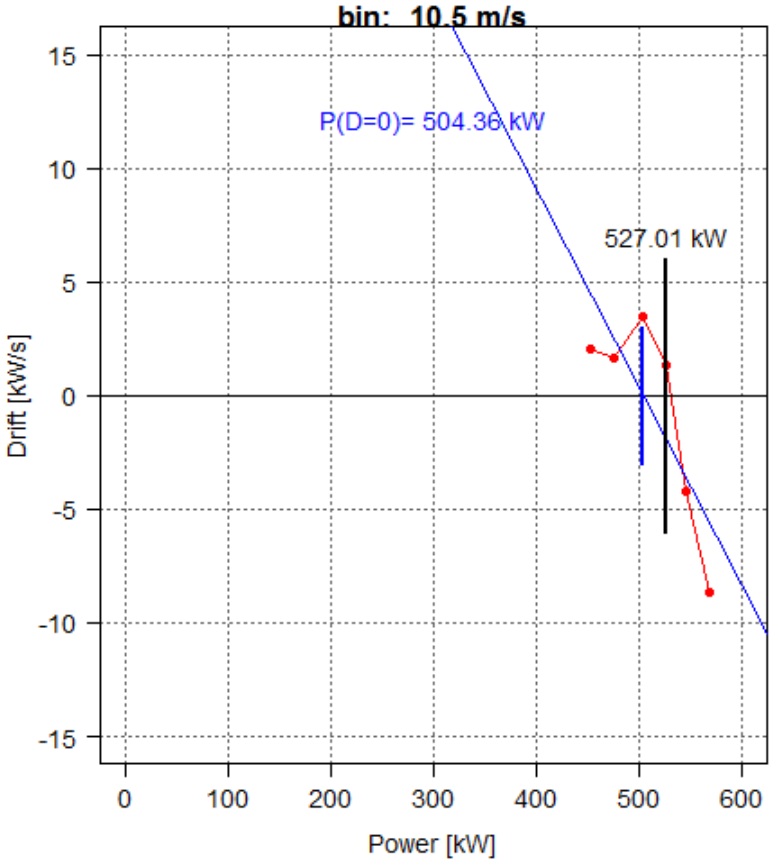
bin: 10.5 m/s
P(D=0)= 504.36 kW
527.01 kW
Drift [kW/s]
Power [kW]
15
10
5
0
-5
-10
-15
0
100
200
300
400
500
600

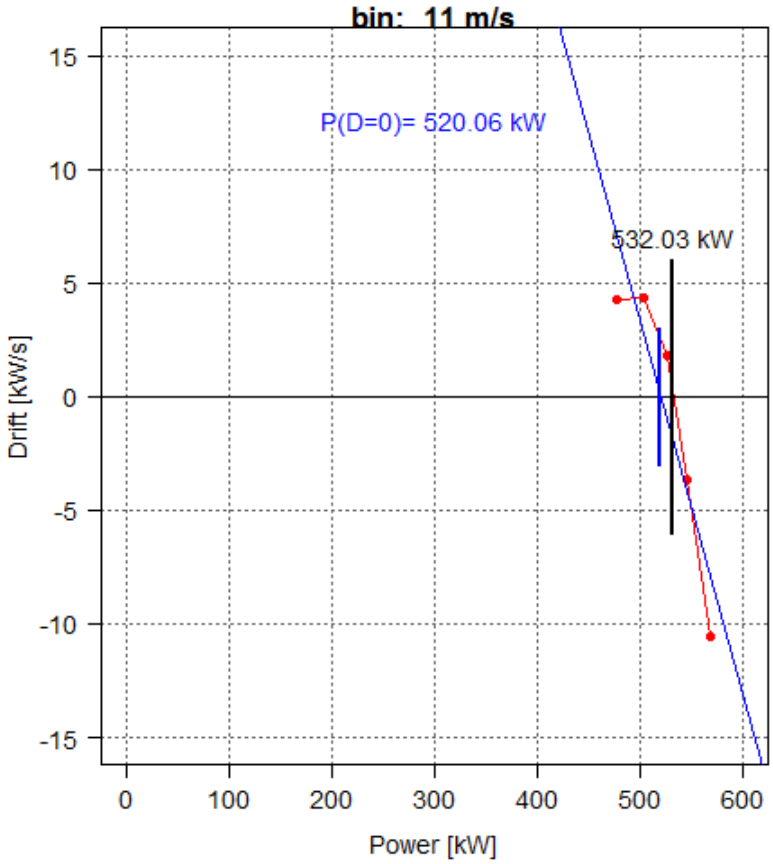
bin: 11 m/s
P(D=0)= 520.06 kW
532.03 kW
Drift [kW/s]
Power [kW]
15
10
5
0
-5
-10
-15
0
100
200
300
400
500
600

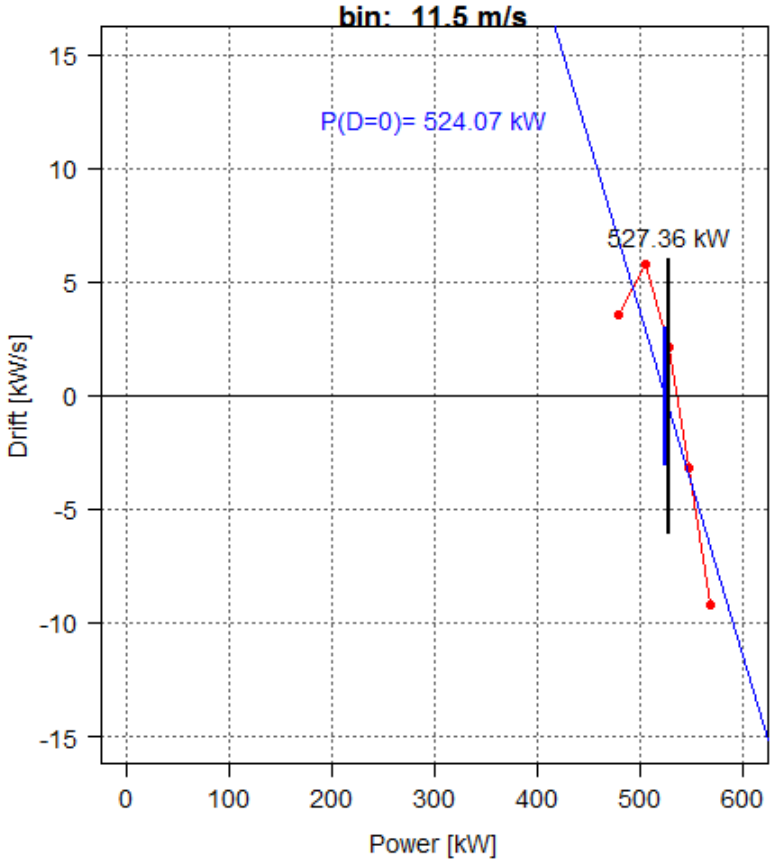
bin: 11.5 m/s
P(D=0)= 524.07 kW
527.36 kW
Drift [kW/s]
Power [kW]
15
10
5
0
-5
-10
-15
0
100
200
300
400
500
600

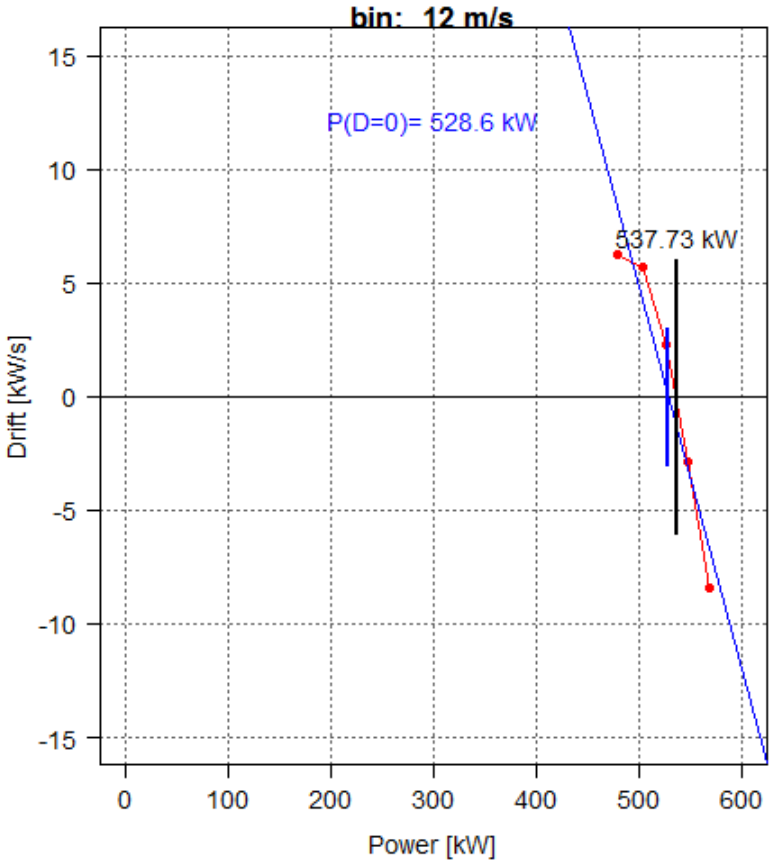
bin: 12 m/s
P(D=0)= 528.6 kW
537.73 kW
Drift [kW/s]
Power [kW]
15
10
5
0
-5
-10
-15
0
100
200
300
400
500
600

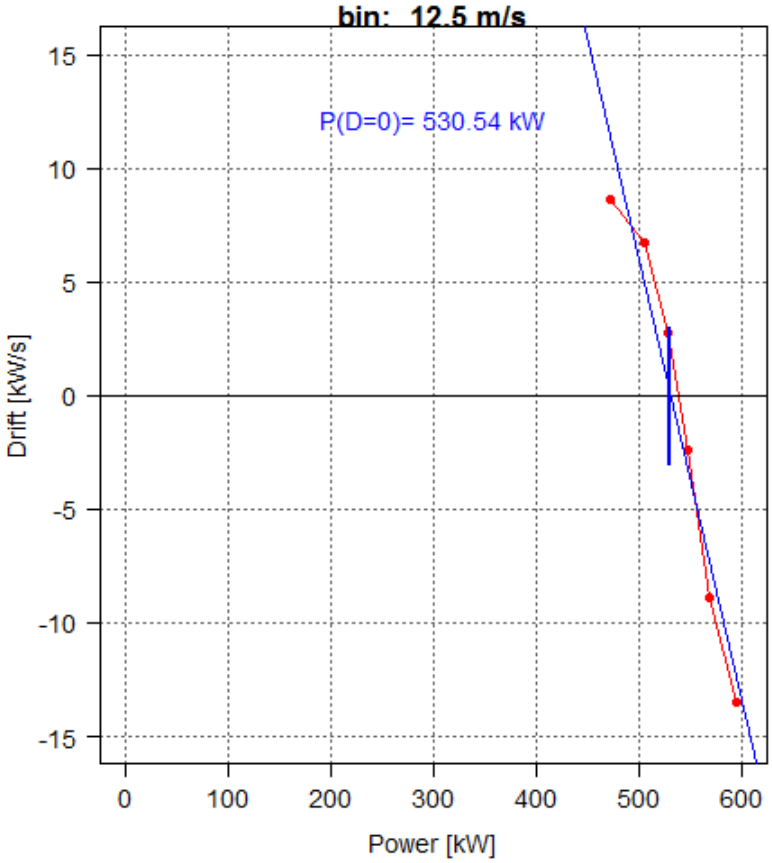
bin: 12.5 m/s
P(D=0)= 530.54 kW
Drift [kW/s]
Power [kW]
15
10
5
0
-5
-10
-15
0
100
200
300
400
500
600

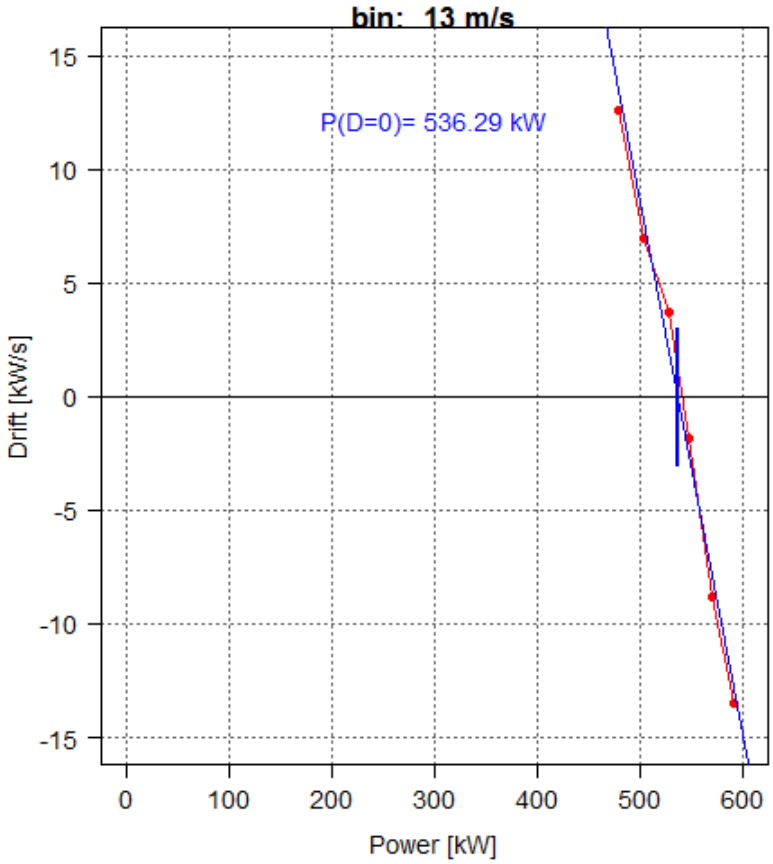
bin: 13 m/s
P(D=0)= 536.29 kW
Drift [kW/s]
Power [kW]
15
10
5
0
-5
-10
-15
0
100
200
300
400
500
600

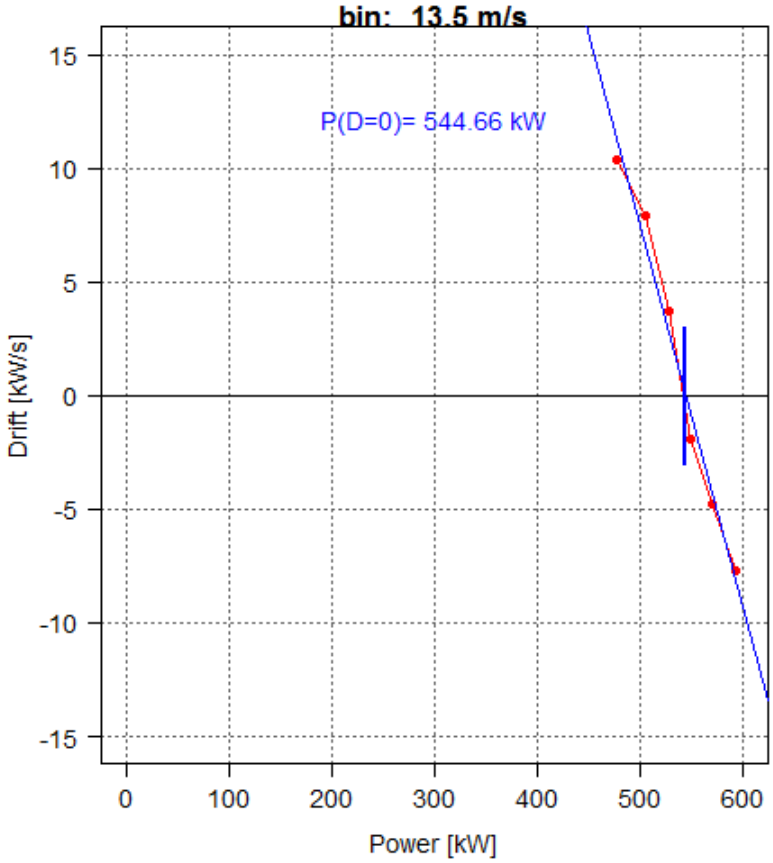
bin: 13.5 m/s
P(D=0)= 544.66 kW
Drift [kW/s]
Power [kW]
15
10
5
0
-5
-10
-15
0
100
200
300
400
500
600

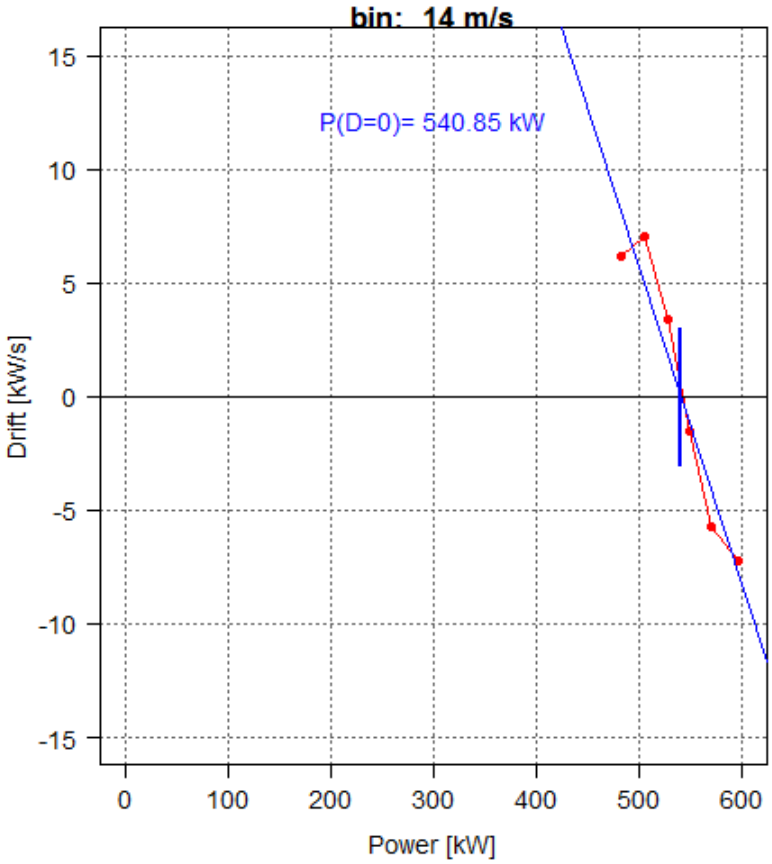
bin: 14 m/s
P(D=0)= 540.85 kW
Drift [kW/s]
Power [kW]
15
10
5
0
-5
-10
-15
0
100
200
300
400
500
600

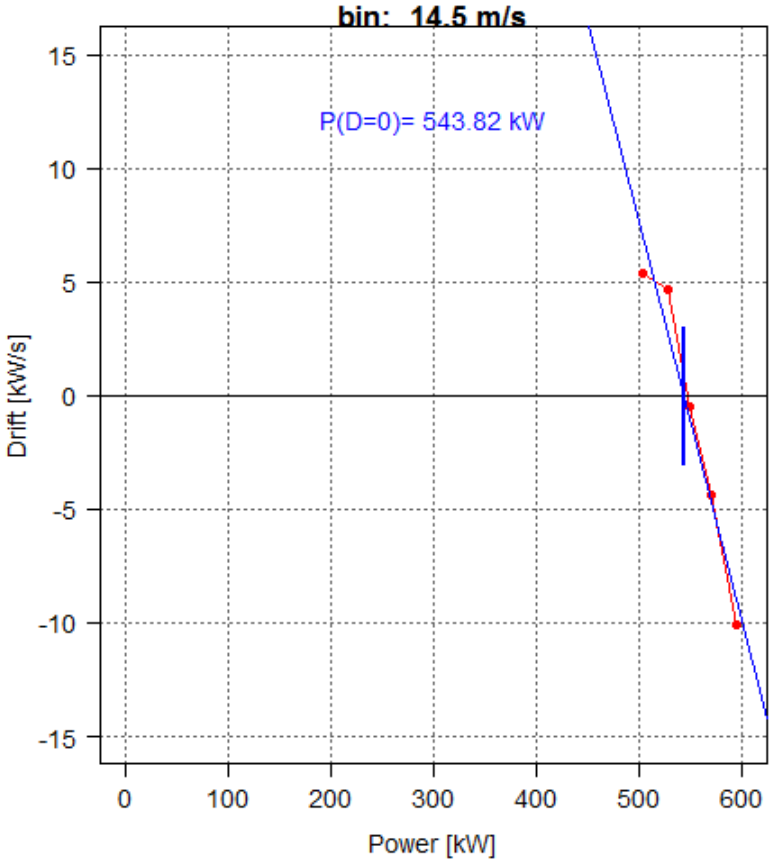
bin: 14.5 m/s
P(D=0)= 543.82 kW
Drift [kW/s]
Power [kW]
15
10
5
0
-5
-10
-15
0
100
200
300
400
500
600

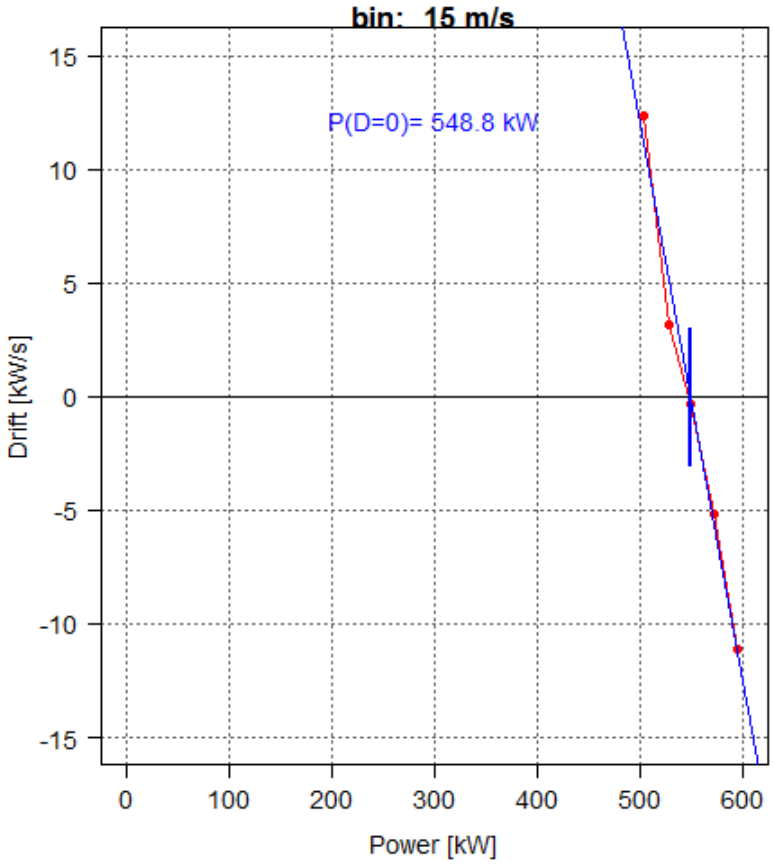
bin: 15 m/s
P(D=0)= 548.8 kW
Drift [kW/s]
Power [kW]
15
10
5
0
-5
-10
-15
0
100
200
300
400
500
600

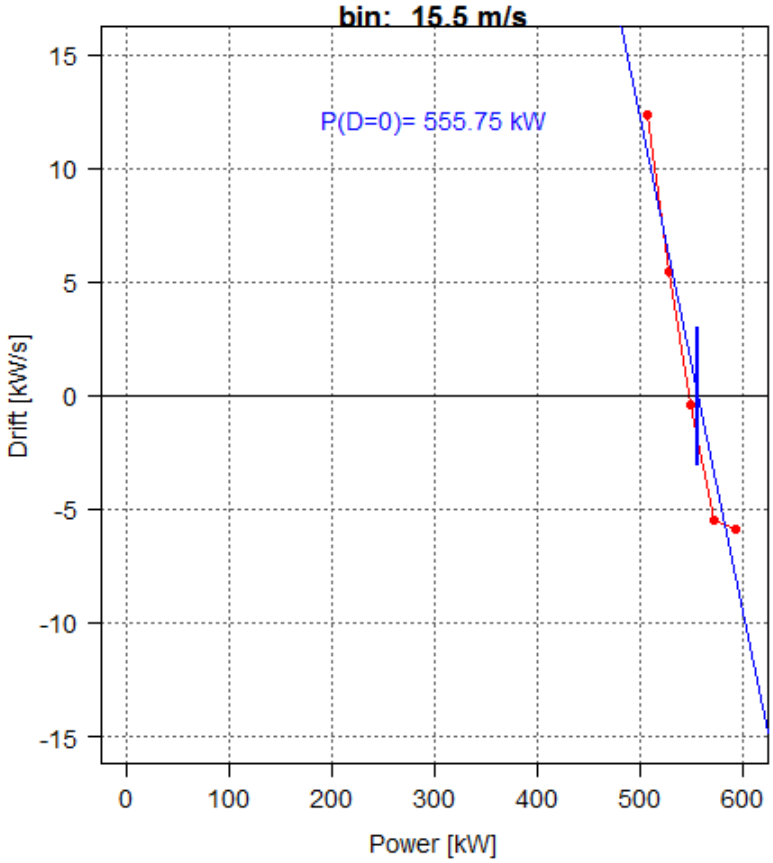
bin: 15.5 m/s
P(D=0)= 555.75 kW
Drift [kW/s]
Power [kW]
15
10
5
0
-5
-10
-15
0
100
200
300
400
500
600

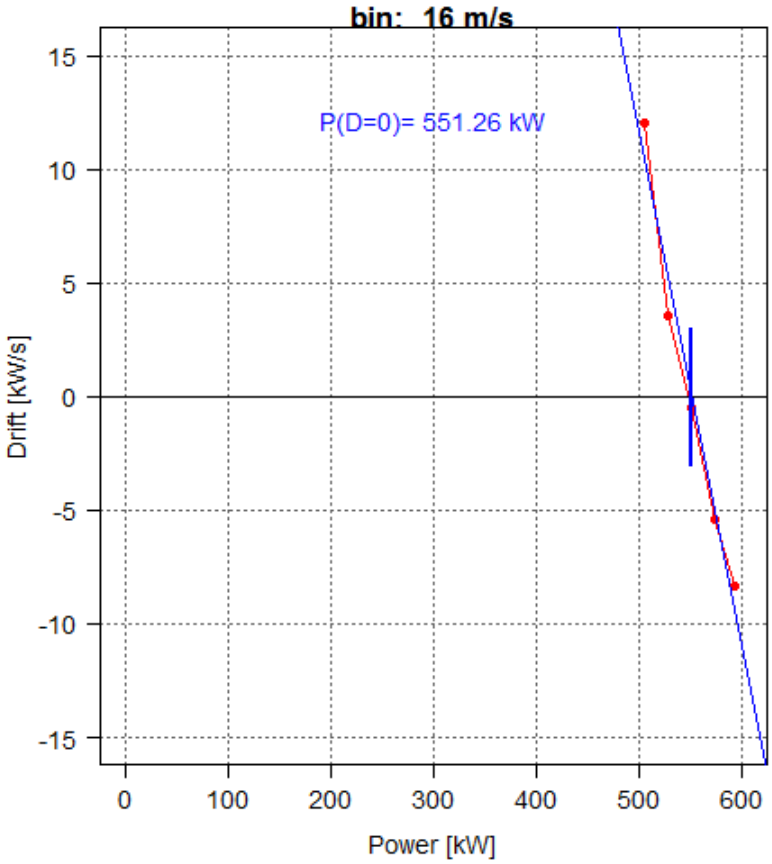
bin: 16 m/s
P(D=0)= 551.26 kW
Drift [kW/s]
Power [kW]
15
10
5
0
-5
-10
-15
0
100
200
300
400
500
600

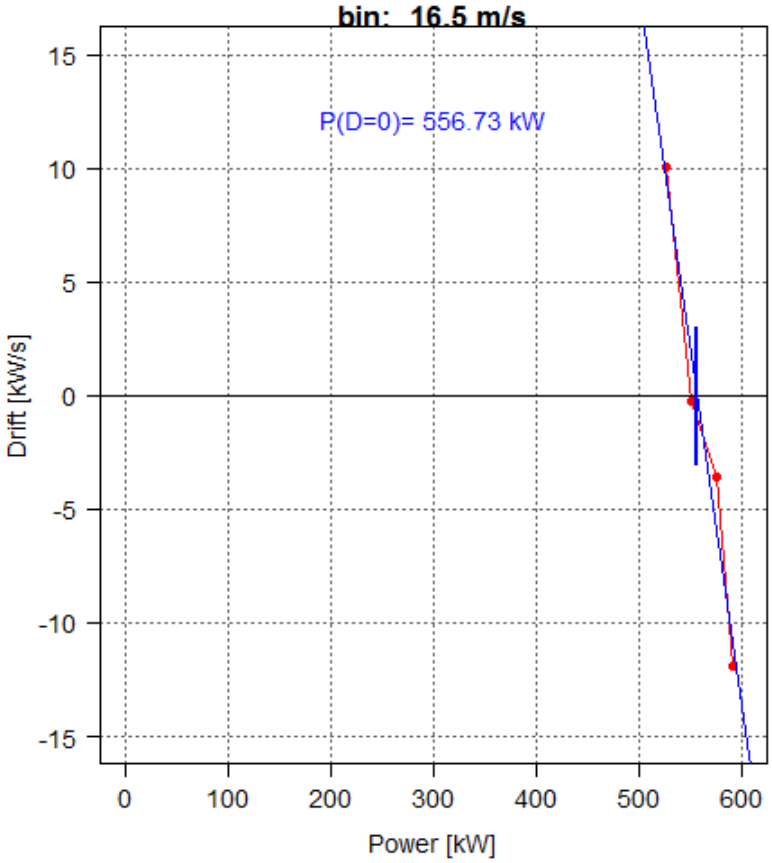
bin: 16.5 m/s
P(D=0)= 556.73 kW
Drift [kW/s]
Power [kW]
15
10
5
0
-5
-10
-15
0
100
200
300
400
500
600

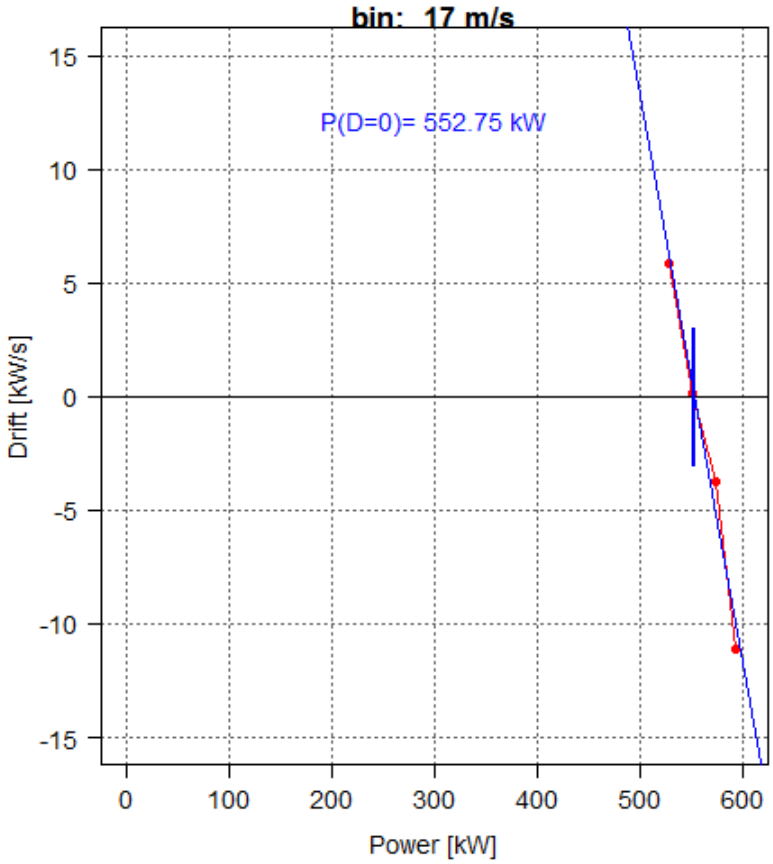
bin: 17 m/s
P(D=0)= 552.75 kW
Drift [kW/s]
Power [kW]
15
10
5
0
-5
-10
-15
0
100
200
300
400
500
600

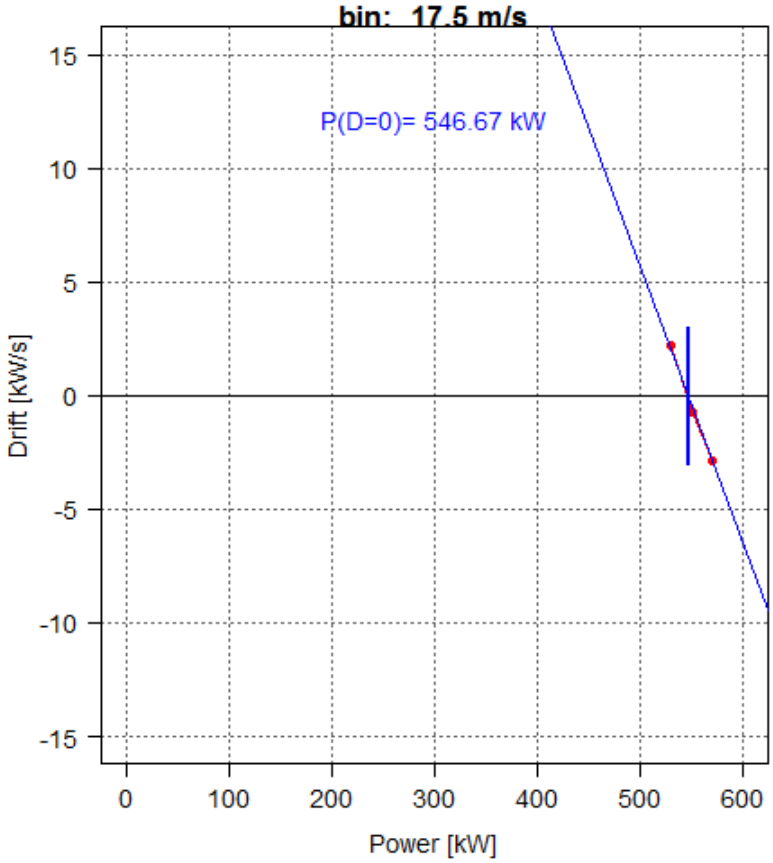
bin: 17.5 m/s
P(D=0)= 546.67 kW
Drift [kW/s]
Power [kW]
15
10
5
0
-5
-10
-15
0
100
200
300
400
500
600

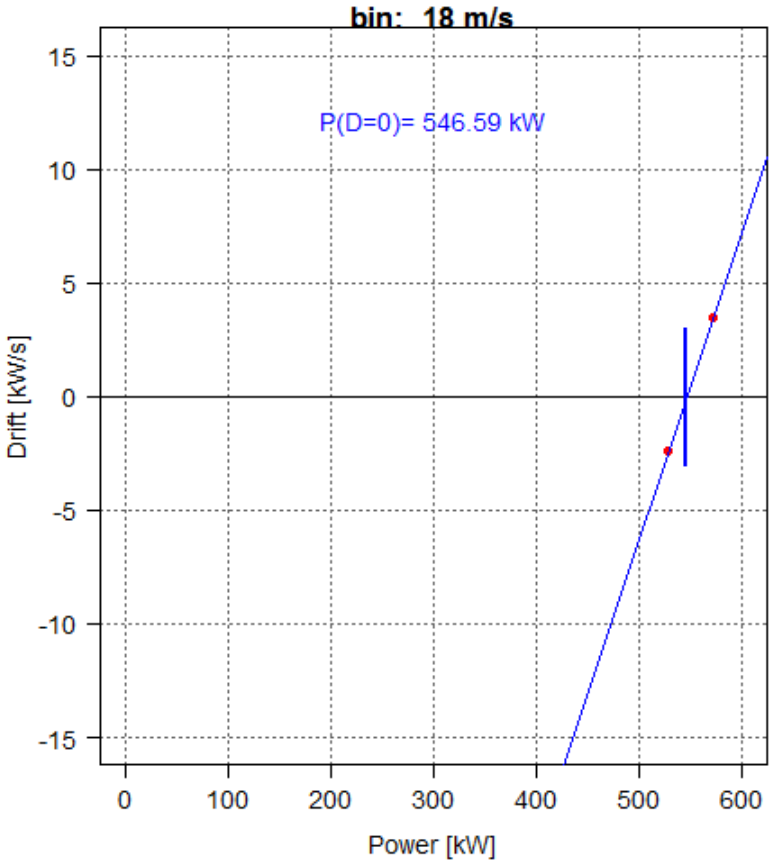
bin: 18 m/s
P(D=0)= 546.59 kW
Drift [kW/s]
Power [kW]
15
10
5
0
-5
-10
-15
0
100
200
300
400
500
600

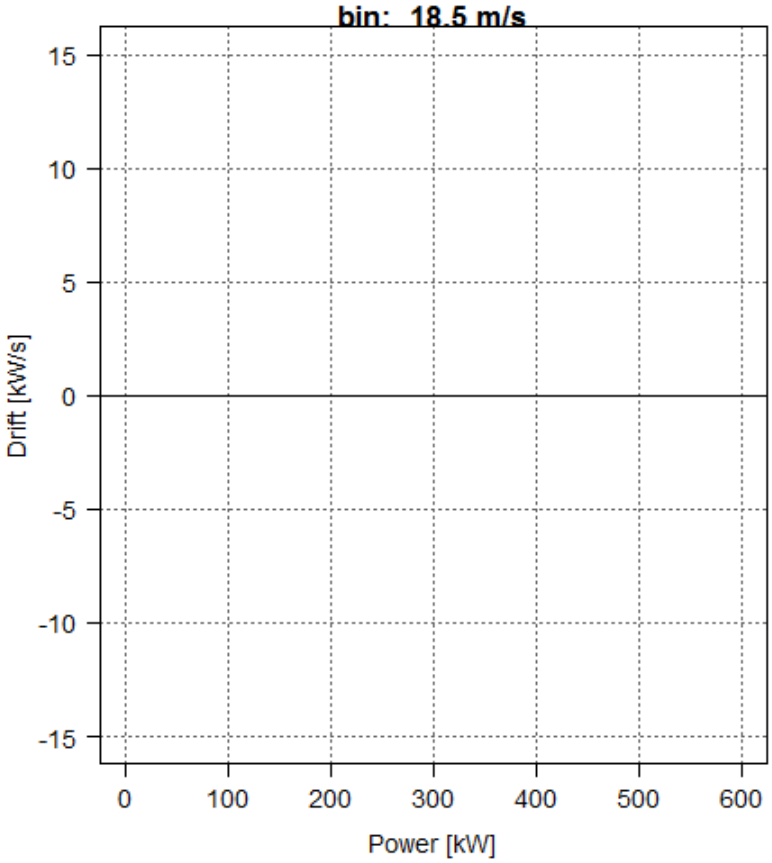
bin: 18.5 m/s
Drift [kW/s]
Power [kW]
15
10
5
0
-5
-10
-15
0
100
200
300
400
500
600

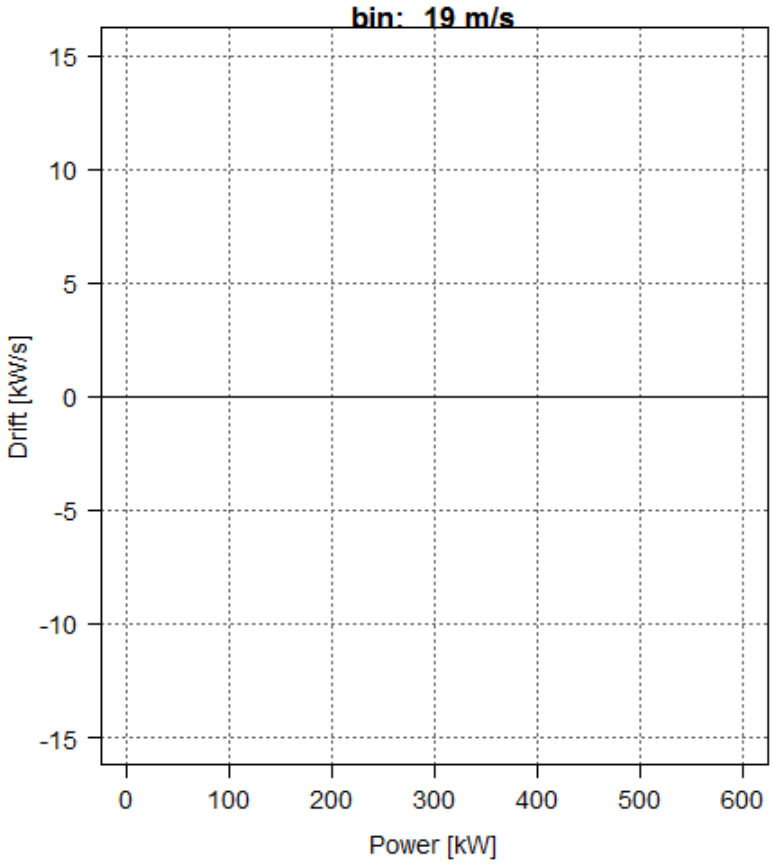
bin: 19 m/s
15
10
5
0
-5
-10
-15
Drift [kW/s]
0
100
200
300
400
500
600
Power [kW]

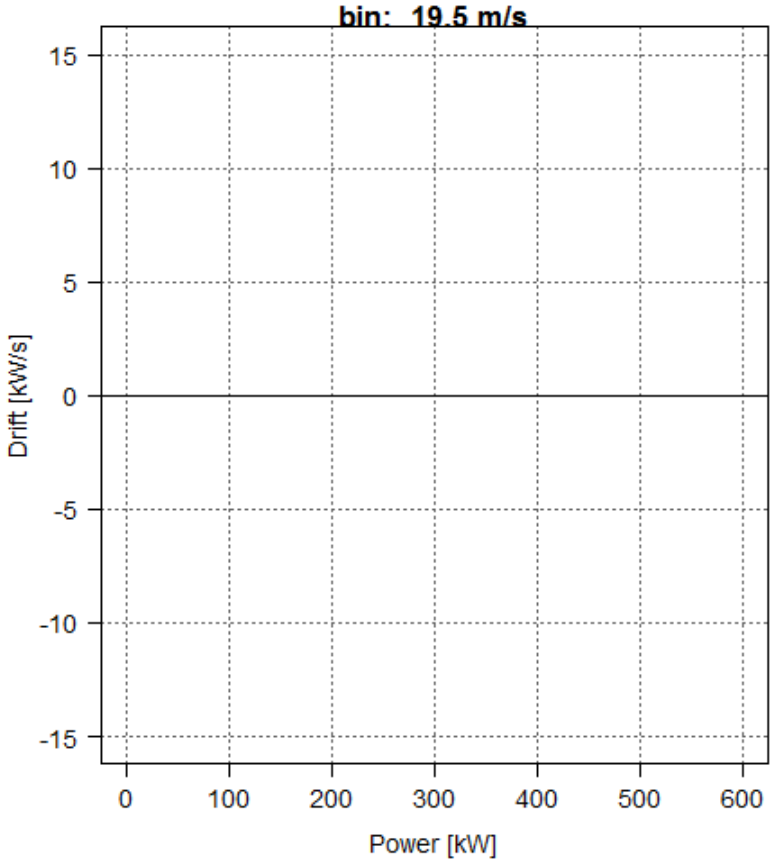
bin: 19.5 m/s
15
10
5
0
-5
-10
-15
Drift [kW/s]
0
100
200
300
400
500
600
Power [kW]

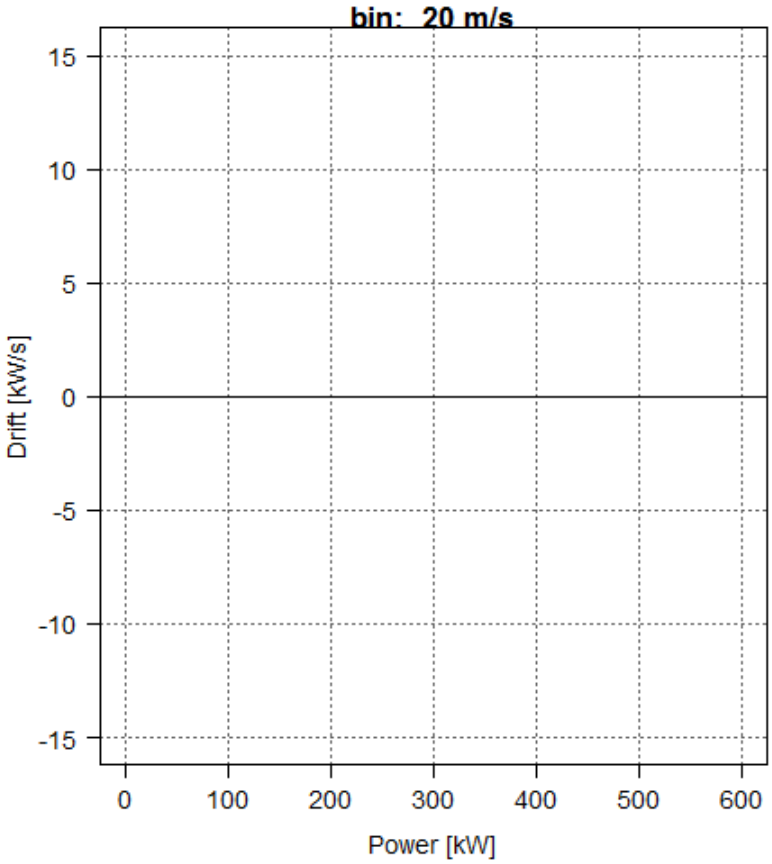
bin:  20 m/s
15
10
5
0
-5
-10
-15
Drift [kW/s]
0
100
200
300
400
500
600
Power [kW]

# Appendix B
# Wind speed bin drift data for 2MW pitch-regulated wind turbine with spinner anemometer

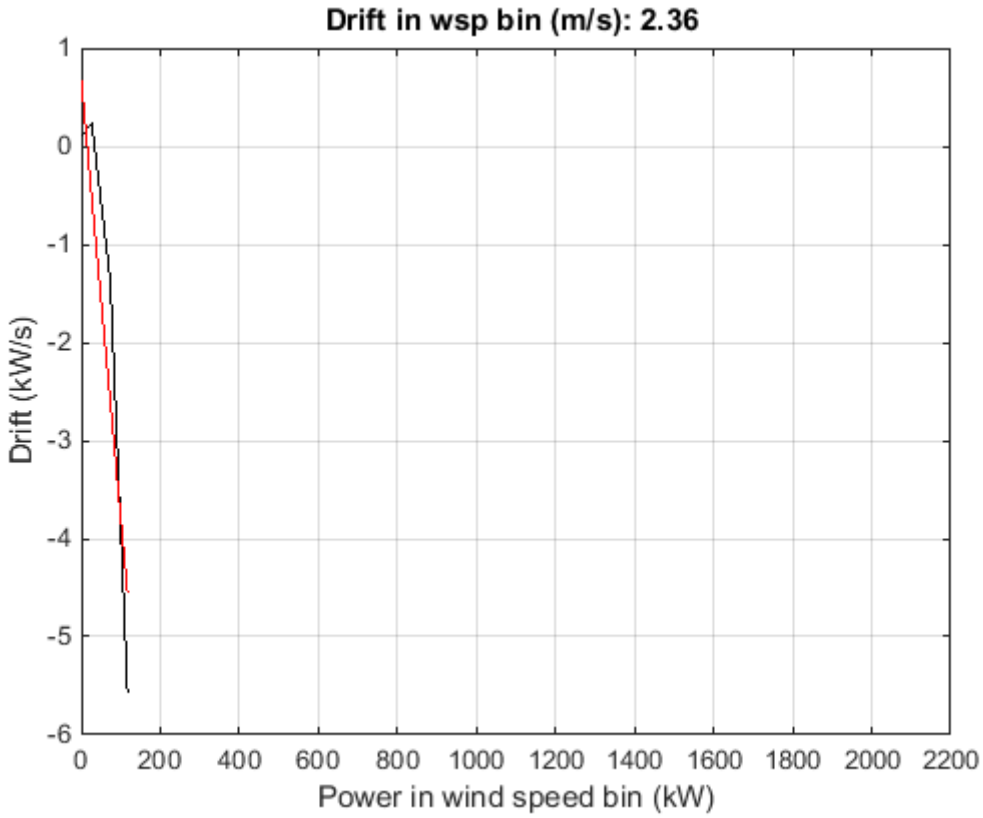

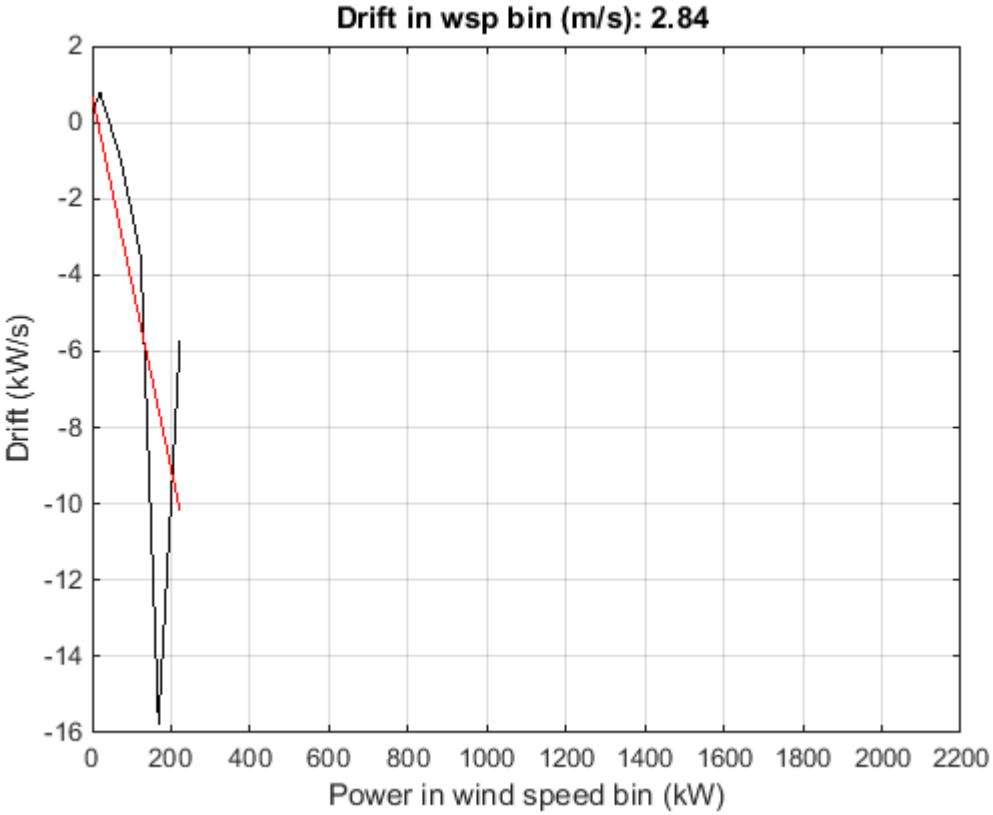
Drift in wsp bin (m/s): 2.84
Drift (kW/s)
Power in wind speed bin (kW)
2
0
-2
-4
-6
-8
-10
-12
-14
-16
0
200
400
600
800
1000
1200
1400
1600
1800
2000
2200

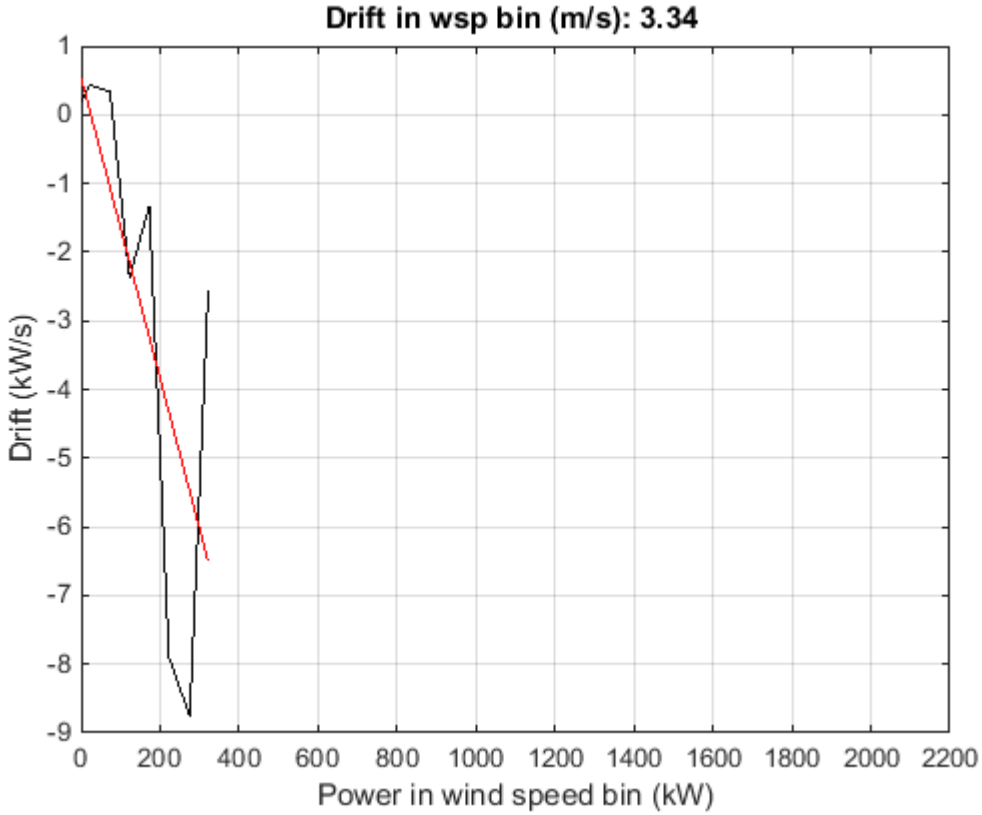
Drift in wsp bin (m/s): 3.34
Drift (kW/s)
Power in wind speed bin (kW)
1
0
-1
-2
-3
-4
-5
-6
-7
-8
-9
0
200
400
600
800
1000
1200
1400
1600
1800
2000
2200

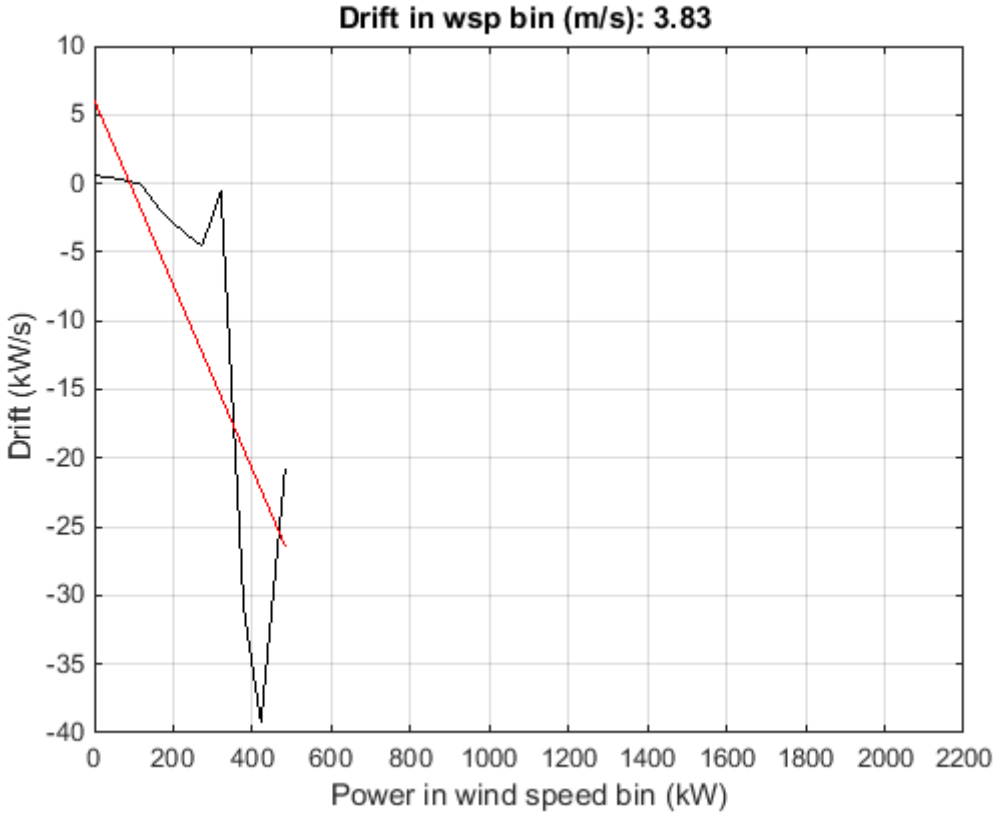
Drift in wsp bin (m/s): 3.83
Drift (kW/s)
Power in wind speed bin (kW)
10
5
0
-5
-10
-15
-20
-25
-30
-35
-40
0
200
400
600
800
1000
1200
1400
1600
1800
2000
2200

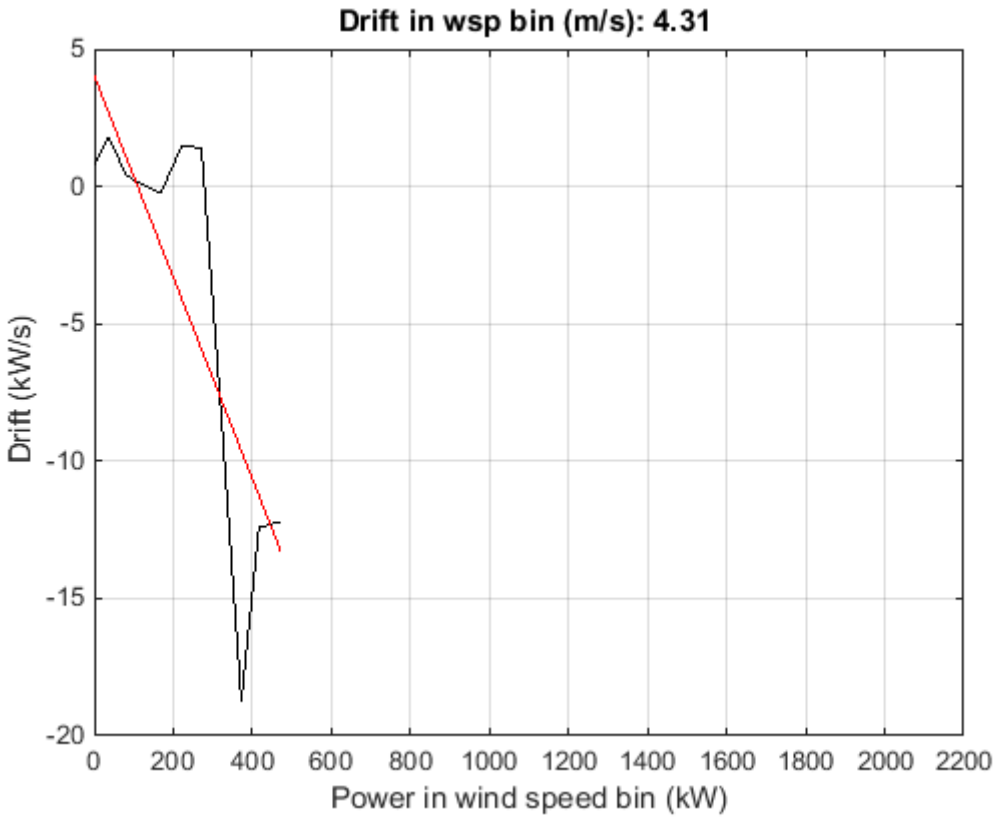
Drift in wsp bin (m/s): 4.31
Drift (kW/s)
Power in wind speed bin (kW)
5
0
-5
-10
-15
-20
0
200
400
600
800
1000
1200
1400
1600
1800
2000
2200

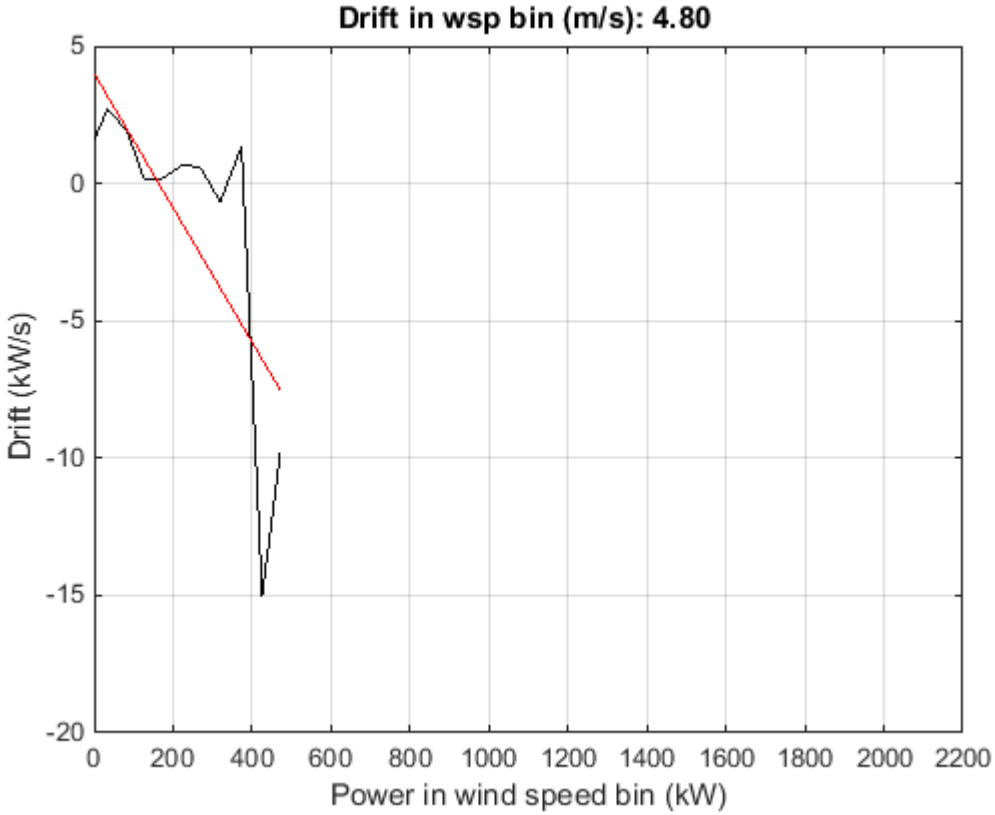
Drift in wsp bin (m/s): 4.80
Drift (kW/s)
5
0
-5
-10
-15
-20
0
200
400
600
800
1000
1200
1400
1600
1800
2000
2200
Power in wind speed bin (kW)

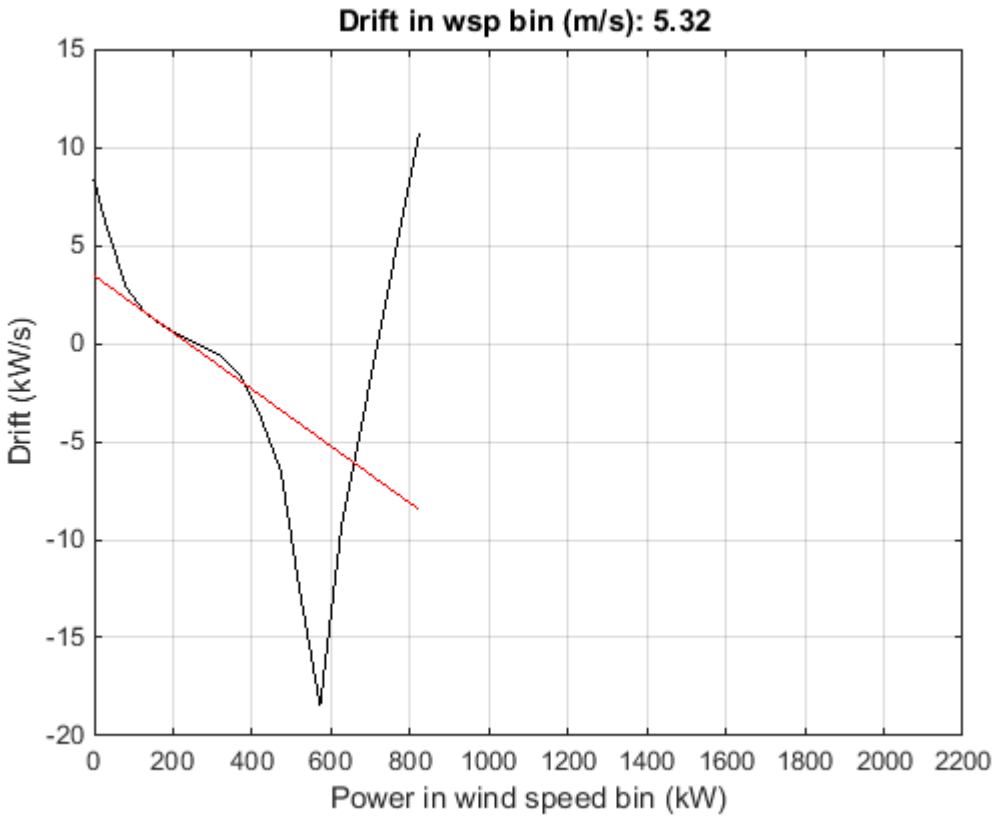
Drift in wsp bin (m/s): 5.32
Drift (kW/s)
15
10
5
0
-5
-10
-15
-20
0
200
400
600
800
1000
1200
1400
1600
1800
2000
2200
Power in wind speed bin (kW)

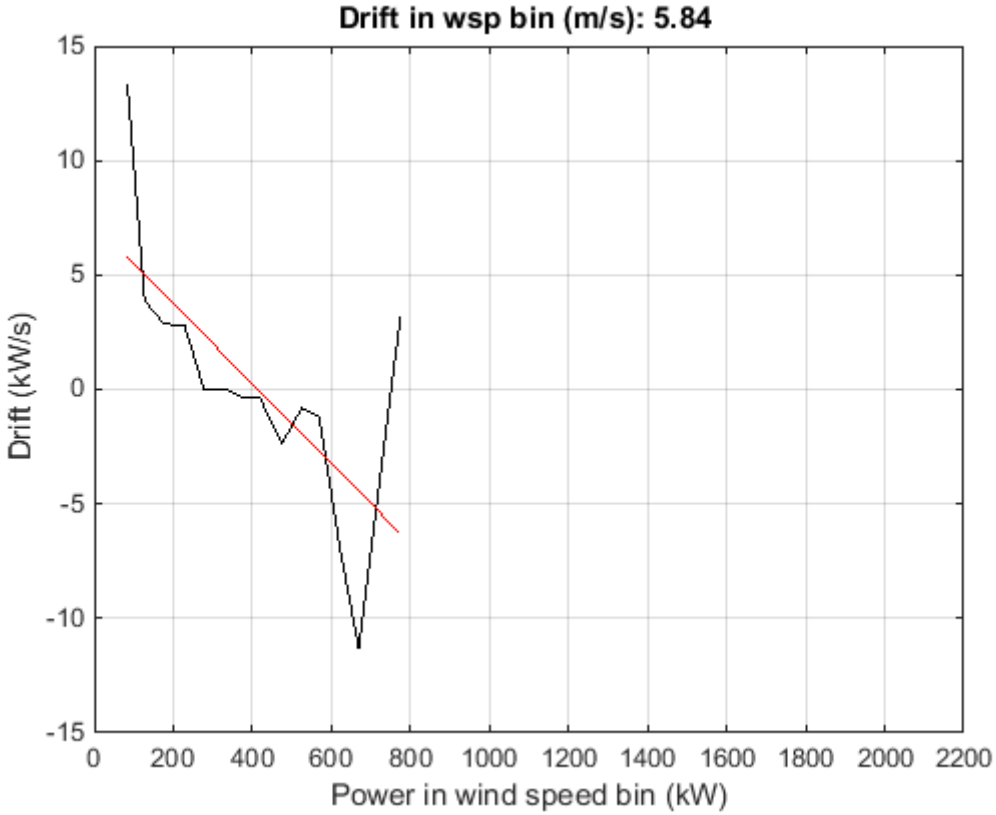
Drift in wsp bin (m/s): 5.84
Drift (kW/s)
15
10
5
0
-5
-10
-15
0
200
400
600
800
1000
1200
1400
1600
1800
2000
2200
Power in wind speed bin (kW)

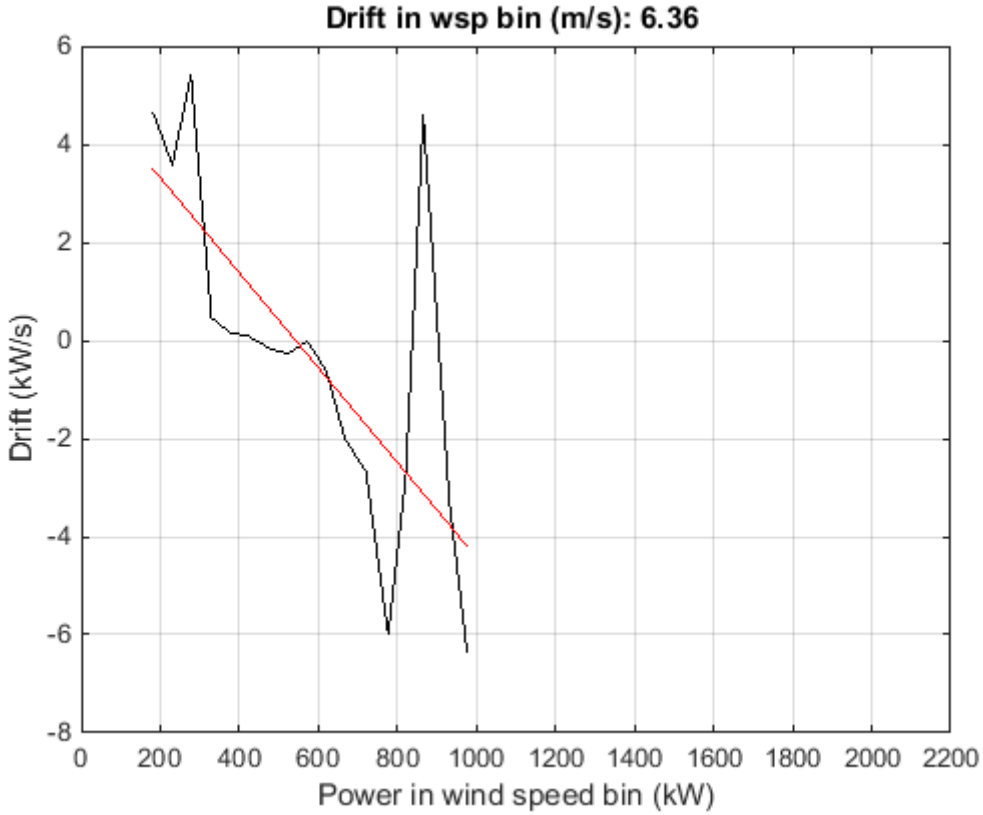
Drift in wsp bin (m/s): 6.36
Drift (kW/s)
6
4
2
0
-2
-4
-6
-8
0
200
400
600
800
1000
1200
1400
1600
1800
2000
2200
Power in wind speed bin (kW)

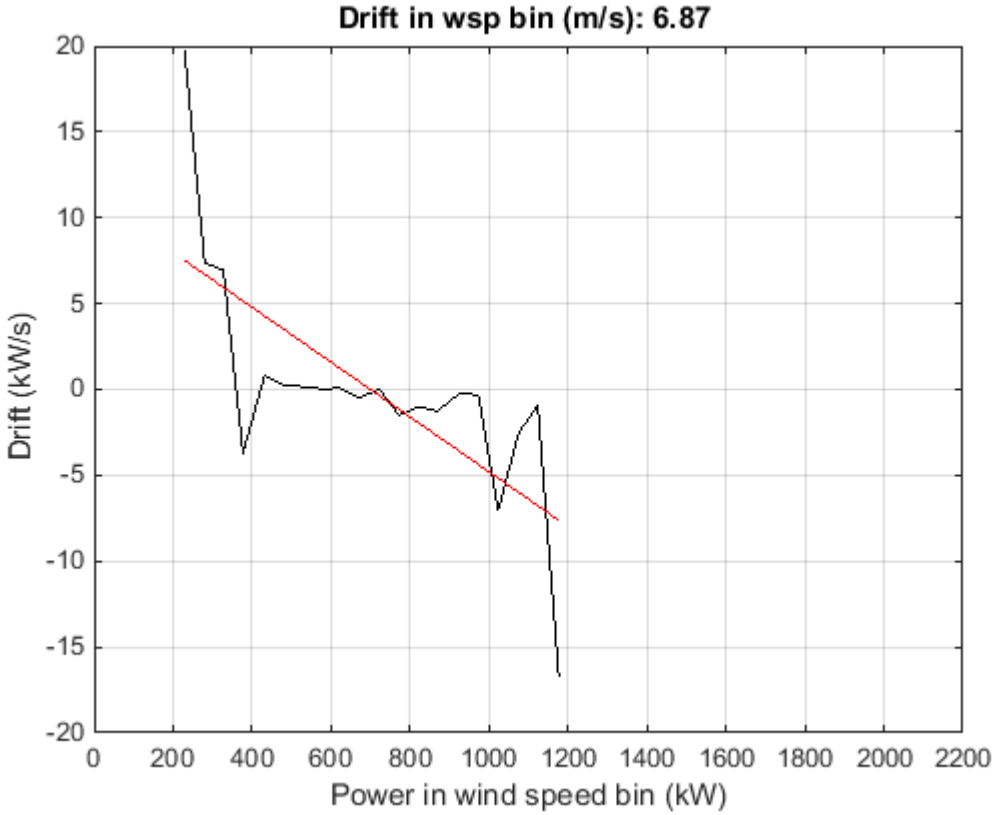
Drift in wsp bin (m/s): 6.87
Drift (kW/s)
Power in wind speed bin (kW)
20
15
10
5
0
-5
-10
-15
-20
0
200
400
600
800
1000
1200
1400
1600
1800
2000
2200

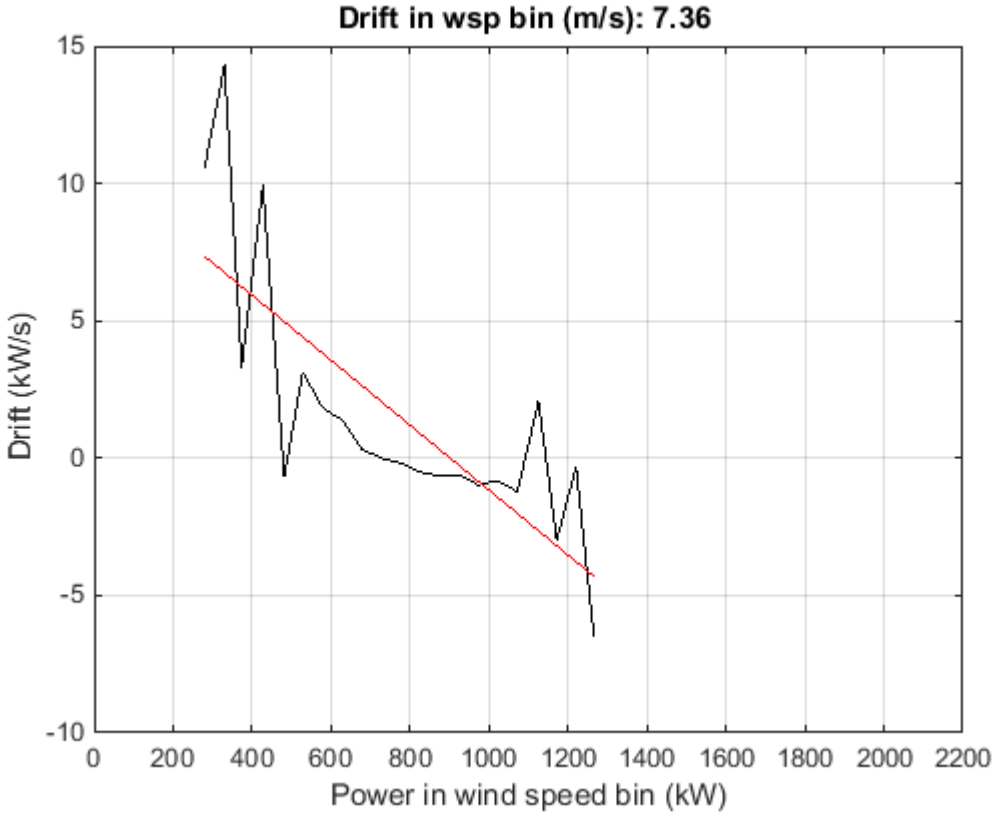
Drift in wsp bin (m/s): 7.36
Drift (kW/s)
Power in wind speed bin (kW)
15
10
5
0
-5
-10
0
200
400
600
800
1000
1200
1400
1600
1800
2000
2200

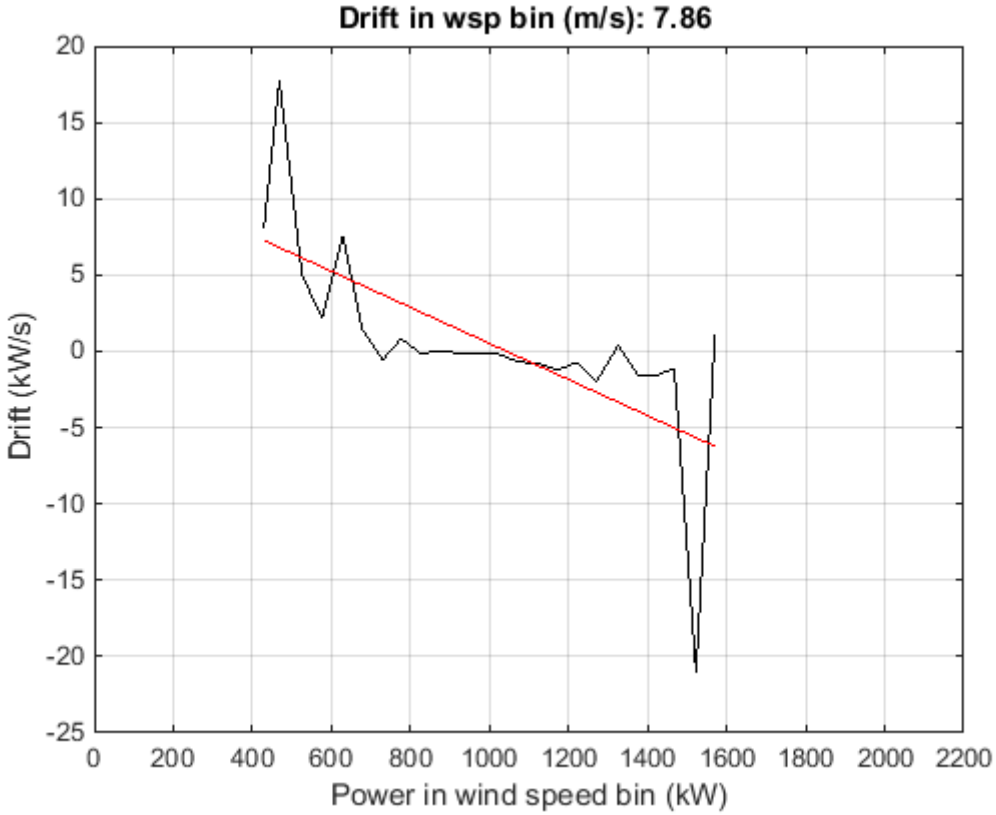
Drift in wsp bin (m/s): 7.86
Drift (kW/s)
Power in wind speed bin (kW)
20
15
10
5
0
-5
-10
-15
-20
-25
0
200
400
600
800
1000
1200
1400
1600
1800
2000
2200

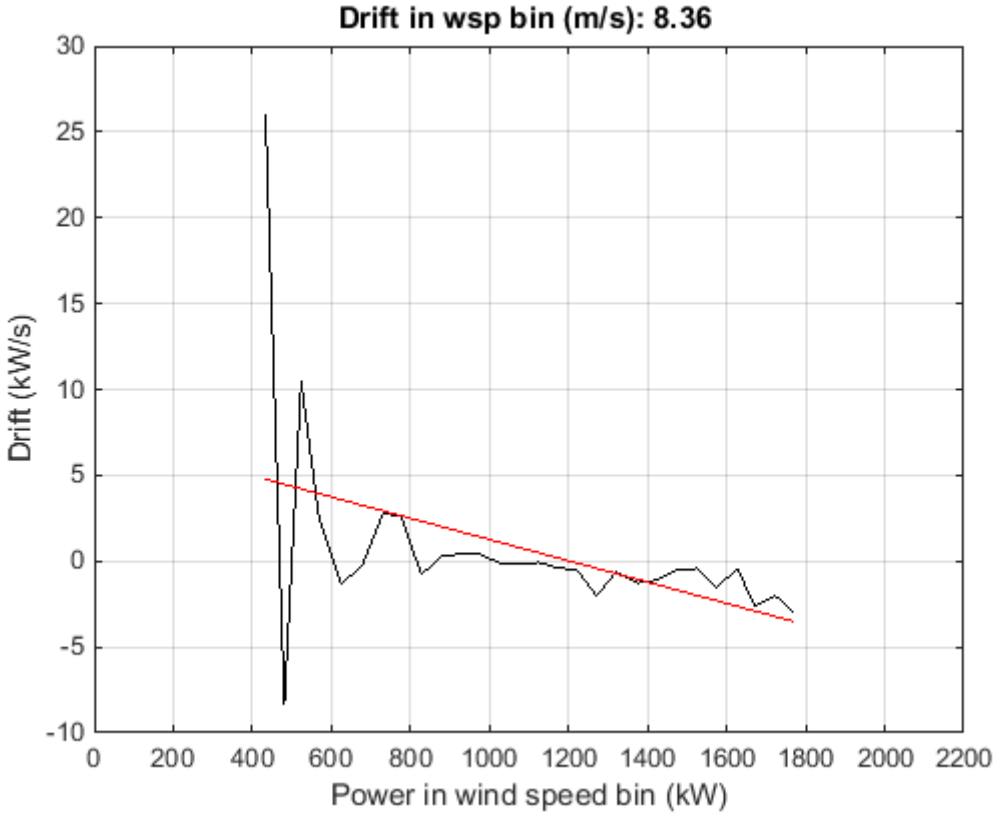
Drift in wsp bin (m/s): 8.36
Drift (kW/s)
Power in wind speed bin (kW)
30
25
20
15
10
5
0
-5
-10
0
200
400
600
800
1000
1200
1400
1600
1800
2000
2200

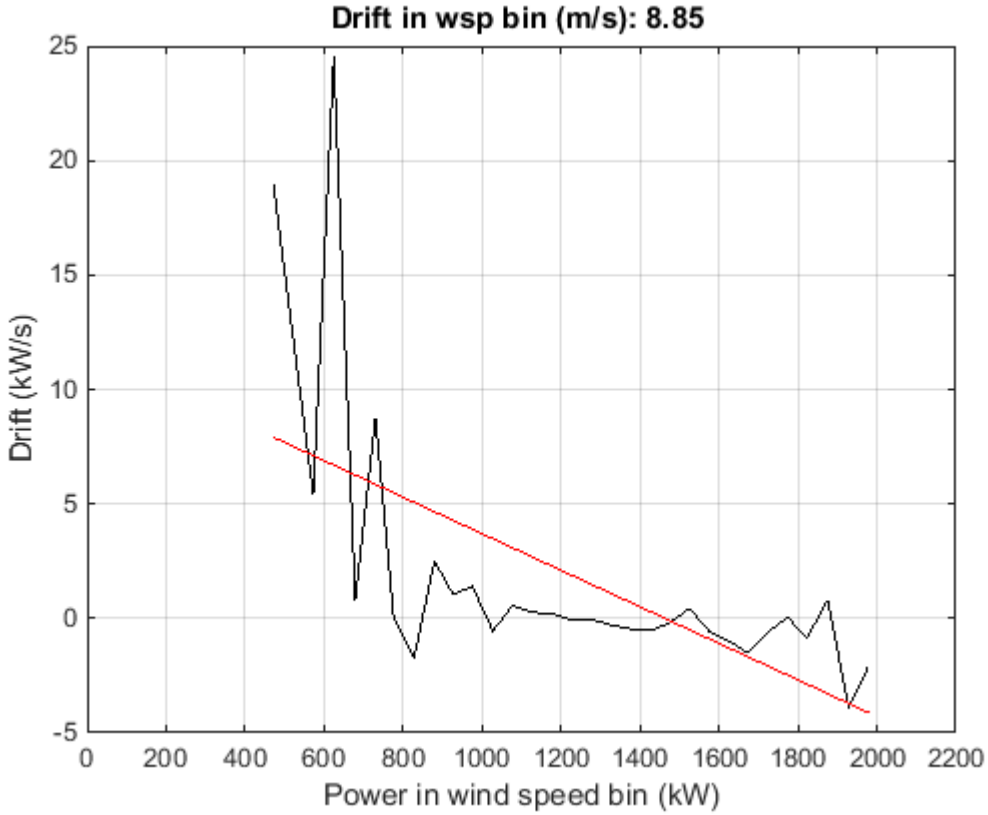
Drift in wsp bin (m/s): 8.85
Drift (kW/s)
Power in wind speed bin (kW)
25
20
15
10
5
0
-5
0
200
400
600
800
1000
1200
1400
1600
1800
2000
2200

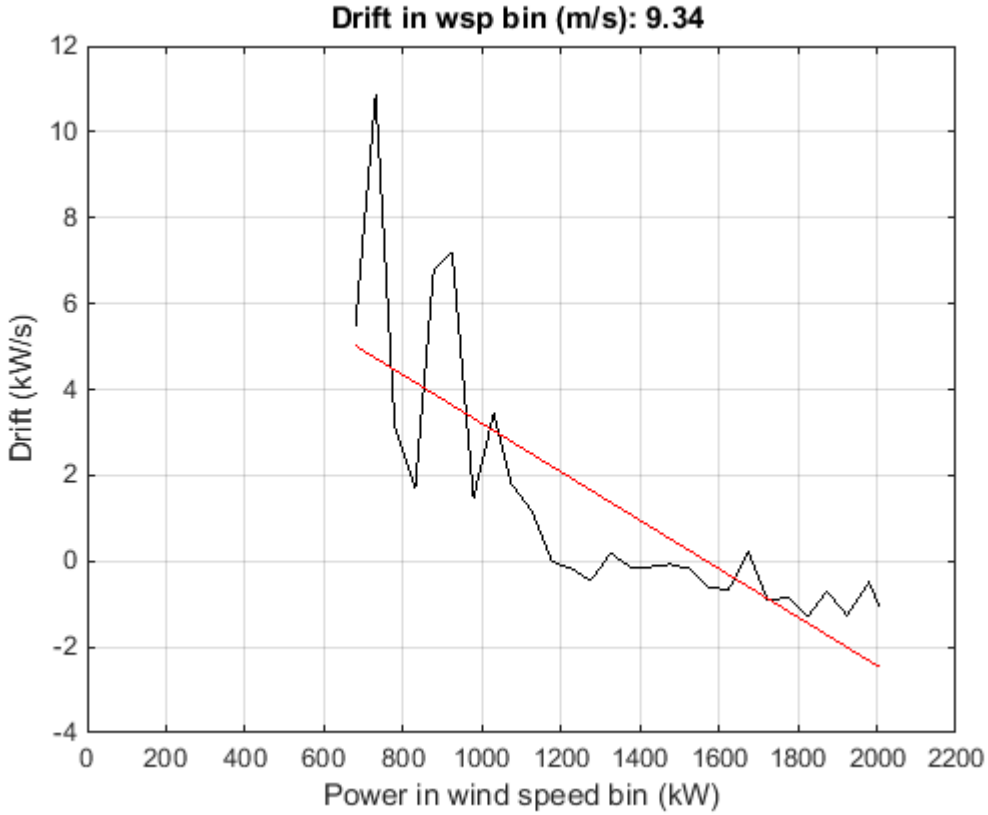
Drift in wsp bin (m/s): 9.34
Drift (kW/s)
Power in wind speed bin (kW)
12
10
8
6
4
2
0
-2
-4
0
200
400
600
800
1000
1200
1400
1600
1800
2000
2200

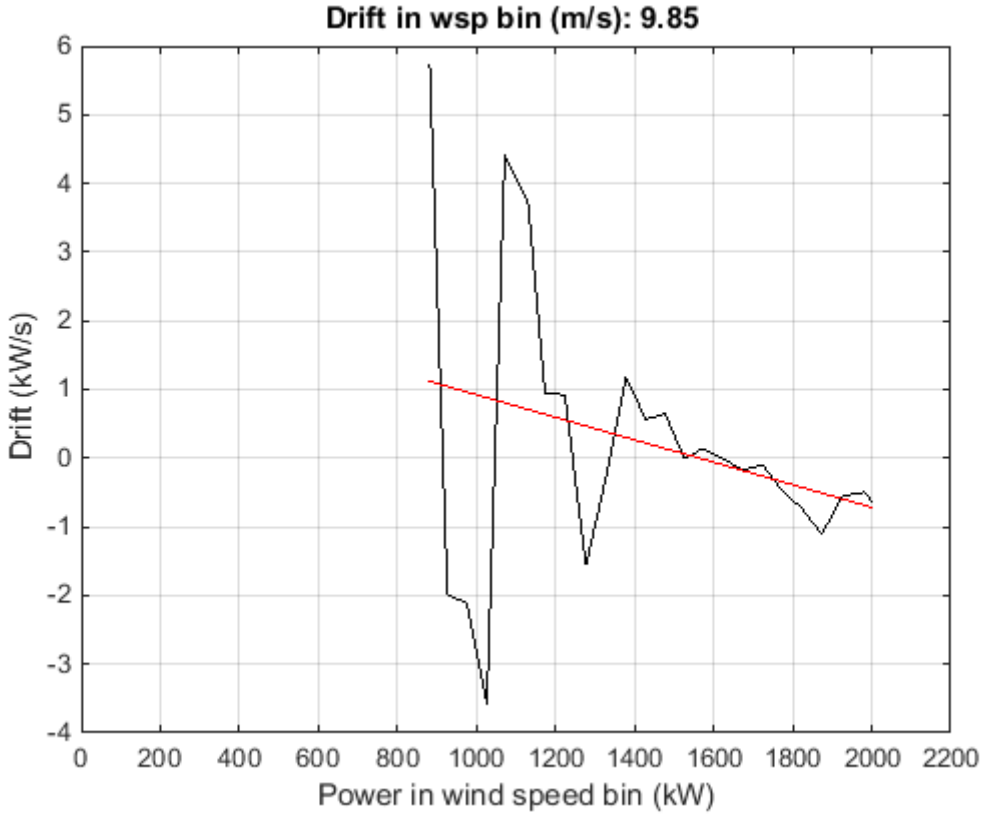
Drift in wsp bin (m/s): 9.85
Drift (kW/s)
Power in wind speed bin (kW)
6
5
4
3
2
1
0
-1
-2
-3
-4
0
200
400
600
800
1000
1200
1400
1600
1800
2000
2200

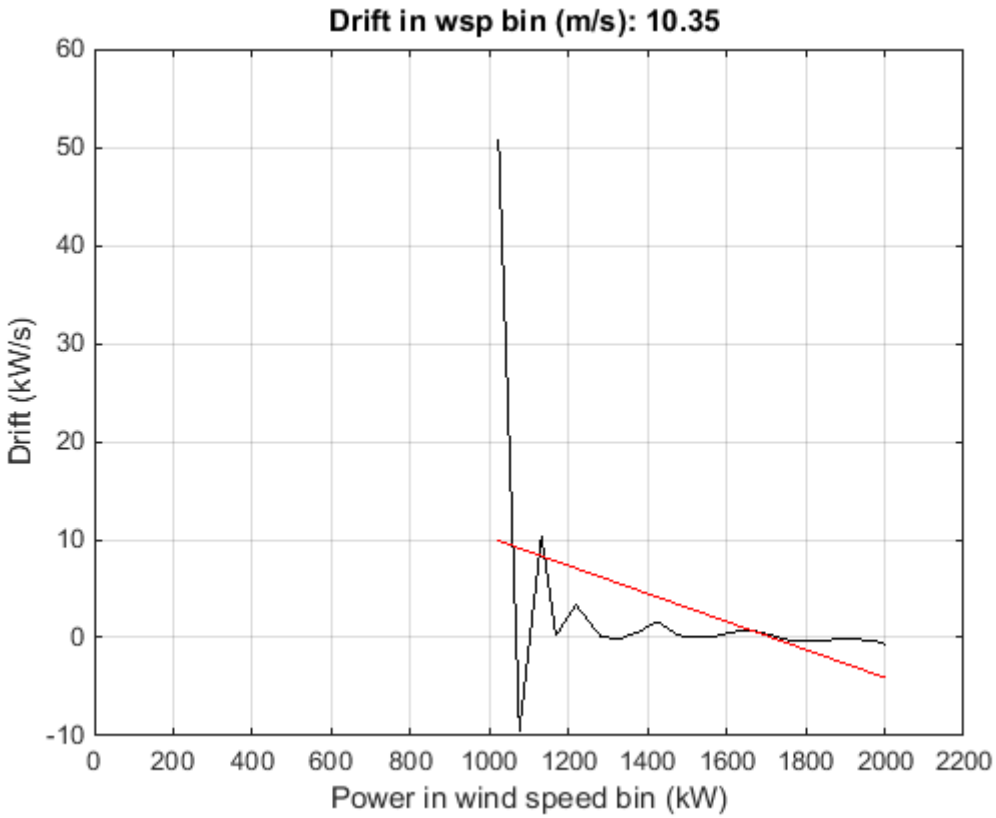
Drift in wsp bin (m/s): 10.35
Drift (kW/s)
Power in wind speed bin (kW)
60
50
40
30
20
10
0
-10
0
200
400
600
800
1000
1200
1400
1600
1800
2000
2200

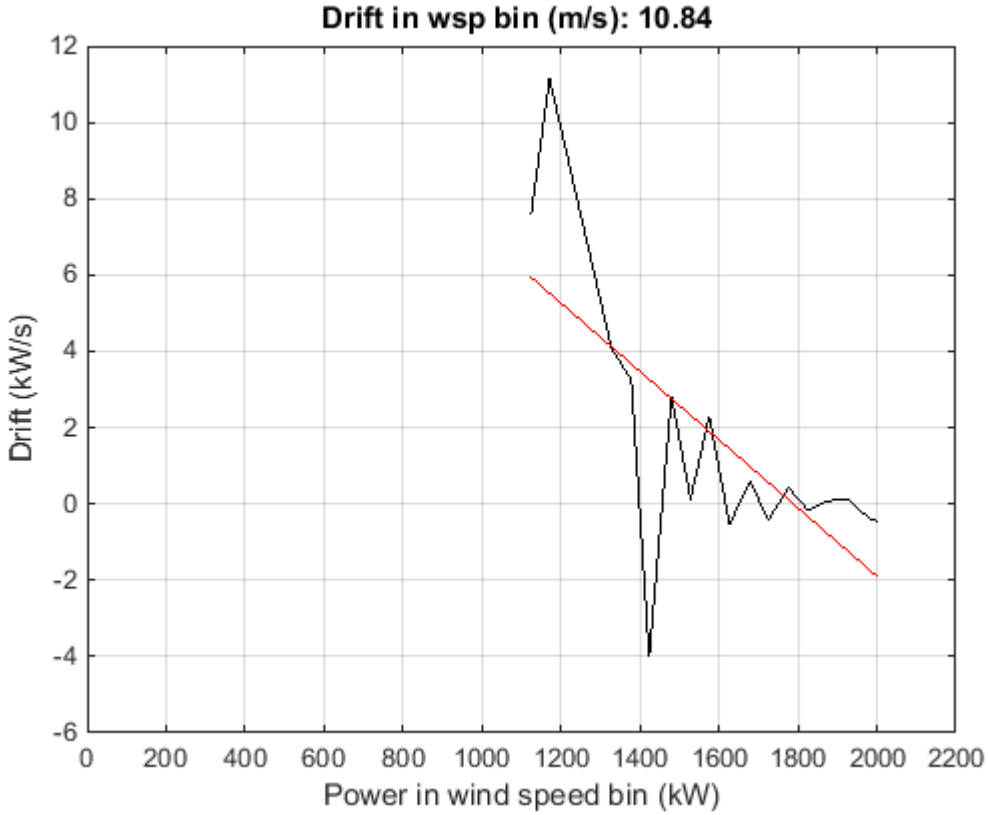
Drift in wsp bin (m/s): 10.84
Drift (kW/s)
Power in wind speed bin (kW)
12
10
8
6
4
2
0
-2
-4
-6
0
200
400
600
800
1000
1200
1400
1600
1800
2000
2200

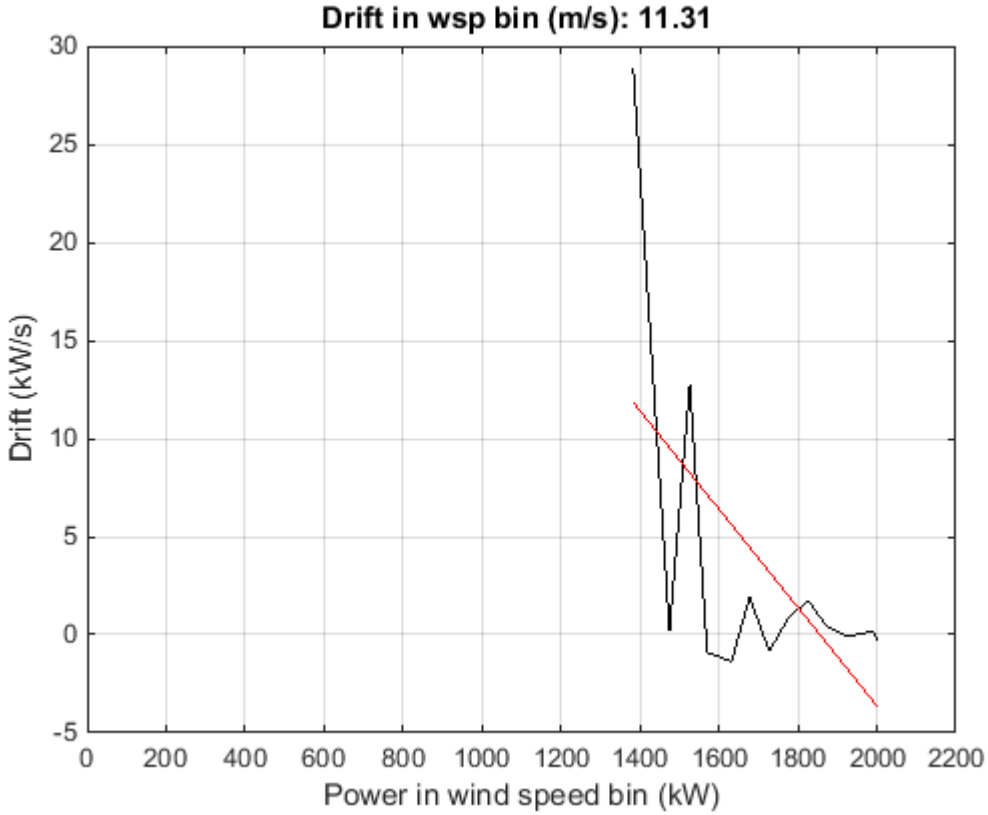
Drift in wsp bin (m/s): 11.31
Drift (kW/s)
Power in wind speed bin (kW)
30
25
20
15
10
5
0
-5
0
200
400
600
800
1000
1200
1400
1600
1800
2000
2200

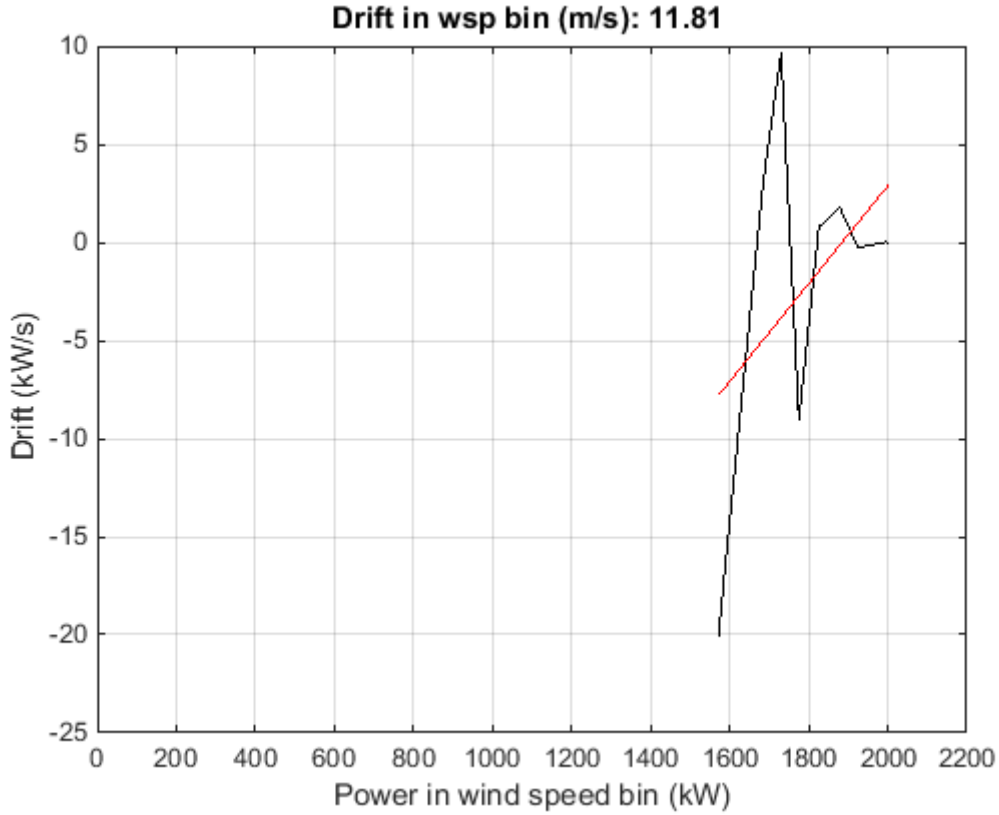
Drift in wsp bin (m/s): 11.81
Drift (kW/s)
Power in wind speed bin (kW)
10
5
0
-5
-10
-15
-20
-25
0
200
400
600
800
1000
1200
1400
1600
1800
2000
2200

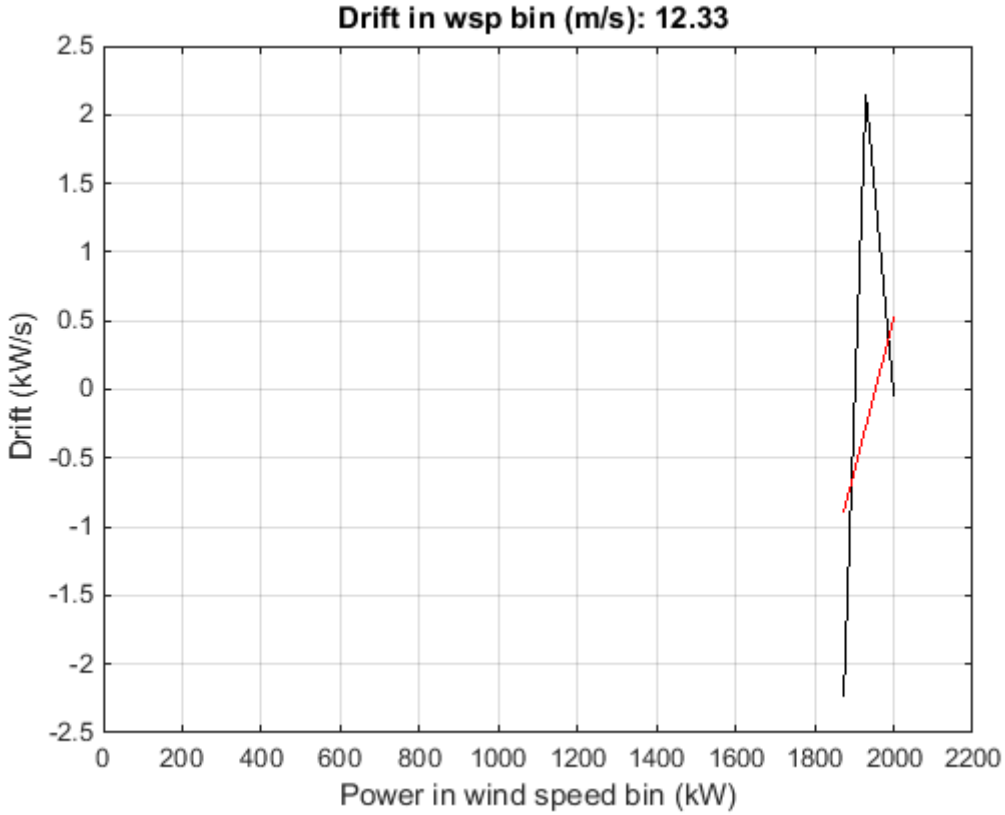
Drift in wsp bin (m/s): 12.33
Drift (kW/s)
Power in wind speed bin (kW)
2.5
2
1.5
1
0.5
0
-0.5
-1
-1.5
-2
-2.5
0
200
400
600
800
1000
1200
1400
1600
1800
2000
2200

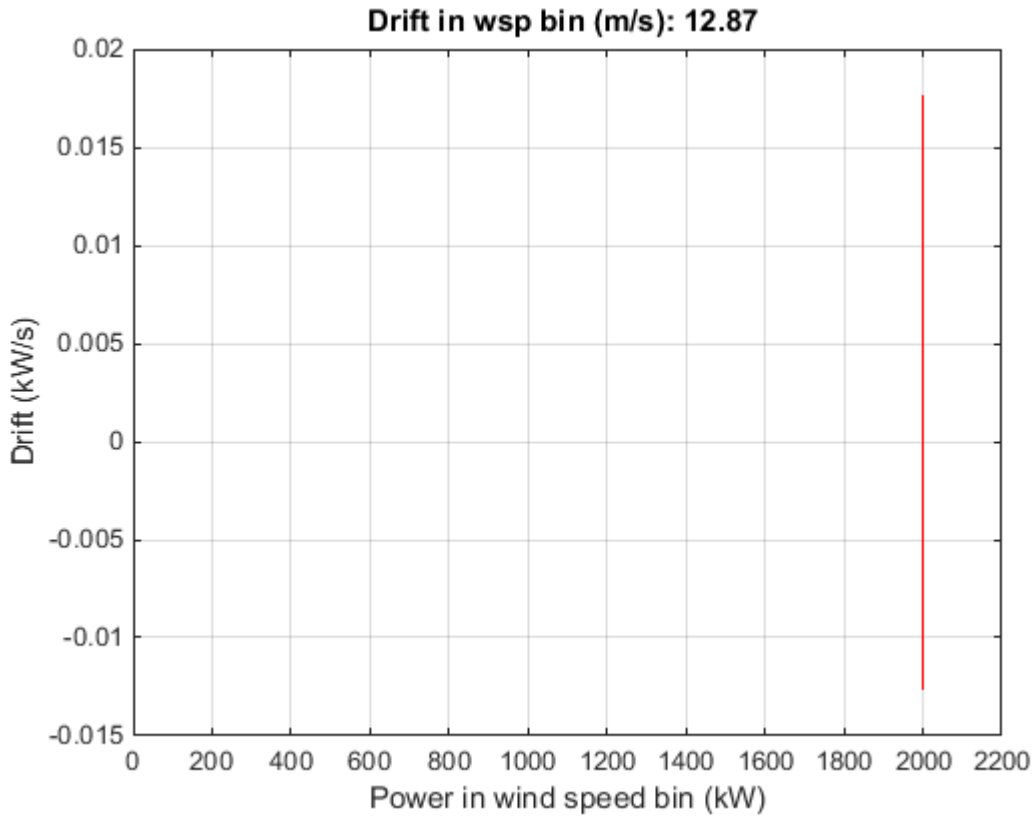
Drift in wsp bin (m/s): 12.87
0.02
0.015
0.01
0.005
0
-0.005
-0.01
-0.015
Drift (kW/s)
0
200
400
600
800
1000
1200
1400
1600
1800
2000
2200
Power in wind speed bin (kW)

DTU Vindenergi er et institut under Danmarks Tekniske Universitet med en unik integration af forskning, uddannelse, innovation og offentlige/private konsulentopgaver inden for vindenergi. Vores aktiviteter bidrager til nye muligheder og teknologier inden for udnyttelse af vindenergi, både globalt og nationalt. Forskningen har fokus på specifikke tekniske og videnskabelige områder, der er centrale for udvikling, innovation og brug af vindenergi, og som danner grundlaget for højt kvalificerede uddannelser på universitetet.

Vi har mere end 230 ansatte og heraf er ca. 60 ph.d. studerende. Forskningen tager udgangspunkt i 9 forskningsprogrammer, der er organiseret i tre hovedgrupper: vindenergisystemer, vindmølleteknologi og grundlag for vindenergi.

**Technical University of Denmark**
**DTU Vindenergi**
**Frederiksborgvej 399**
**Bygning 125**
**4000 Roskilde**
**Telefon 45 25 25 25**
**info@vindenergi.dtu.dk**
**www.vindenergi.dtu.dk**